PERFORMANCE OF AN ANISOTROPIC MAGNETO-RESISTIVE ELECTRICAL ENERGY METER

FREDRICK MACHARIA KAGUCIA

A Thesis Submitted to the Graduate School in Partial Fulfillment of the Requirements for the Masters of Science Degree in Industrial Engineering Systems and Management of Egerton University

EGERTON UNIVERSITY

SEPTEMBER, 2025

DECLARATION AND RECOMMENDATION

Declaration

This thesis is my original work and has not been presented in this University or any other for the award of a degree.

Signature: …… Date:.04/09/2025……

Fredrick Macharia Kagucia

BM12/1330/04

Recommendations

This thesis has been submitted with our approval as University Supervisors:

Signature: …… Date:.05/09/2025…..……

Dr. Owino George O

Department of Industrial and Energy Engineering,

Egerton University

Signature: …… Date:.06/09/2025…..……

Dr. Franklin M. Manene

Department of Electrical and Control Engineering,

Egerton University

COPY RIGHT

DEDICATION

I dedicate this work to my wife Mrs. Asenath Nyambura, sons and daughters for their long patience, moral and material support during the entire period of study.

ACKNOWLEDGEMENTS

I wish to express my sincere thanks to the Egerton University Management for giving me study leave to pursue my postgraduate studies. My thanks also go to my supervisors, Dr. Owino George O. and Dr. Franklin M. Manene of Egerton University for their support and guidance. Special thanks and sincere gratitude go to Prof. D. M. Nyaanga of Egerton University for his tireless support, encouragement and unreserved guidance in the realization of this thesis. My sincere thanks also go to my workmate Mr. John Muniu who thoroughly went through the thesis draft and made very useful comments and corrections. This thesis could not have been completed without the unreserved support of Mr. Joseph Mwangi for his contribution in C-programming and PCB etching.

I wish to recognize Mr. G. G. Maina of the Department of Electrical and Control Engineering for supporting me with laboratory equipment, Mr. Sila Morris and Mr. Otundo for their contributions in the availability of laboratory equipment, setting them up for data collection and their will to sit long hours during the data collection. I also wish to appreciate all the technical staff for their support and suggestions during experimentation and everyone who, in one way or the other, contributed to the success of this thesis.

ABSTRACT

Electro-mechanical energy meters provide an excellent combination of simplicity and reliability and have been used for over a hundred years. They only indicate units consumed and need for additional functionalities made the transition to solid-state electrical energy meters a necessity. Most energy meters use traditional current sensors which have shortcomings like thermal drift, limitation of frequency range, cost, size and lack of electrical isolation. In this research an Anisotropic Magneto-Resistive (AMR) current sensor which overcomes the above disadvantages was tested and found to have a linear characteristic suitable for electrical energy metering. A digital electrical energy meter based on the AMR current sensor was designed using Proteus 8 Professional software, basic electronic components and an Arduino micro microcontroller which sampled and processed supply voltage and current signals through a C-code program. The meter displayed accurate output results of supply voltage, current, power factor (pf), 'real-time' power consumption and cumulative electrical energy (kWh) on a Liquid Crystal Display (LCD). Test-runs lasting 5 minutes were conducted and repeated on electrical loads using the developed AMR meter, Powertek and laboratory multimeters. Analysis of variance was performed on recorded data using Statistical Analysis of Systems (SAS). Means of currents, voltages and pf measured on different meters including the AMR meter were found not to be significantly different at $\alpha = 0.05$. In one of the test runs, analysis of variance on data from four energy meters gave electrical energy means of 0.1197^{a}, 0.1233^{a}, 0.1233^{a} and 0.1333^{a}. Since the means were followed by the same letters, it implied that the means were not significantly different at $\alpha = 0.05$ and the performances of the energy meters were therefore similar. The results showed that the AMR meter performed competitively against common domestic electrical energy meters and also displayed more useful information. Although in the performance analysis the error bars overlapped, further study need to be carried out to investigate on how the errors could be reduced at low current loads.

TABLE OF CONTENTS

LIST OF TABLES

LIST OF FIGURES

LIST OF PLATES

LIST OF ABBREVIATIONS

AC	Alternating Current
ACEEE	American Council for an Energy-Efficient Economy
ADC	Analogue to Digital Converter
AMM	Automated Meter Management
AMR	Anisotropic Magneto-Resistive
AMRg	Automated Meter Reading
AMI	Advanced Metering Infrastructure
ANSI	American National Standards Institute
CoFeSiB	Cobalt-Ferrous-Silicon-Boron alloy
CRO	Cathode Ray Oscilloscope
CT	Current Transformer
DAC	Digital to Analogue Converter
DC	Direct Current
DSP	Digital Signal Processing
EEPROM	Electrically Erasable Programmable Read Only Memory
EMF	Electromotive Force
$Fe_{81}Si_{19}$	Permalloy (81% Fe, 19% Si)
$Fe_{83}P_{10}C_{7}$	83% Fe, 10% P and 7% C alloy
GMI	Giant Magneto-Impedance
GUI	Graphical User Interface
IC	Integrated Circuit
IEC	International Electro-technical Commission
KEBS	Kenya Bureau of Standards
kWh	kilo-Watt-hour
LCD	Liquid Crystal Display
LPF	Low Pass Filter
MCU	Microcontroller Unit
OPAMP	Operational Amplifier
PCB	Printed Circuit Board
PBM	Power measured by Blue Meter (BM)
PFM	Power measured by AMR meter

VBM	Voltage measured by Blue Meter (BM)
VFM	Voltage measured by AMR meter
IBM	Voltage measured by Blue Meter (BM)
IFM	Current measured by AMR meter
pfBM	Voltage measured by Blue Meter (BM)
PfFM	Power factor measured by AMR Meter
EM1	Double decimal point electrical energy meter (Meter No. 1)
EM2	Single decimal point electrical energy meter (Meter No. 2)
EM3	Electro-mechanical electrical energy meter (Meter No. 3)
EBM	Electrical energy measured by ‘Blue Meter’ (BM)
EFM	Electrical energy measured by AMR meter
pf	Power factor
RMS (or rms)	Root Mean Square

CHAPTER ONE
INTRODUCTION

1.1 Background of the study

Electromechanical meters have served electricity consumers well for over a century and have been used in Kenya for many years. Their design was optimized to provide an excellent combination of simplicity and reliability. However, these meters lack the additional functionalities needed to integrate customers with a smart grid, such as real-time bills, range of measured quantities and communication capability. For these reasons, the transition to solid-state electrical energy meters has not therefore been one of choice, but of necessity (Seal & McGranaghan, 2010).

Analogue meters are being replaced with state-of-the-art electronic digital energy meters on a large scale. However, the reliability of electronic components has been a concern and many experts believe that the electronic meters will not survive like their electromechanical predecessors (Chaluvadi, 2008). Despite well-developed traditional and alternate sources of electricity, there are many problems with regard to distribution, metering and billing of electrical energy and measurement of its consumption (Ashiquzzaman *et al.*, 2012). However, revenue mobilization starts with effective and accurate metering, production of error-free bills and effective collection exercises (John, 2012).

Electrical residential-smart meters are expensive. They measure the consumption of electrical energy in frequent intervals and communicate that information at least daily to the utility firm for monitoring and billing purposes. Smart meters are a fundamental element for the future smart grid of electricity. However, smart metering does not only affect the future development of the smart grid, but motivates the rational management of the electrical energy consumption in houses and buildings (Kamilaris, 2012). The American Council for an Energy-Efficient Economy (ACEEE) reviewed more than 36 different residential smart metering and feedback programs internationally. Their conclusion was that “to realize potential feedback-induced savings, smart meters must be used in conjunction with in-home displays and well-designed programs that successfully inform, engage, empower and motivate people” (Kamilaris, 2012). Automatic meter reading offers additional functionality such as real-time power outage notification, power quality monitoring and transferring that data to a central database for billing, trouble-shooting and analyzing.

The accuracy of energy meters depends upon the various accuracies of the sensors used in the analogue input circuits, the sampling process, the Analogue to Digital Conversion (ADC) and of digital calculations (Hribik *et al.,* 2004). For planning and monitoring purposes, the power supply companies need to estimate the loading of the distribution network. Modern electricity distribution utilities need accurate load data for pricing and tariff planning, distribution network, customer service and billing. The mission of power supply providers is to service the customer's needs of electric energy at optimal costs. Usually the only source of information of the customer's energy use comes from the customer billing meters (Seppälä, 1996).

Despite the high accuracy of digital meters, the sensors used possess inherent errors which contribute to inaccurate bills. Most digital electronic energy meters in the market utilize low resistance shunts, current transformers and the Hall-effect based current sensors. Shunts offer Direct Current (DC) and Alternating Current (AC) sensing, good accuracy, low offset and cost. They do not provide electrical isolation, have a high thermal drift and insert a voltage drop in the electrical circuits (Koon, 1999). Current transformers are low-cost and provide electrical isolation, but can only work in AC circuits. They have the disadvantages of a limited frequency range, hysteresis, eddy losses, saturation and nonlinearity especially at large currents.

Hall-effect based sensors provide electrical isolation and operate from DC to high frequency (200 kHz) but have limitations in cost, size, linearity and temperature performance. A Rogowski coil which is air-cored has no hysteresis, saturation or non-linearity and is becoming very common in domestic installations in the United States of America (USA). It relies on measuring the magnetic field but is more susceptible to external magnetic field interference than the current transformer (Koon, 1999). The ferromagnetic Anisotropic Magneto-Resistive (AMR) sensor (19% Fe, 81% Ni) is manufactured using thin film technology (Friedrich & Kunze, 2000). It possesses intrinsic characteristics such as temperature stability, corrosion resistance, good electromagnetic properties, high reliability, small size and light weight. AMR current sensors can be used in smart meters.

Evidence shows that energy feedback information provided by smart meters can enable consumers to reduce consumption by 5-15%. Statistics show that if every domestic user in the UK reduced electricity consumption by 10%, then the users would not only reduce their bills by 10%, but six power stations could be closed and reduce the UK's CO_2 output by six million tons per year (Kelly, 2011).

The electronic energy meters used in Kenya display the digital read-out of the electrical energy consumed and are read monthly for billing purposes. They lack additional functionalities like real-time power consumption, power factor, available terminal voltage and current drawn by the load. The additional information read off from the meters would make the consumers more aware of their energy usage.

This research aimed at designing and fabricating an electrical energy meter using an AMR current sensor and analyzing its performance against some selected common electrical energy meters used in domestic installations. The study showed that the performance of the meter was not significantly different from the selected meters at 0.05 level of significance. In addition to the usual electrical energy (kWh) readout, the designed AMR electrical energy meter was able to display the "real-time" power consumption, current drawn by the load, power factor (pf) and consumer's terminal voltage which are useful to both the consumers and power supply companies.

1.2 Statement of the problem

The problem with single phase electrical energy meters installed in domestic premises in Kenya and other countries is that they don't display additional information essential in enlightening consumers and utility providers the supply voltage, current, power factor and "real-time" power consumption at the source. If such information is provided, consumers would be continuously informed about their consumption and power factors which they could easily and conveniently improve through a competent technician. Consumers continuously complain about their supply voltage fluctuations and service providers at times connect their meters for monitoring purposes. Consumers and also the service providers could monitor this from installed meters and arrest the problem before electrical equipment burn out. This research aims at solving such problems by designing and developing an electrical energy meter which provides additional information.

1.3 Objectives

The broad objective was to develop an electrical energy meter by sampling the load supply voltage and current signal derived from an Anisotropic Magneto-Resistive (AMR) sensor and determine its performance.

The specific objectives were:

(i) To determine the output/input relationship of the AMR current sensor and its suitability in the design and fabrication of a single phase electrical energy meter.

(ii) To sample and process consumer's terminal voltage and load current signals and display accurate voltage, current, power factor, 'real-time' power consumption and electrical energy on a Liquid Crystal Display (LCD).

(iii) To determine the performance of the AMR electrical energy meter.

1.4 Research questions

(i) What is the output/input relationship of the AMR current sensor and is it suitable in the design and fabrication of a single phase electrical energy meter?

(ii) Are consumer's terminal voltage and load current signals sampled and processed to display accurate voltage, current, power factor, 'real-time' power consumption and electrical energy on a Liquid Crystal Display (LCD)?

(iii) How is the performance of the AMR electrical energy meter?

1.5 Justification of the study

Many consumers' loads are growing from small domestic consumptions to small industrial loads. Today, electrical loads in homes include chaff cutters, maize mills, electrical drills and cutters, arc-welding machines, fridges and fluorescent fittings which draw currents at lagging power factors. The large currents drawn by the lagging power factor loads translate into high bills. These bills could be reduced if the consumers were continuously informed about their electricity usage through digital displays on energy meters.

There are many complaints of low supply voltages at consumer terminals which cause malfunctions and losses of equipment/appliances that pass with no compensation to the customers. The study has shown that displays of supply voltage, load current, power factor, 'real-time' power consumption and cumulative electrical energy are achievable. This could solve the above problems through regular monitoring, improving their power factors, switching off unnecessary loads and reporting to electricity service providers for their response. The customers would not only benefit from improved power supply quality but also in reduced bills. The electricity service providers would also benefit in faster monitoring of power consumption, voltage fluctuations (quality), cheaper equipment/installations as a result of lower current ratings and increased customer connectivity resulting from saved electrical energy. The performance of new meters entering the market is not usually compared with that of existing meters. This creates a problem of introducing into the market lower quality meters. The performance of the new AMR electrical energy was compared with several meters used by electricity companies and was found to have similar accuracies.

1.6 Scope and limitation

This study was based on a 25A AMR current sensor and an Arduino micro microcontroller. The metering was limited to single phase 240V, 50 Hz supply with a maximum load current of 25A. The design and fabrication of the electrical energy meter utilized locally available materials (except the AMR sensor). Fabrication of a suitable dc power supply for the current sensor, OPAMPS, Arduino Micro and the LCD was a big challenge and was not achieved. It was finally purchased.

The experimental set-up was based on electrical loading using 240V 100W incandescent bulbs and 1.2M × 36W fluorescent fittings and measurements of voltage, current, power factor, 'real-time' power consumption, and electrical energy. The supply voltage and temperature fluctuations were not controlled and were assumed to have no major effects on the experiments. The measurements on the laboratory Powertek meter ('Blue Meter (BM)') were used as the reference to the other instrument readings. The performance of the meters was evaluated against KEBS-certified instruments in the laboratory of Electrical and Control Engineering Department. The following electrical energy meters were used for comparison:

i. Single Phase Static Meter Class 1.0 EM101-1 5(100) A, 240V, 50 Hz.
ii. Single Phase Static Meter Class 1.0 DDS9999 10(40) A, 220V, 50 Hz.
iii. Electric Watt-hour Meter Class 2.0 20(100) A, 220V, 50Hz, Model 28.

CHAPTER TWO
LITERATURE REVIEW

2.1 Introduction

This section covers reviewed literature and applications of current sensors used in metering electrical energy. The most common current sensors used for electricity metering are resistive shunts, Hall-effect sensors and current transformers. Due to the rapid growth in manufacturing technology, new sensors have been developed and are shown in a comparison table. The voltage and current signal acquisition transducers need to be selected depending on the application. A general block diagram of practical single phase meters have been used to illustrate applications of current transducers, signal conditioning and processing, display and other features. Relevant equations have been used in various sections and some have been used in the development of the signal processing software.

2.2 General block diagram

The accuracy of energy metering is a function of measurement error, which depends on the precision of voltage and current sensors. Current measurement is considered to be more challenging because it requires a wider range of measurements and processing of a wider range of frequencies that are present in the current signal (Volokhin *et al.*, 2017). These sensors have advantages and disadvantages that are subject to their applications. A general block diagram for a solid-state energy meter showing voltage and current transducers, ADCs, digital signal processing and display is shown in Figure 2.1.

The figure shows how current and voltage signals are acquired through current and voltage transducers which transform them to suitable and appropriate signals for sampling by their respective Analogue-to-Digital Converters (ADCs). The digital signals are then fed to the digital signal processor which, through a suitable code, processes the digital signals to electrical energy which is displayed using appropriate digital units. The Electrically Erasable Programmable Read Only Memory (EEPROM) stores temporary data as well as the cumulative consumed electrical energy information.

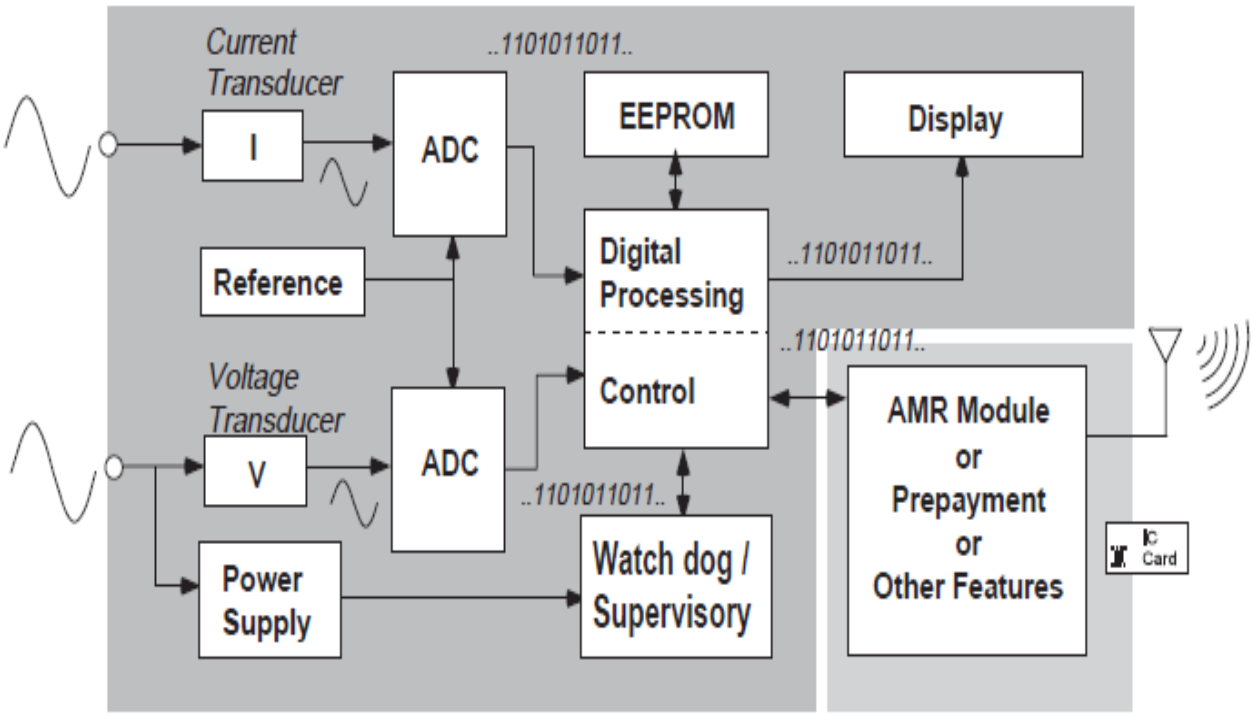

Figure 2.1: General block diagram for a solid-state energy meter.

(http//www.welwyn-tt.com)

Supervisory and control provides communication protocol to/from the EEPROM and Automatic Meter Reading (AMR). The AMR module sends electrical energy data to the electricity service provider for billing purposes through appropriate signal transmission media. A prepayment feature provides a means through which the consumer pays for units to be consumed in advance.

2.3 Low Resistance current shunt

Current shunt is the lowest cost solution available today (Koon, 1999). It offers good accuracy at low cost and the current measurement is simple. Though popular it has self-inductance which results in a noticeable error at low power factor (Kaplan, 2002). The shunt is fundamentally resistive and has a self-heating problem which makes its use rare among high current energy meters (Koon, 1999). When a large current is to be measured, a Kelvin connection is used since it avoids the error caused by voltage drops in the high current path (Xu & Lorenz, 2002).

Figure 2.2 shows a block diagram of an electrical energy meter having a one decimal point kWh LCD display. The MSP430AFE is a slave-metrology processor while the MSP430F6638 is the

host/application processor (Hou & Yu, 2011). The key components are the voltage and current transducers. In this application the current signal is acquired through a resistive shunt transducer while the voltage signal is acquired through a potential divider.

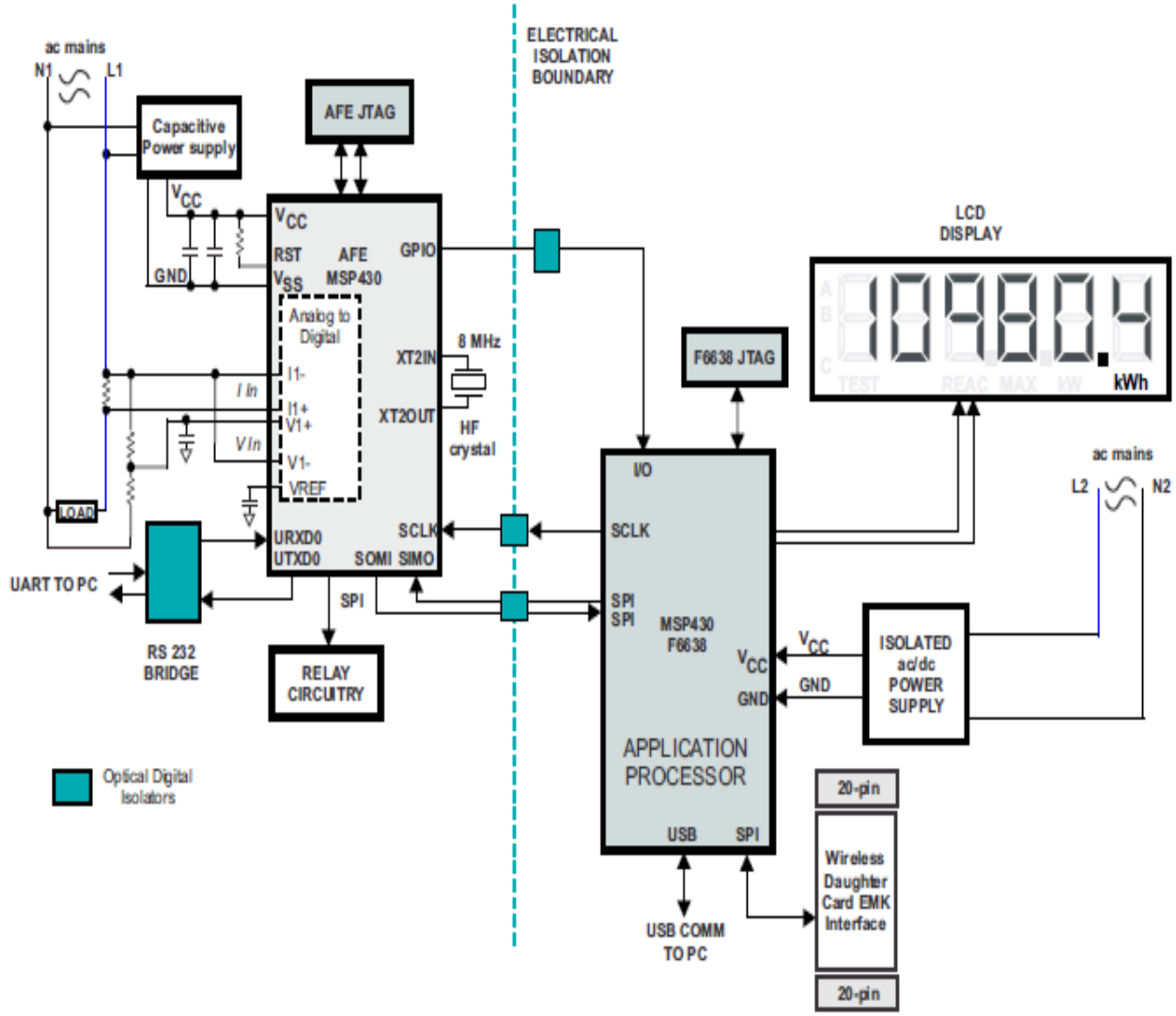

Figure 2.2: Use of current shunt in an electrical energy meter (Hou & Yu, 2011).

The meter has an USB communication port to a Personal Computer (PC) and a wireless feature which may be used for automatic billing. The supply voltage (0 to V_{CC}) to the application processor is derived from the alternating current mains.

2.4 Current transformer

Current Transformers (CTs) are commonly used sensors among today's high current solid-state electrical energy meters. Because of the magnetizing current, a CT sensor has a typical small phase shift of 0.1 to 0.3 degrees (Koon, 1999) and if not calibrated, it will lead to a noticeable

error at low power factor because of the parasitic inductance. Large currents may cause a CT to saturate but this problem is solved by using ferrite materials with very high permeability. However, these types of CTs have inconsistent and larger phase shift compared with the conventional iron core CTs (Koon, 1999). Figure 2.3 shows a single-phase energy meter application using processors from Texas Instruments.

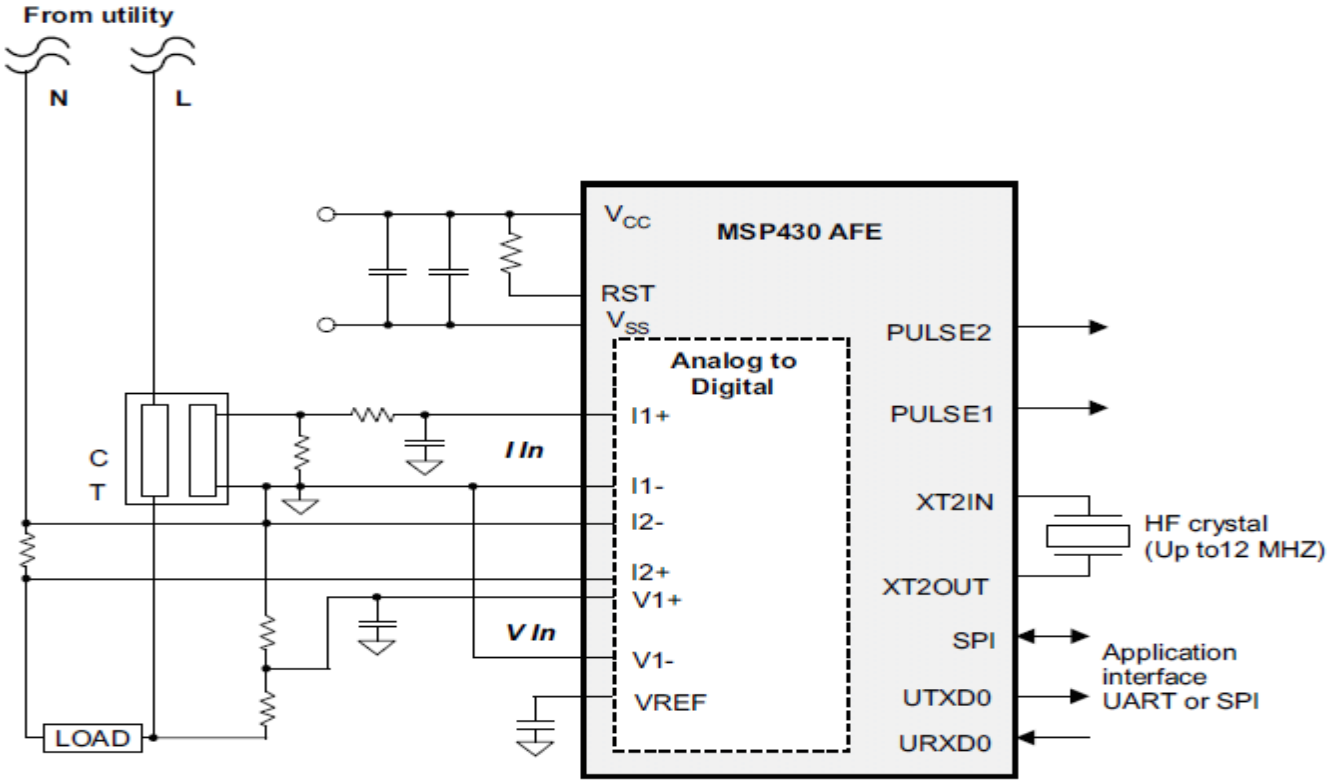

Figure 2.3: Application of a CT and a current shunt in a single phase energy meter (Hou & Yu, 2011).

In this design, a Current Transformer (CT) and a shunt are used for tamper detection in which the current in the live and neutral conductors are measured and compared. If a difference exists, it is an indication that some tampering of the installation has been done and an illegal connection has been done. The choice of the CT is based on current transducers and the voltage divider resistors for the voltage channel depend on the manufacturer and current range required for energy measurements (Hou & Yu, 2011).

2.5 Hall-effect sensor

Hall-effect is the production of a transverse voltage in a current-carrying conductor (usually a semiconductor) in a magnetic field (Horowitz, 1989). Hall-effect sensors are capable of measuring a very large current but have limitations in cost, size, linearity and temperature performance. The offset and temperature drift are dependent on the Hall element and the amplifier (Friedrich & Kunze, 2000). The push-pull amplifier drives a nulling coil. This results

in sensors always operating at or near zero magnetic flux, eliminating dependence on the linearity of the core and hall generator (Drafts, 2004).

Shahrara (2011) utilised NNC–30GFP (the NNC series from LEM Co.) current transducer to design a wireless energy meter based on the ATmega32 AVR microcontroller and whose block diagram is shown in Figure 2.4. Two full bridge rectifiers are used after the voltage and current transducers. This set-up has the disadvantage of voltage drops across the diodes which introduce errors especially at low signal values. Two Zero Cross Detectors in the current and voltage channels were used for determining the power factor.

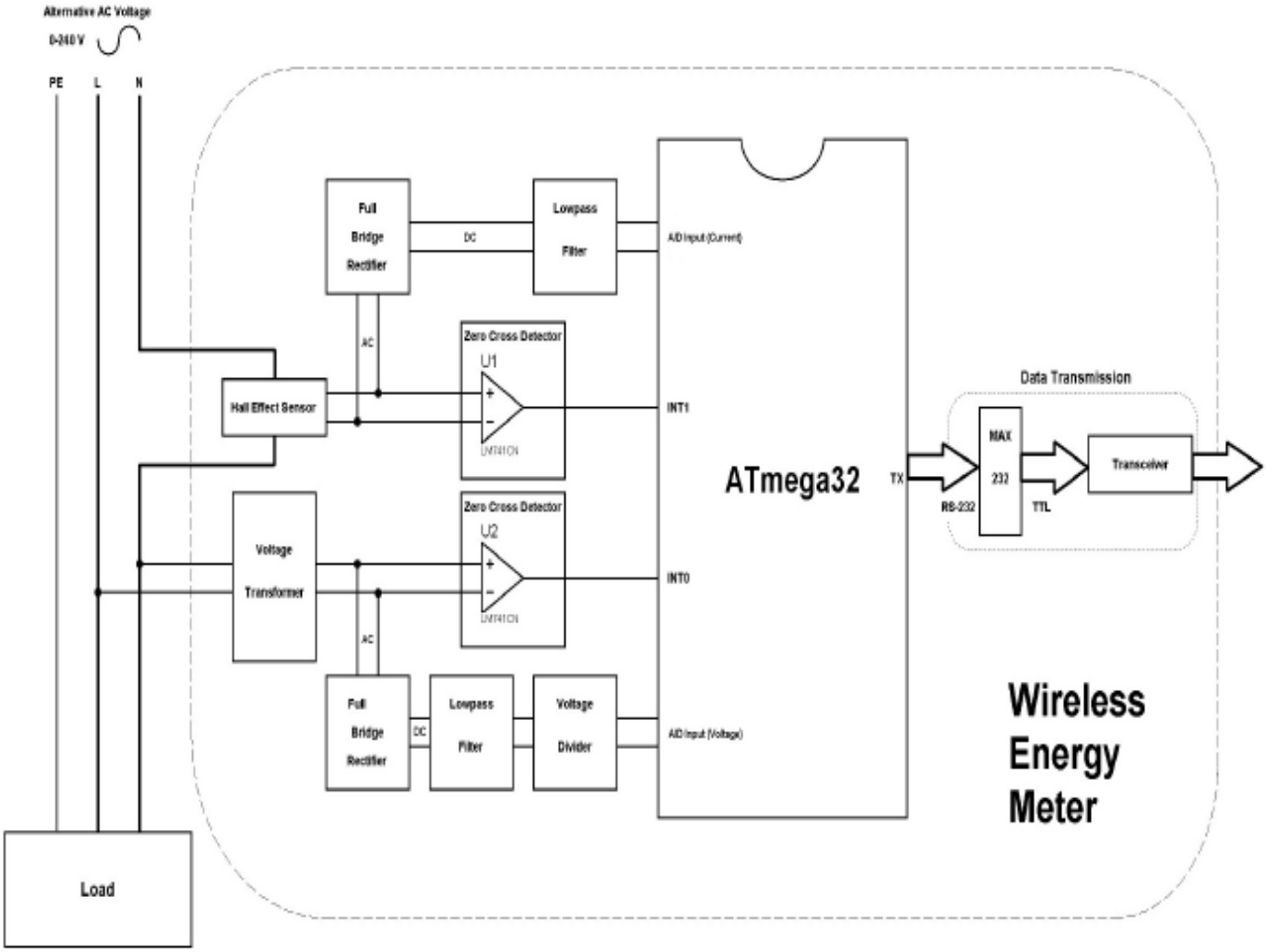

Figure 2.4: Electrical energy meter using a Hall-effect sensor (Shahrara, 2011).

However, the problem with this kind of arrangement is that for small signals, a considerable voltage drop across the diodes contributes to inaccuracies in the acquired signals and ultimately to the overall accuracy of the electrical energy meter.

2.6 Rogowski coil

A simple Rogowski coil is an air-cored inductor which has a mutual inductance with the conductor carrying the primary current (Ripka, 2004). Precise Rogowski coils have both magnetic and electrostatic shielding to suppress interference and the electromotive force (emf) induced in a rectangular air-core Rogowski coil is given by equation 2.1.

$$e.m.f = M\frac{di}{dt} \tag{2.1}$$

where,

$\frac{di}{dt}$ is the rate of change of current and M is the mutual inductance.

It relies on measuring the magnetic field and therefore makes this type of coil more susceptible to external magnetic field interference when compared with the CT (Koon, 1999). Rogowski coils with digital integrator are used for power meters in the USA (Ripka, 2004).

2.7 Ferromagnetism

The study of magnetism in amorphous materials began with the discovery of ferromagnetism in a glassy material, $Fe_{83}P_{10}C_{7,}$ produced by quenching from a melt (Elliot, 1990). Iron, Nickel and Cobalt are the only ferromagnetic metals at room temperature. All ferromagnets have Curie temperature T_c (about 1043 K for iron), above which the ferromagnetic phase is transformed into a paramagnetic one as a result of thermal agitation (Kittel, 1986). Some of the important technological applications of amorphous materials are based on Iron, Nickel-Iron and Cobalt (McCurrie, 1994).

2.7.1 Magneto-resistive sensors

Magneto-resistance is the property of a material that results in a change of resistance when exposed to a magnetic field. An Anisotropic Magneto-Resistive (AMR) sensor is made by depositing a very thin film of Permalloy (19% Fe and 81% Ni) onto a substrate (metals, ceramics or polymers). When a magnetic field is applied to the film, the magnetic domains "swing" round and the electrical resistance changes by around 2-3%.

The linear characteristics of the AMR resistor is achieved by the use of the barber pole structure in which the current is forced to flow in a direction 45˚ with respect to the magnetic field (Hübschmann and Schneider, 1996). GMR sensors are known to detect weak magnetic fields and are therefore utilized in many biomedical and industrial applications. GMR sensors (for example, Philips KMZ) consist of patterned NiFe thin film structures in a Wheatstone bridge configuration equipped with barber pole structures for output linearization (Hauser *et al*., 2006).

Figure 2.5 shows a schematic diagram of an NT Series AMR sensor manufactured by F.W. Bell.

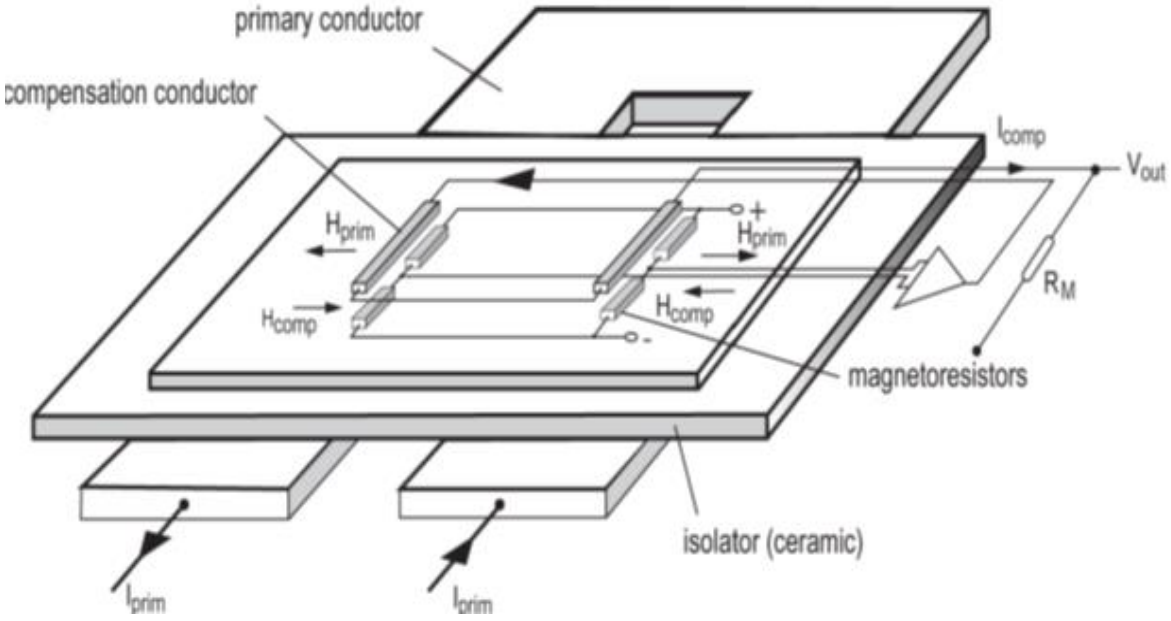

Figure 2.5: Schematic diagram of an AMR sensor (Friedrich *et al.*, 1999).

The basic resistance of the AMR resistor (R_0) is 1.7 kΩ which will change by an amount dR given by;

$$dR = R_O\left(\Delta R/R\right)\sin\alpha\left(1-\sin^2\alpha\right)^{0.5} \qquad (2.2)$$

where,

$(\Delta R/R)$ is set by the properties of the material and α is the angle between the current flow and the resultant field (Mason, 2003).

The NT series current sensors have a high linearity (0.1%) and low temperature sensitivity, an output voltage $V_{out} = \pm 2.5V$ at a nominal current $\pm I_{PN}$, a basic high accuracy of $\pm 0.3\%$ I_{PN} and uses a surface area of $2.6cm^2$ on the PCB (Friedrich *et al.*, 1999). The sensor is only sensitive to measured current through the primary bus bar.

To expand the current range of AMR sensors, a very clever and cost-effective solution for the measurement of high currents, especially in series application was presented at PCIM'99 in Nuremberg, Germany, where it drew considerable attention (Friedrich & Kunze, 2000). In this case, it was a current sensor placed into a slot in a 200A copper bus bar.

2.7.2 Comparison of current sensors

There are various current sensors available in the market but limitations dictate their applications as shown in Table 2.1 (Ziegler *et al.*, 2009).

Table 2.1 Performance comparison of current sensor

Types of sensor	Performance						
	Band width	DC capable	Accuracy	Thermal drift	Isolated	Range	Power loss
Shunt resistor							
• Coaxial	MHz	Yes	0.1%-2%	25-300	No	kA	W-kW
• SMD	kHz-MHz					mA-A	mW-W
Copper Trace	kHz	Yes	0.5%-5%	50-200	No	A-kA	mW
Current Transformer	kHz-MHz	No	0.1%-1%	<100	Yes	A-kA	mW
Rowgoski	kHz- MHz	No	0.2%-5%	50-300	Yes	A-MA	mW
Hall Effect (Open loop, Core-less)	kHz	Yes	0.5%-5%	50-1000	Yes	A-kA	mW
Fluxgate	kHz	Yes	0.001-0.5%	<50	Yes	mA-kA	mW-W
AMR Effect (Closed loop Core-less)	kHz	Yes	0.5%-2%	100-200	Yes	A	mW
Core-less, Open loop (GMR, AMR, Hall-effect)	kHz	Yes	1%-10%	200-1000	Yes	mA-kA	mW
Fiber Optic Current Sensor	kHz-MHz	Yes	0.1%-1%	<100	Yes	kA-MA	W

The choice of the current sensor generally depends on the application. From the Table, the most common current sensors in electrical energy meters are found among the top five in the table. The bottom four are not common despite their high accuracies. The size, cost, accuracy and availability are some of the factors considered when making a choice of an application. Often, the engineer will face a trade-off between cost, bandwidth, power loss, and accuracy (Ziegler *et al.*, 2009).

2.7.3 Related research works and gaps

Electronic sensor market has experienced a rapid growth in recent years, driven by the Internet of Things (IoT). Sensors of various types are employed in multiple domains to sense and collect data, assisting in improving the production efficiency and facilitating our lives (Yan *et al*., 2022). Most of the smart sensors required in smart living are in the field of spintronics. Based on distinct underlying mechanisms, spintronic sensors are normally categorized into Anisotropic Magneto Resistance (AMR), Giant Magneto-Resistance (GMR), and Tunneling Magneto-Resistance (TMR) sensors (Yan *et al*., 2022. Test results from Tunneling Magneto-Resistance TMR31 current sensor showed a linear relationship between its output voltage and current flowing through it with a sensitivity of 15.5 mV/A (Enrique *et al*., 2017).

One of the factors that affect the choice of current sensors is cost and this has made it rare to carry out research using spintronic sensors. A large research gap exists in the application of the AMR current sensor for electrical energy metering and hence the need for this research.

2.8 Operation of electrical energy meter

If $v(t) = V_m \sin \omega t$ and $i(t) = I_m \sin(\omega t + \Phi)$ are the respective instantaneous values of the voltage and current, then the instantaneous power $p(t)$ consumed by the load is given in equation 2.3 (Muñoz *et al*., 2009);

$$p(t) = v(t) \times i(t) = V_m I_m \sin \omega t \times \sin(\omega t + \Phi) \quad (2.3)$$

where,

V_m and I_m are the respective maximum voltage and current values,

ω is the angular velocity in rad / s,

t is time in seconds and

Φ is the phase angle between voltage and current.

The active power, P over a time, T corresponds to the average value of $p(t)$ as given by equation 2.4 (Muñoz e*t al.*, 2009);

$$P = \frac{1}{T} \int_0^T p(t)dt \quad (2.4)$$

The average power which is equal to active power dissipated in the load is given by;

$$P = VI \cos \Phi \quad (2.5)$$

where,

V and I are the respective RMS values of the voltage and current and,

Φ is the phase angle between the voltage and current.

Figure 2.6 shows a power triangle that illustrates the above terms.

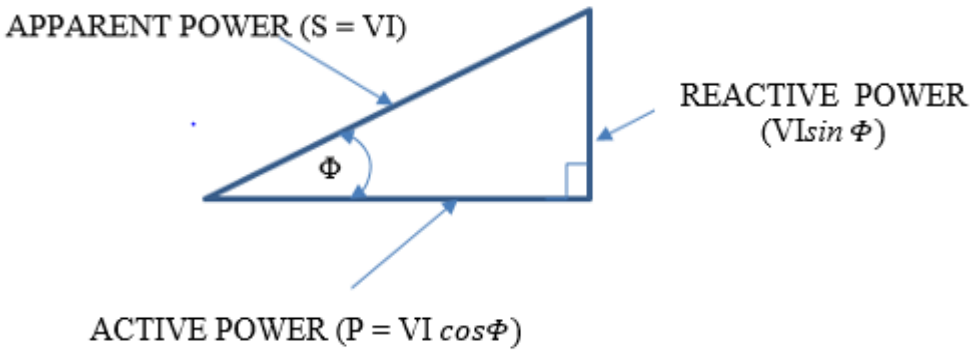

Figure 2.6: Power triangle (Nayak, 2013)

The RMS values of voltage and current in equation 5 over a period T are calculated using equations 2.6 and 2.7 respectively (Pinto e*t al.*, 2006).

$$V = (\tfrac{1}{T}\int_0^T v^2(t)dt)^{\frac{1}{2}} \tag{2.6}$$

$$I = (\tfrac{1}{T}\int_0^T i^2(t)dt)^{\frac{1}{2}} \tag{2.7}$$

The apparent power, S (Volt-Amperes) and power factor (pf) are given by equations 2.8 and 2.9, respectively;

$$S = VI \tag{2.8}$$

$$pf = \frac{P}{S} = \cos\Phi \tag{2.9}$$

The electrical energy supplied to the load over a time period, T is given by equation 2.10.

$$E = \int_0^T p(t)dt \tag{2.10}$$

2.8.1 Single-phase induction electrical energy meter

In a single phase induction energy meter, the voltage coil is connected across the mains and the current coil carries the load current. The rotating element is usually an aluminium disc whose spindle is supported by bearings at both ends. The electrical energy units consumed are registered through a worm and gear mechanism by a mechanical counter which can be read directly in kilowatt-hours (Jones, 1987).

The flux densities due to the voltage and current coils may be obtained using the Biot and Savart law. If the law is applied to an induction type energy meter, the flux density (B_{cc}) due to the current through the current coil is given by equation 2.11 (Megraw *et al.*, 2002),

$$B_{cc} = \frac{\mu_0 N_{cc} I r_{cc}^2}{2\left(x_{cc}^2 + r_{cc}^2\right)^{3/2}} \tag{2.11}$$

where,

$\mu_0 = 4\pi \times 10^{-7} A/M$, N_{cc} = number of circular loops, I = current through coil,

r_{cc} = radius of the coil and x_{cc} = distance from coil to disk.

The flux density B_v due to the voltage across the voltage coil is given by;

$$B_v = \frac{\mu_0 N_{vc} \left(\frac{V}{R_{coil}} \right) r_{vc}^2}{2\left(x_{vc}^{\ 2} + r_{vc}^2 \right)^{3/2}} \tag{2.12}$$

where,

N_{vc} = number of circular loops, V = voltage across voltage coil,

R_{coil} = resistance of voltage coil, r_{vc} = radius of the coil and

x_{vc} = distance from voltage coil to disk.

The mathematical model for the induction-type meter is given by equation 2.13 (Megraw *et al.*, 2002).

$$Energy = k \int \frac{\mu_0 N_{cc} I r_{cc}}{(x_{cc} + r_{cc})^{3/2}} r_{disk} \frac{1}{R_{Disk}} \frac{d}{dt} \iint \frac{N_{vc} \left(\frac{V}{R_{coil}} \right) r_{vc}^{\ 2}}{\left(x_{vc}^{\ 2} + r_{vc}^{\ 2} \right)} dA dt \tag{2.13}$$

where,

k = a measurement constant, r_{disk} = radius of disk and R_{Disk} = resistance of disk.

The electrical energy consumed by the load is related to the torque τ on the disk by;

$$Energy = k \int \tau dt \tag{2.14}$$

From equation (2.13), it is seen that electrical energy is directly proportional to the product of voltage (V) and current (I) supplied to the load. This is expected since energy is the current multiplied by potential difference, all integrated with respect to time (Megraw *et al.*, 2002).

2.8.2 Electronic energy meters

The digital meter relies on a process called analog-to-digital conversion (Collins, 1999). Electronic solutions are difficult to tamper with and offer superior accuracy with higher functionality than their electromechanical predecessors which can't achieve the dynamic range and accuracy of lower cost electronic meters with as low as ±0.1% accuracy. Each 0.1% improvement in meter resolution can make a significant impact on revenues for the utility (Kaplan, 2002). The new microcontroller technology allows designers to build energy meters that are competitive in price with traditional devices while maintaining the required IEC 1036 Class 1 accuracy of ± 1% for domestic applications. Microcontrollers also allow the easy incorporation of added features, such as RMS voltage, current and peak demand as local electric utility companies desire to implement them (Chattopadhyay, 2005).

2.9 Signal processing

The ADC takes samples or "snap shots" of the analogue signals at discrete instances of time. The discrete time signals are in turn converted to numeric values by the Analogue to Digital Converters (ADC). Once the analogue signals are in the numeric or digital format, digital circuits (e.g. microprocessors) can easily and reliably process them (Collins, 1999). In one of the single phase digital energy meters based on the ADE7755 energy metering IC (Daigle, 1999), two ADCs digitize the voltage signals from the current and voltage transducers at a selected sampling rate. If $v(t) = V_m \cos(\omega t)$ and $i(t) = I_m \cos(\omega t)$, then the equation for the instantaneous real power signal for unity power factor is given by:

$$p(t) = v(t) \times i(t) \tag{2.15}$$

The output frequency is proportional to the average real power which can in turn be accumulated to generate real energy information (Daigle, 1999).

Electrical power is the product of voltage and current. If repeated measurements of both instantaneous voltage v_{i_k} and current i_{i_k} are made and a total of their products over time accumulated, the average power and energy consumed for N samples at a sampling rate F_s may be obtained from equations 16 and 17 respectively (Chattopadhyay, 2005).

$$P_{average}(watts) = \frac{1}{N} \sum_{k=1}^{N} V_{i_k} I_{i_k} \tag{2.16}$$

$$E_{consumed}(watt\,\mathrm{sec}onds) = \frac{\frac{1}{N} \sum_{k=1}^{N} V_{i_k} I_{i_k}}{F_s} \tag{2.17}$$

Instantaneous sampling does not directly use power factor. The value of the phase angle is essentially embedded in the instantaneous voltage and current measurements (Chattopadhyay, 2005) as in equation 2.18;

$$P_{active} = \frac{1}{T} \int_0^T v(t) \times i(t) dt = V \times I \times cos\Phi \tag{2.18}$$

The discrete time equivalent is given by;

$$P_{active} = \frac{1}{N} \sum_{n=0}^{N-1} v_n \times i_n \tag{2.19}$$

where,

$v(n)$ and $i(n)$ are the respective sampled voltage and current values and

N is the number of samples.

The integral calculations for the voltage and current presented in equations 2.6 and 2.7 are replaced by digital summations, according to the signal sampling rate. The RMS values of voltage and current are respectively obtained by expressions 2.20 and 2.21 (Pinto e*t al.*, 2006);

$$V = (\frac{1}{N}\sum_{n=1}^{N} v_n{}^2)^{\frac{1}{2}} \tag{2.20}$$

$$I = (\frac{1}{N}\sum_{n=1}^{N} i_n{}^2)^{\frac{1}{2}} \tag{2.21}$$

The apparent power S is achieved by multiplying the RMS values of voltage and current while the pf is obtained from the active and apparent power calculations using equation 9.

2.10 Microcontrollers

A microcontroller is a single Integrated Circuit (IC) containing all the circuitry of a microprocessor-based system necessary for most control applications. The main difference is that microcontrollers also incorporate on-board RAM, EEPROM (for program and data storage) and peripherals which would be externally interfaced on a microprocessor system. This arrangement simplifies the design of microcontroller systems (Beştepe, 2004). The microcontroller executes operations that allow the acquisition of the electrical signals to be measured, then executes the necessary calculations to obtain the desired parameters, and finally performs the numeric to character data transformations and place the results in the LCD. It has in-built facilities like the ADCs, EEPROM, Timer and Flash Memory that simplify the hardware (Pinto e*t al.*, 2006).

The advantage of ATmega 328 microcontroller over the other microcontrollers is that it simplifies the amount of hardware and software development needed in order to get a system running. It is open source software and can be extended by experienced programmers. ATmega 328 microcontroller has simple and clear programming environment and also a quicker writing code (Srividyadevi *et al.,* 2010).

2.11 Requirements for ADC energy metering

Energy metering requires ADCs with high resolution (e.g. 16 bits), a sampling rate of at least 2000 to 4000 samples per second - at least twice the highest frequency content of the signal.

ANSI and IEC standards specify for measurements up to the 20th harmonic (1kHz or 1.2 kHz) depending on the line frequency, low cost (the end application is particularly cost sensitive, especially in residential metering applications) and it must not consume excessive power (Collins, 1999).

2.12 The LCD screen

Usually, a 16×2 LCD (2 lines with 16 characters per line) is used to display the meter reading. It contains two registers - the data and command registers. The data register is used to send any type of data to the LCD. A command register is used to send addresses that initialize the LCD (Al-Omary *et al.*, 2011).

2.13 Automatic meter reading

Automatic Meter Reading (AMRg) system has to be cost-effective which means reducing the costs of implementation and maintenance while providing a robust and reliable performance (Arun *et al.*, 2012). It offers additional functionality including real-time readings, power outage notification, power quality monitoring and transferring that data to a central database for billing, troubleshooting and analyzing (Azasoo, 2012). A Graphical User Interface (GUI) is used to manage all Short Message Service (SMS) readings, e-billing and updating the database. GUI computes the monthly bill and notifies it to the consumer through the SMS facility (Ambedkar *et al.*, 2017).

Automated Meter Reading was introduced in North America to read difficult-to-read meters placed at inaccessible locations and hazardous-to-access meters. Metering technologies have improved over the years, from electromechanical meter to Automated Meter Reading (AMRg), Automated Meter Management (AMM) and Advanced Metering Infrastructure (AMI) (Veerabadhra, 2011).

2.14 Smart maters

A smart meter is usually an electrical energy meter that records consumption of electric energy in intervals of an hour or less and communicates that information at least daily back to the utility for monitoring and billing purposes. A smart meter differs from traditional AMRg in that it enables two-way communications with the meter (Azasoo, 2012). Prepaid metering requires the customer to make advance payment before electricity usage while postpaid metering involves payment of energy consumed after usage (Shomuiywa *et al.*, 2013). This energy metering technology is being implemented on a large scale in Kenya

2.15 DC power supply

One of the challenging aspects of solid-state meter design is the design of the power supply unit (Collins, 1999). To reduce the weight of the energy meter, a transformer-less power supply is used. Fast switching of digital circuits is usually a source of noise that causes unwanted interference on analogue signals. Therefore, to minimize interference within the Printed Circuit Board (PCB), the Radio Frequency (RF) section is placed on the opposite corner to the digital components and power supply (Gloria, 2010).

2.16 Voltage measurement

Voltage division is the most preferred way to divide down the line voltage based on Ohm's law. The output voltage V_{out} due to an input voltage V_{in} is given by equation 2.22 (Nayak, 2013);

$$V_{out} = V_{in} \times \frac{R_{11}}{R_{11}+R_{12}+R_{13}} \tag{2.22}$$

where,

V_{in} is the voltage across the three series-connected resistors.

Voltage V_{out} across resistor R_{11} becomes the input signal to the voltage channel of the energy meter. In one of the prepaid energy meters, a voltage divider is made using 1MΩ ($R_{12}+R_{13}$) and 1kΩ (R_{11}) in series (Haque *et al.*, 2011). Assuming the input voltage is 240 volts, the output voltage becomes,

$$V_{out} = 240 \times \frac{1000}{1001000} = 239.76mV \cong 240mV \tag{2.23}$$

V_{out} is then scaled up to 240 volts for power and energy computations using the software.

2.17 Calibration

Resistor R_{11} in equation 2.22 is connected in series with a binary-weighted resistor chain for attenuating the line voltage. The attenuated voltage provides varying signals for processing and display. These voltages are then compared with voltages measured by a reference meter. The chain allows the meter to be accurately calibrated using a successive approximation technique (Collins *et al*., 1999).

2.18 Comparison of performance of energy meters

The performance of energy meters for various loads is usually not known by the consumers. Tests were carried out on 11 different meters in the power quality laboratory in the Department of Electrical Engineering of the Helsinki University of Technology TKK (Espoo, Finland). The results were presented in graphical form. The results showed that the meters had average errors varying from 2% to 19% and that the meter with the 2% error was the cheapest (Liikkanen *et al*., 2009). From these results, it is possible that a consumer may unsuspectingly overpay by almost 20%. For this reason, meters should be tested against standard energy meters available at standard laboratories (KEBS in the case of Kenya).

From the study carried out in Helsinki University of Technology, there is a need to develop other new energy meters that utilize sensors manufactured using new technologies with an aim of reducing errors in energy meters. In this research, the attractive characteristics of AMR current sensor were exploited in the design of the new energy meter in an attempt to solve the underlying problems.

CHAPTER THREE

MATERIALS AND METHODS

3.1 Introduction

This study aimed at designing and fabricating a digital electrical energy meter which would display on a Liquid Crystal Display (LCD) the supply current, consumer's terminal voltage, power factor, real-time power consumption and electrical energy. The current and voltage signals were respectively derived from an AMR current sensor and supply voltage through resistive voltage division. The electrical energy meter was designed using Proteus 8 Professional software and a Printed Circuit Board (PCB) fabricated. The components were then soldered to the PCB. A code was written in C-language and stored in the Microcontroller's EEPROM for processing the signals from which the other variables were derived. The signal conditioning circuits were then tested for accuracy by displaying current and voltage on the meter's LCD. The fabricated electrical energy meter was then tested against selected meters.

3.2 Relationship between sensor output voltage and its current

It was important to carry out tests to ascertain the characteristics of the AMR current sensor and specifically determine the relationship between its output voltage and input current. Figure 3.1 shows the set-up that was used to carry out this test.

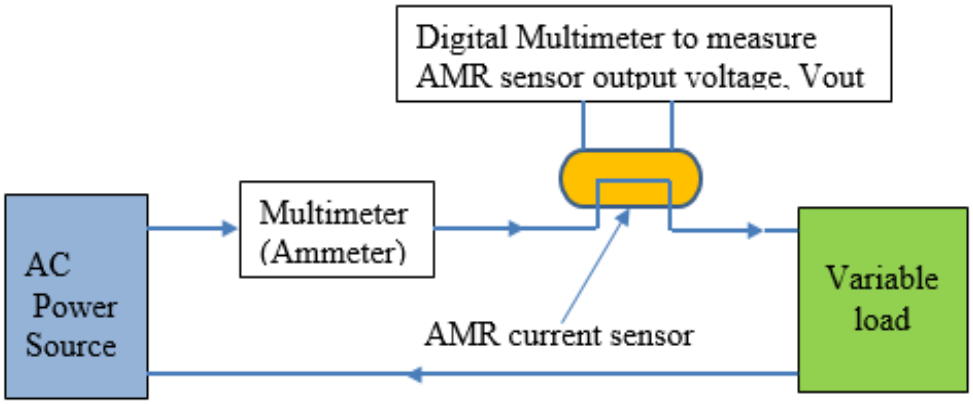

Figure 3.1: Experimental set-up for output voltage and current.

This was meant to help in assessing its suitability in electrical energy measurements. Various resistive and inductive loads (100W bulbs and 1.2M × 36W fluorescent fittings) were connected in parallel and voltages and currents recorded as in Table 3.1.

Table 3.1 Electrical loads for testing the current sensor

Electrical loads	Bulbs (W)	Fluorescent fittings (W)
L1	0	36
L2	200	0
L3	400	36
L4	400	0
L5	600	36
L6	700	36
L7	500	180
L8	1000	144
L9	1000	108
L10	1200	0
L11	1100	180

3.3 Design and Fabrication of AMR Electrical Energy Meter

It was necessary to design and fabricate a meter which could display the above variables. The design of the digital electrical energy meter was based on the conceptual block diagram in Figure 3.2 in which, the current sensor was connected in series with the electrical load. The AMR sensor output was the input to the signal conditioning circuit which outputted a suitable current signal for processing by the microcontroller. The supply voltage was connected to a successive approximation voltage divider network whose output (mV) was supplied to a voltage signal conditioning circuit. The output of the circuit was fed to the microcontroller for processing. Both voltage and current signals were separately summed up with DC voltages of +2.5V to 'lift' them above zero volts so that they would be suitable for processing by the microcontroller. This ensured that the microcontroller terminals didn't go negative.

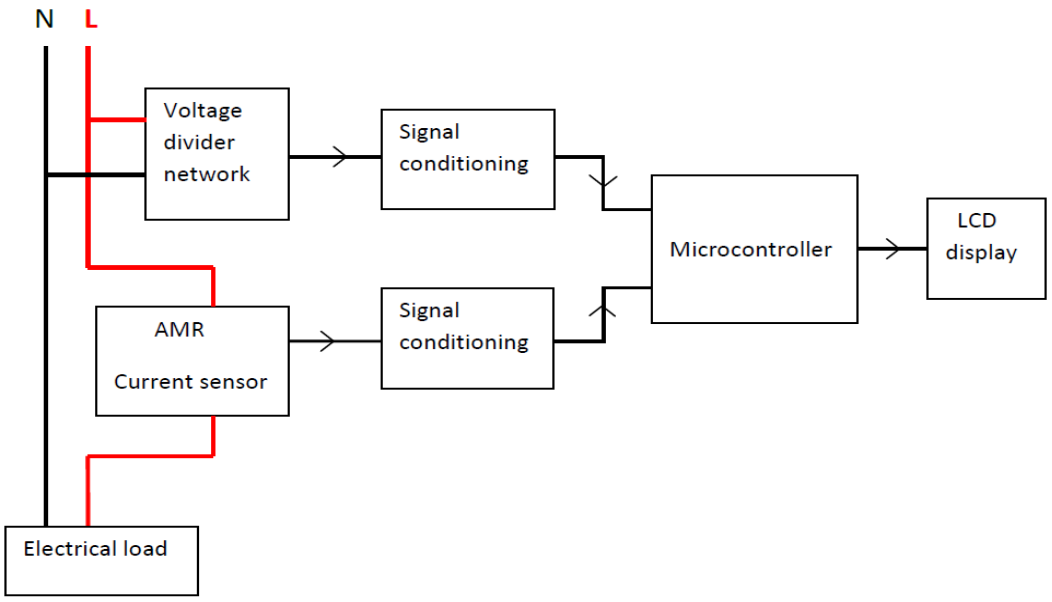

Figure 3.2: Block diagram of the designed electrical energy meter.

The power factor, power and electrical energy were derived from the voltage and current signals. The microcontroller processed all the five variables and outputted the results to the Liquid Crystal Display (LCD).

The design process was divided into hardware, fabrication and software developments. The supply voltage required for the current sensor and operation amplifiers was ±12V while that of the microcontroller and LCD was +5V. Since the design and fabrication of a suitable power supply for this purpose was quite a challenge, time-consuming and probably a full project on its own, the power supply was purchased.

3.3.1 Current signal conditioning channel

The maximum sensor current in this application was 25A (rms) and the output voltage from the sensor representing this current was 2.5V (rms). The current signal conditioning channel would have a peak-to-peak value of 7.0711V and a negative peak value of 3.5355V. If this voltage was to be applied to the input channel of the microcontroller, it would make the microcontroller input channel negative (-3.5355V).

The microcontroller does not accept negative voltages and therefore this voltage signal had to be 'lifted' positively by a dc voltage of 2.5V. The dc off-set was obtained from the 5V supply through a potential divider circuit consisting of R_{25} (30K) and R_{24} (10K) as shown in Figure 3.3.

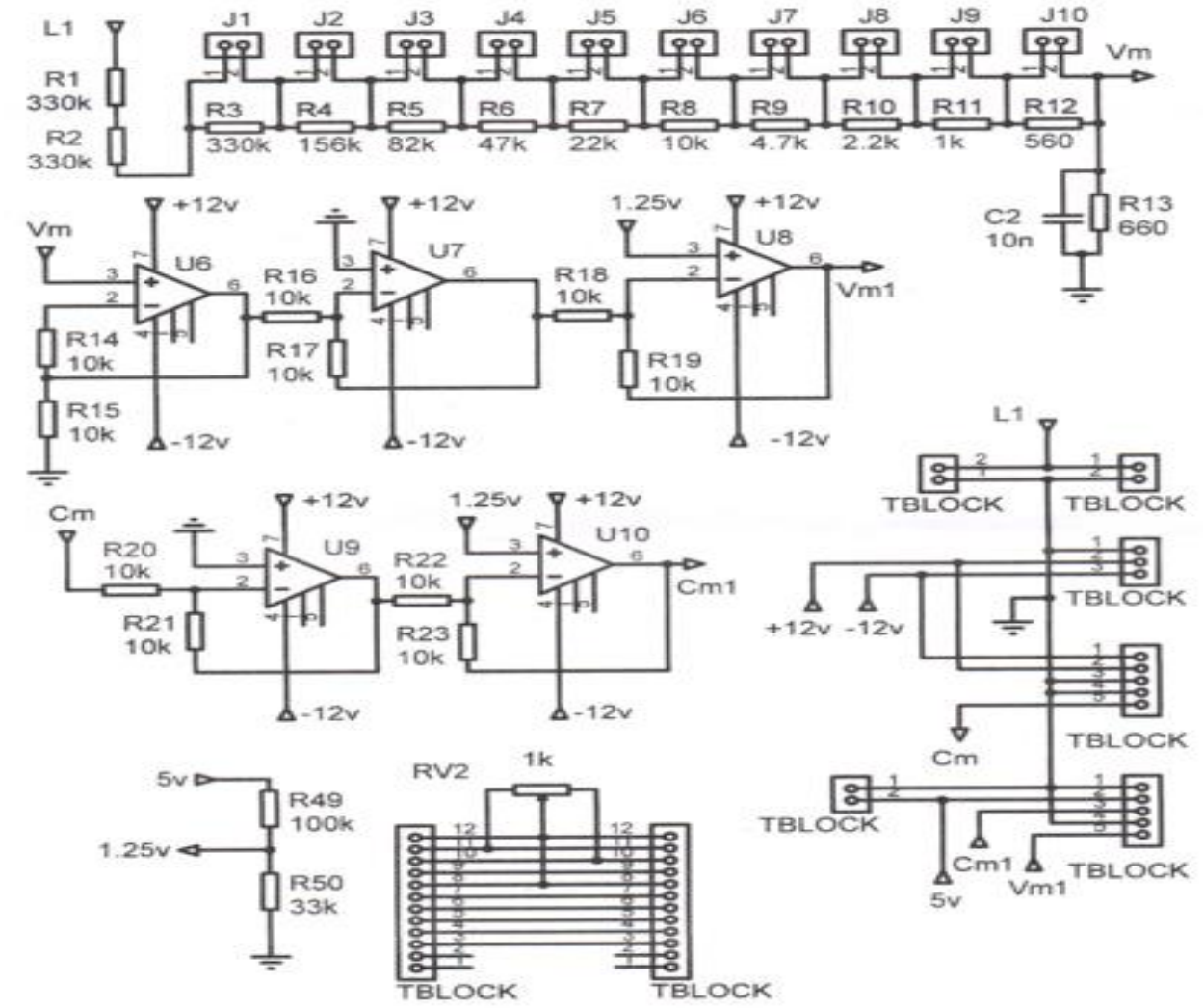

Figure 3.3: Testing schematic diagram**.**

The 1.25V (dc) potential across R_{24} was doubled (1+10K/10K) by the non-inverter (OPAMP U_5, R_7 and R_8) to give 2.5V (actual measured dc offset on the fabricated meter was 2.31V). With a rated sensor current of 25A and an output of 2.5V, the voltage at the microcontroller terminals would be $2.31 \pm \sqrt{2} \times 2.5V$ giving a maximum value of 5.8455V and a minimum of -1.2255V. This voltage would not only make the input terminals of the microcontroller negative but also exceed the microcontroller supply voltage of 5V.

Since the microcontroller does not accept negative voltages, the signal was divided by two to give 1.25V (a peak-to-peak value of 3.5355V). The maximum voltage at the input terminals of the microcontroller would be given by $2.31 \pm \sqrt{2} \times 1.25V$ (resulting to a maximum value of 4.0777V and a minimum of 0.5422V). These voltages would be within the microcontroller supply voltage of 5V and would meet the microcontroller input conditions.

In Figure 3.3, the current signal conditioning circuit consists of two unity gain buffers made up of OPAMPs U_4 and U_5 and four 10K resistors with no signal inversion. The output of the channel consists of 2.31V dc off-set and the sinusoidal signal proportional to the sensor current. The microcontroller would sample a signal with a minimum of 0.5422V and a maximum of 4.0777V. The sampled signal would have a maximum positive peak signal of $4.0777-2.31=1.7677V$ and a maximum negative peak of $0.5422-2.31=-1.7678V$. The positive and negative peaks would be equal with a common dc off-set reference of 2.31V. The negative sign was factored in the software so that the readings would be positive. The sampled data would be mapped to the range '0 to $2^{10}-1$'. The dc offset voltage of 2.31V (512 bits) and a multiplying factor of the signal by 2 were also factored in the software.

3.3.2 Voltage signal conditioning channel

It was required to reduce the supply voltage from 240V to a voltage less than 5V (peak-to-peak) at the terminals of the microcontroller. For that reason a resistive potential divider circuit was designed to give a proportional output of 0.24V (240mV) to be wired to the microcontroller input terminals. The voltage signal conditioning channel is shown in two separate sections in Figure 3.3 (resistive voltage division and voltage amplification).

For the voltage signal to be almost in the range of the current signal (Vpeak of 1.7678V), 0.24V was multiplied by $1+47K/10K=5.7$ (actual value was 5.75) using OPAMP U_1, R_1 and R_3. The peak voltage was given by $V_{peak}=\sqrt{2}\times 0.24\times 5.75=1.9516V$. This amplification also improved the signal-to-noise ratio in the voltage channel.

Using Proteus 8 Professional design software, it was possible to test these sections separately. The voltage signal was off-set by a dc voltage of 2.31V (as described in current signal conditioning) to prevent the input terminal of the microcontroller from going negative. The peak signal at the terminal of the microcontroller would be $2.31\pm 1.9516V$ (a maximum peak of 4.2616V and a minimum peak of 0.3584V). The voltage signal would rise from 2.31V to 4.2616V and fall to 0.3584V. The sampled values would be equal if both positive and negative half cycles were to be identical.

If the supply voltage was to change by ±10%, the voltage at the input terminal would be $2.31\pm\sqrt{2}\times 0.264\times 5.75=2.31\pm 2.1468V$ (a maximum peak of 4.4568V and a minimum peak

of 0.1632V. This would ensure that the maximum voltage available at the microcontroller input terminal would always be positive (this satisfied the microcontroller input signal conditions).

3.3.3 Successive approximation voltage divider network

The supply voltage to the meter was 240V. In this design, the resistor chain had 13 resistors (R_{11} through R_{23}) as shown in Figure 3.3. Resistors R_{11} and R_{12} had a resistance of 330 kΩ each while R23 had a resistance of 660Ω. The three resistors had a total resistance of 660660Ω. R_{13} had a resistance of 330 kΩ and the subsequent resistances were approximately half of their preceding values. Under normal working conditions, all resistors except R_{11}, R_{12} and R_{23} were short-circuited with zero resistance jumpers. The voltage across R_{23} (660 ohms) for a supply voltage of 240V was $V_{out} = \frac{240 \times 660}{660000 + 660} = 239.76 \cong 240\,mV$. If the resistors R_{22} through R_{13} in that order were opened, each at a time (and left open as the others were progressively opened), successive approximation voltages were obtained across R_{20} as shown in Appendix G (a). The voltages available across 660Ω would be 240V to approximately 120V (100 to 50%).

In the implemented design shown in Figure 3.6, the resistors are labelled R_1 through R_{13}. The measured resistances had variances from those in Figure 3.3. The output voltages across R_{13} (653Ω) were expressed as a percentage of the supply voltage because they varied with the supply voltage as shown in Appendix G (b). For supply voltages of 240V and 220V, the outputs across R_{13} would be 239.76mV and 219.78mV respectively (approximately 240mV and 220mV). With all the jumpers opened, the outputs were 50.5% of the supply voltage (121.2mV and 111.1mV for inputs of 240V and 220V respectively). The switching order to get the outputs (mV) across R_{13} was from jumpers J_{10} through J_1.

3.3.4 Anti-aliasing circuit

Anti-aliasing circuit was necessary at the input terminals of the microcontroller to prevent possible distortion due to sampling by the ADC. A simple Resistor-Capacitor (R-C) Low Pass Filter (LPF) with a roll-off of 20dBs/decade was designed and constructed to attenuate any possible high frequency voltage signals which would be present. In normal operation, the LPF is made up of series resistors (R_1 and R_2 (660 kΩ)) and R_{13} (660 Ω) in parallel with capacitor C_1 (10*nF*) as in Figure 3.4.

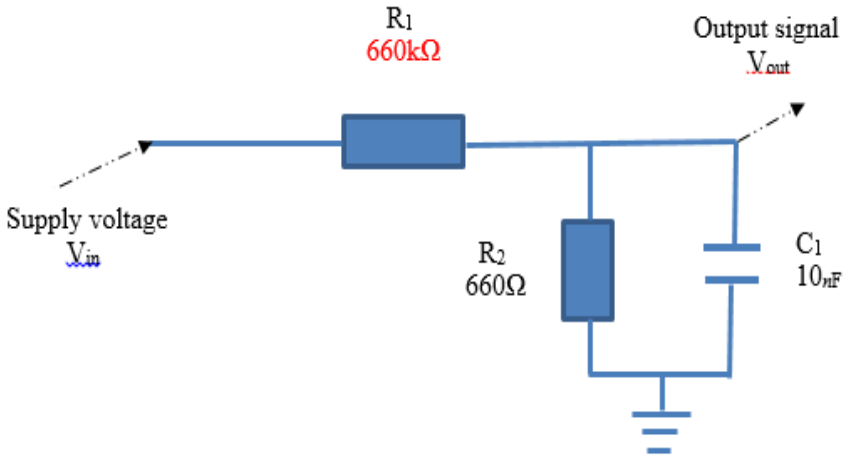

Figure 3.4: Resistor-capacitor LPF filter

Figure 3.5 shows the gain/frequency response of the R-C LPF. The "0" and "-3dB" points are at approximately 1 kHz and 24 kHz respectively.

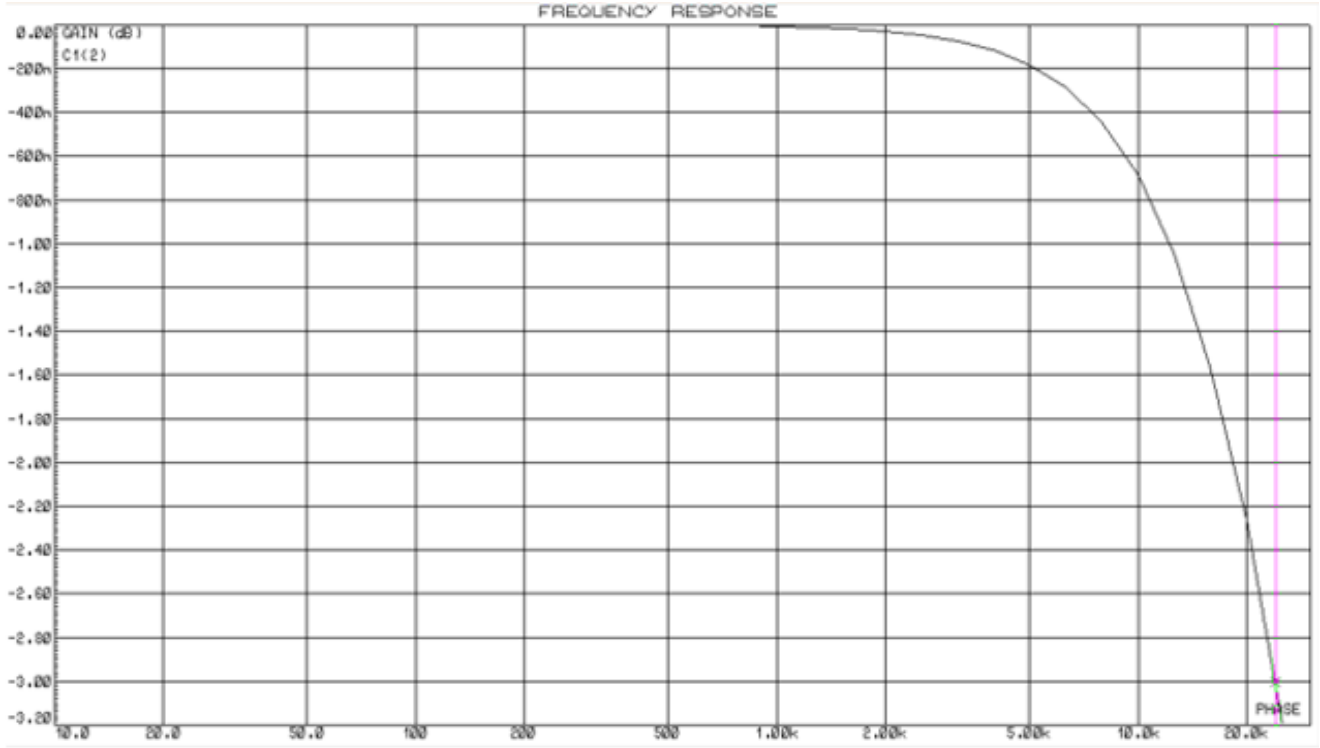

Gain (dB)

Frequency (kHz-log scale)

Figure 3.5: Gain-frequency response of LPF filter

Electrical and electronic loads cause high frequency harmonic currents to flow in metering equipment. High frequency signals should therefore be included in metering. IEC1036 standard requires that in electrical energy metering, sampling should include signals up to the 20th harmonic (20×50 Hz = 1 kHz). Based on this and in obedience to Shannon's Theorem,

(sampling frequency should be at least twice the highest frequency signal available), the minimum sampling frequency was 2 kHz and was used in this application.

It is seen from the graph that signals up to 1 kHz (20^{th} harmonic) would pass through the filter and appear at the input of the microcontroller for sampling. It was deduced from the graph that high frequency signals above 50 Hz generated by electrical devices like rectifiers and welding machines could be adequately captured by this filter as recommended by IEC1036 standards.

3.3.5 Fabrication

The fabrication involved etching the PCB and the implementation of the circuit shown in Figure 3.6 designed using Proteus 8 Professional Software. Figure 3.3 shows the main circuits that were tested before mounting and soldering the components on the PCB. This made it necessary to test all the sections of the circuit to ascertain that they were all operating according to the design. The AMR current sensor, Arduino micro Microcontroller and the LCD are not shown. The complete schematic diagram used in the fabrication is shown in Figure 3.6. It includes all the components used in the design and fabrication. This circuit was tested before the fabrication and it was found to be operating according to the design.

(a) AMR schematic diagram

The schematic circuit diagram of the designed and fabricated AMR electrical energy meter is shown in Figure 3.6. The load was connected in series with the AMR current sensor and therefore the sensor current was the same as the load current. The AMR current sensor was rated at 25A with a proportional maximum output voltage of 2.5V (RMS). This voltage was divided by 2 through R_{26} and R_{27} to give 1.25V which was the input to the current signal conditioning section. The block has two unity gain amplifiers comprising OPAMPs U_3 and U_4, resistors R_{18}, R_{19}, R_{20} and R_{21}. The dc off-set of +1.25V was provided by voltage division using R_{22} and R_{23}.The off-set was doubled ($1+R_{21}/R_{20}$) through the non-inverting amplifier comprising OPAMP U_4, R_{21} and R_{20} to give +2.5V (measured dc off-set was +2.31V). The sinusoidal input current signal was to be 'lifted' by +2.31V so that the input terminals of the microcontroller would always remain positive for the rated load and sensor current.

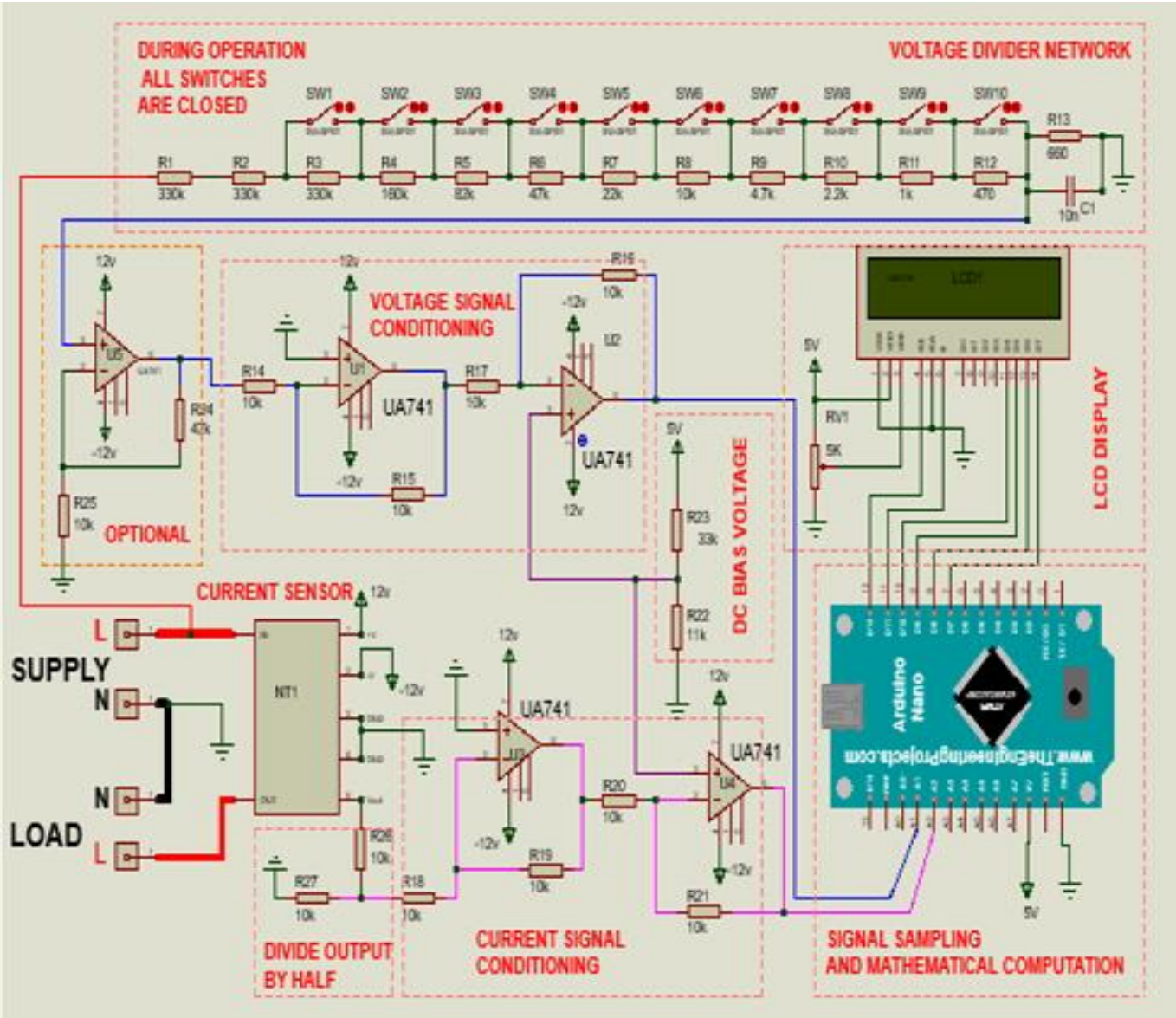

Figure 3.6: Schematic diagram of the constructed electrical energy meter.

The meter's voltage signal was proportional to the supply voltage and was derived through voltage division (2×330kΩ and 660Ω). For a normal supply of 240V, the output voltage across 660Ω would be 240V×660/(2×330000+660) = 239.76mV (240mV). To obtain a voltage close to the one in the current channel, the 240mV was multiplied by 5.7 (1+47 kΩ/10 kΩ) using the non-inverting amplifier comprising OPAMP U_5, resistor R_{24} (47 kΩ) and R_{25} (10 kΩ). The actual value was 5.75 and therefore the peak value was 5.75×√2×240mV = 1.952V.

The multiplication factor of 5.75 and 1000 (to convert 240mV to 240V) was factored through software. As in the case of the current channel, the voltage signal was off-set by a dc voltage of +2.31V to ensure that the input terminal of the microcontroller always remained positive for all values of the supply voltage.

(b) PCB layouts

Some of the considerations made in the hardware design included correct component sizes, component layout and mounting, lead sizes, hole-positioning, drilling of holes, analogue and digital grounds. It was necessary in some cases (missing components in Proteus library) to carry out size measurements on the actual components and transfer them to the board**.**

Proteus 8 Professional software was used to draw the schematic diagram shown in Figure 3.6 and produce the PCB layouts shown in Plates 3.1 and 3.2. The layouts on Plate 3.1 were physically examined for any short-circuits before printing on toner transfer paper using a laser printer. The printed layout was then physically transferred to the copper plated board by applying heat (from an iron box) on the paper placed on copper board. The board was then immersed into a solution of Hydrogen Peroxide and Hydrochloric acid at a ratio of 2:1 (Hydrogen Peroxide: Hydrochloric acid) to remove the copper uncovered by the toner. The green. and blue areas show the copper that remained after etching. The conducting paths (green and blue) have end terminations. The hardware components were then soldered on the etched board. Plate 3.2 shows the conducting paths and components for the top and bottom layers.

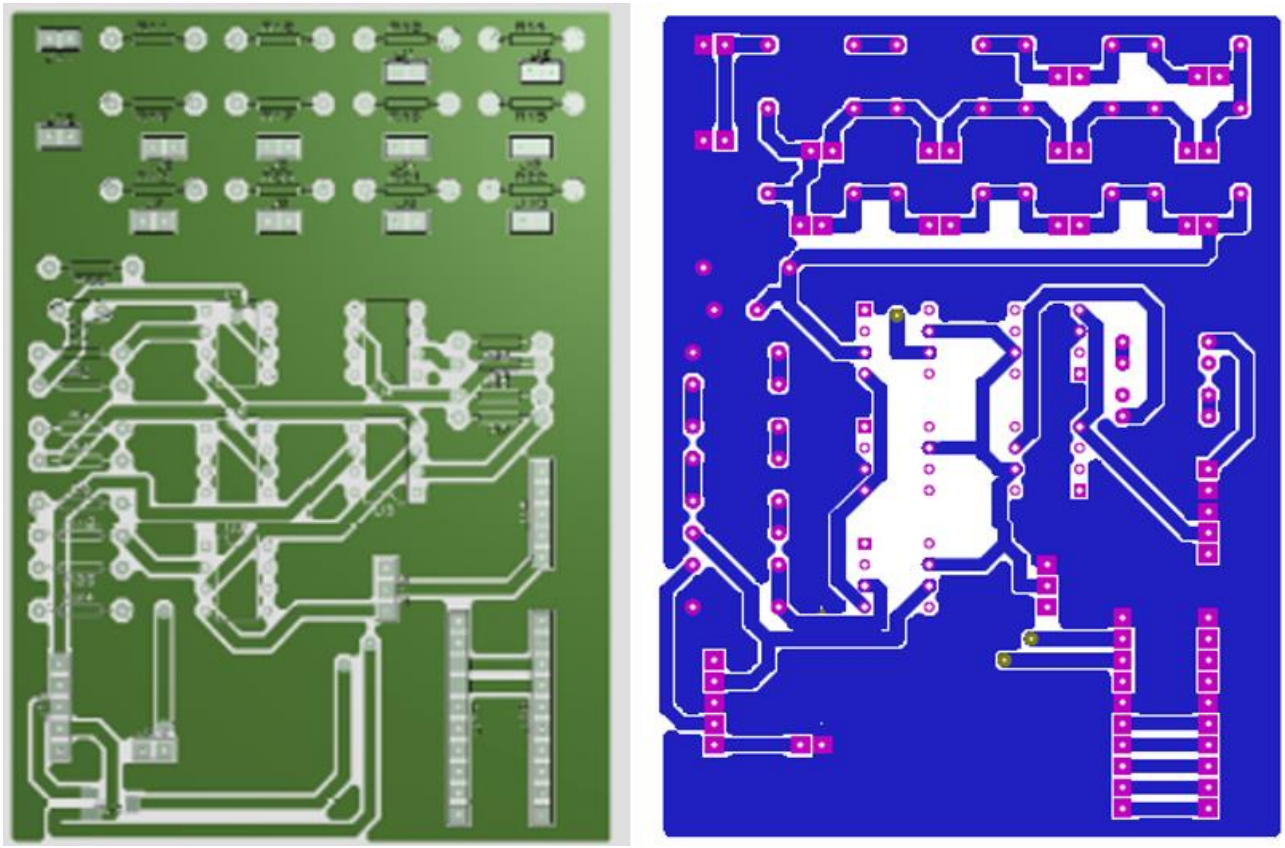

(a) PCB top layer. (b) PCB bottom layer.

Plate 3.1: PCB top and bottom layers without components.

After thorough inspection of the etched board, the microcontroller and the LCD were assembled on the PCB top layout side. The top layer shows the side of the PCB where the components were soldered though there were no components assembled on the bottom layer. The green colour in Plate 3.1 (a) signifies the parts of the copper-plated board which remained with copper after etching while the blue colour in Plate 3.1 (b) represents copper which was not removed after etching. The large green and blue surface areas represent the ground. The other green or blue colours represent the signal paths or dc supply lines to the components.

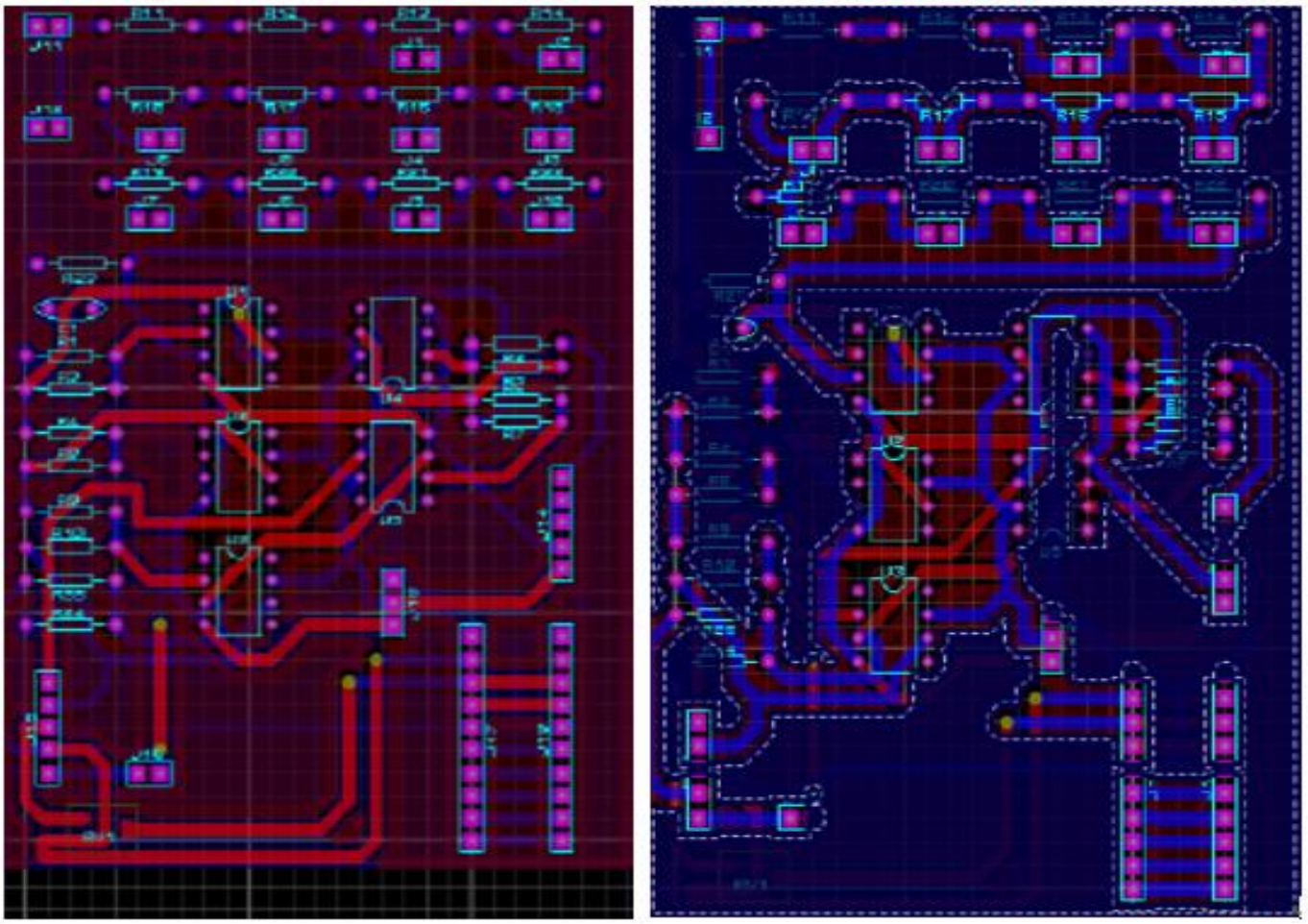

(a) PCB top layer (b) PCB bottom layer

Plate 3.2: PCB top and bottom layers with a few components

Plate 3.2 shows the top and bottom layers with components assembled on the etched copper board. The AMR current sensor, LCD and Arduino Micro Microcontroller are not shown for clarity of the conducting paths. The Arduino Micro was mounted on the top layer using sticking glue while the LCD was mounted above the Micro using studs mounted on the PCB board. The power supply was then assembled near the PCB and connections to various components made.

The electrical connections to Arduino were provided through a connector block shown at the bottom right of the top and bottom layers. After each component assembly and/or soldering, the board was physically checked for any short-circuits.

3.3.6 Development of C-code program

The flow diagram of the developed C-code listed in Appendix A is shown in Figure 3.7. The microcontroller which is the heart of the digital energy meter stored the C- code in an EEPROM, sampled the supply voltage and load current signals, processed them and displayed current, voltage, power factor, 'real-time' power consumption and cumulative electrical energy consumed on a 16 2 LCD.

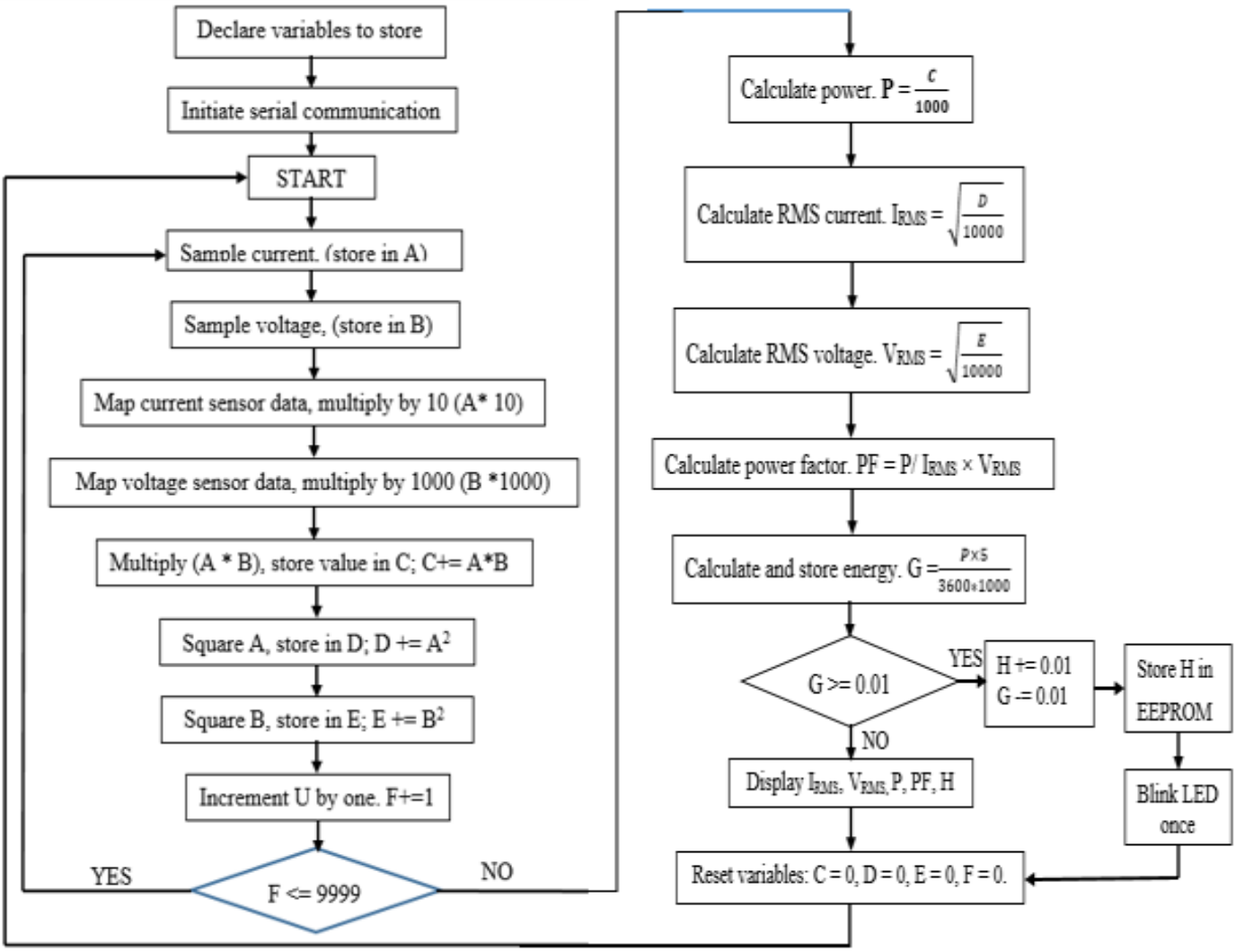

Figure 3.7: Flow diagram of AMR energy meter.

As shown in Figure 3.7, the variables were declared before initializing the program. The current and voltage signals were sampled, converted to digital and stored as variables A and B, respectively. The contents in A were multiplied by 10 to map voltage signal to current. The

contents in B were multiplied by 1000 to map mV to Volts. The two sets of data (A and B) were multiplied to obtain instantaneous power and added to the stored sum as variable C. Only the new sum of the instantaneous power was stored in the memory. This was important because it saved memory space and improved the processing speed. The final value in the memory gave the total power consumed during the 10,000 samples. Each value in A and B was squared to obtain squares of the current (A^2) and voltage (B^2). The squared values were then stored as variables D and E, respectively. The process was repeated for the second set of sampled data and the process continued until 10,000 sets of sampled data had been taken (10,000 sets of data for both current and voltage). After every set of samples, the sampling counter was incremented by 1.

From Figure 3.7, the square roots of the means of the squares of the instantaneous values of current and voltage for the 10,000 samples (variables D and E) were computed to obtain I_{RMS} and V_{RMS}, respectively. The apparent power (Volt-amperes) was computed as the product of I_{RMS} and V_{RMS} whereas the power factor was computed as the ratio of the active power to the apparent power as illustrated in Figure 2.6.

The electrical energy consumed by the load in 5 seconds, (time for 10,000 samples) was computed and stored as variable G. This was repeated until value G was equal to or greater than 0.01 kWh when the electrical energy was incremented by 0.01 kWh and stored as variable H. Theme value was subtracted from G to avoid double entry in the following count. The new value of electrical energy was stored in the EEPROM until it was next incremented. After incrementing H by 0.01 kWh, an LED blinked once to indicate that 0.01 units had been consumed. Every time G was incremented by 0.01 kWh, the LCD displayed the RMS values of current, voltage, power consumed, pf and electrical energy.

3.3.7 Effects of delayed sampling

The microcontroller could not sample the input current and voltage signals to the Analogue to Digital Converter (ADC) channels at exactly the same time. This meant that only one signal to an input channel could be sampled at a time. When the current signal was sampled first followed by the voltage signal, it was found that the sampling time for each signal was 104μs. This was the ADC conversion time for the current signal. If the sinusoidal current and voltage signals had an amplitude of 1A and 1V, respectively, the instantaneous values would be given by $i = 1\sin\omega t$ and $v = 1\sin(w(t + t_d))$.

At $t=0; i=0$, $v=1\sin(100\pi(0+0.000104\times180\div\pi))=0.03267 volts$. This showed that if the sampling was ideal (same time ADC sampling), the sampled values would be equal but due to the delay, this was not possible. Table 3.2 shows values of *i* and *v* over half a cycle and Figure 3.8 shows the effects of sampling *v* after a delay of 112μ*s* over a full cycle.

Table 3.2 Sampling of current and voltage at different times

Time (ms)	$i=1\sin wt(A)$	$i=1\sin(w(t+t_d))(V)$
0	0.0	0.033
2	0.58	0.614
3	0.809	0.828
4	0.951	0.961
5	1.0	0.999
6	0.951	0.941
7	0.809	0.789
8	0.588	0.561
10	0.0	-0.033

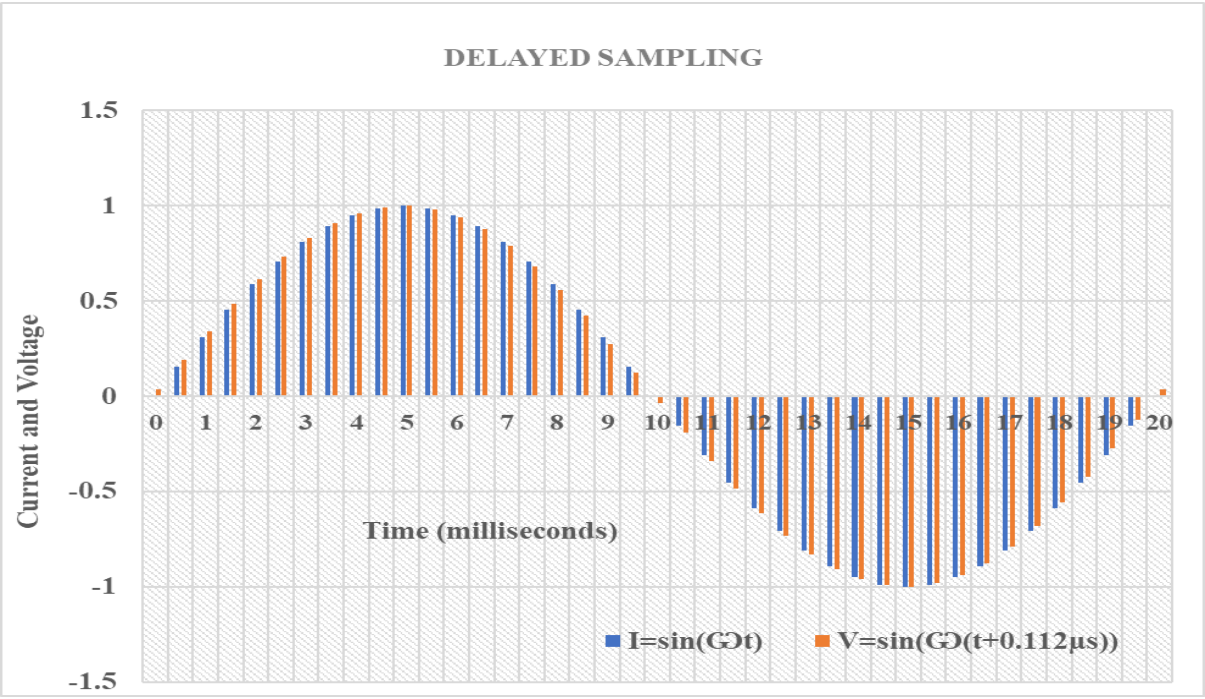

Figure 3.8: Effect of delayed sampling.

It was noted from Figure 3.8 that the instantaneous values of current (*i*) and voltage (*v*) increased sinusoidally from zero to maximum in approximately 5ms (0 to 90º) though current

values were slightly lower than those of voltage but was vice versa after 5ms until 10ms (90º to 180º). Computations of current, voltage, power, power factor and electrical energy for delayed and fundamental voltage conditions using EXCEL showed no significant differences in the results. A delay of 112µs between the two signals was not expected to make a significant difference in the computed variables when the microcontroller was used to sample and process the signals.

The microcontroller's processor speed was 16 MHz, therefore the ADC clock frequency was 16 MHz/128 = 125 kHz (128 was the default division factor). It took 14 clock cycles to complete an ADC conversion. Hence, the time taken to complete one ADC conversion was $14 \times \frac{1}{125000} = 112\ \mu s$ (equivalent to a delay angle of 2.016º). It also took 1 clock cycle (8 μs) to reset from one ADC sampling and start the following ADC sampling. One set of current and voltage samples was therefore to take a time of 232 μs.

3.3.8 Determination of sampling frequency

The results of pilot data from EXCEL revealed that a large sample size produced higher accuracies than a low sample size in the computations of current, voltage, power factor, consumed power and electrical energy. Based on those computed results, a figure of 10,000 samples for each signal channel was used. To determine the maximum number of samples per cycle, 10,000 samples were taken and processed for current and voltage, respectively. These tasks took 4800 *ms* and the following calculations were carried out;

Time taken by one pair of samples = $4800\ \text{ms}/10000$ = 0.480 *ms* (480μs)

Number of samples in 1 complete cycle = $20/0.480 = 41.7$ samples

Sampling frequency =$1/480\mu s = 1000000/480 = 2.0833$ kHz

From the above calculations, the maximum sampling frequency that could be realized using ATmega 328 on the Arduino board was 2.0833 kHz. In order to give the processor more time for data processing a frequency of 2 kHz was chosen. Using this sampling frequency;

Time taken by one sample pair = $1/2000$ = 0.500ms (500µs)

Number of pairs of samples in 1 cycle = $20ms/0.500ms$ = 40

The ADC conversion time for the current and voltage was 232 μs (112 μs for voltage, 112 μs for current and a reset time of 8 μs). A slot of 268 μs was therefore available for the processing

of the data and storing it in the EEPROM before the next sampling cycle commenced. The timing diagram for the sampling process is shown in Figure 3.9.

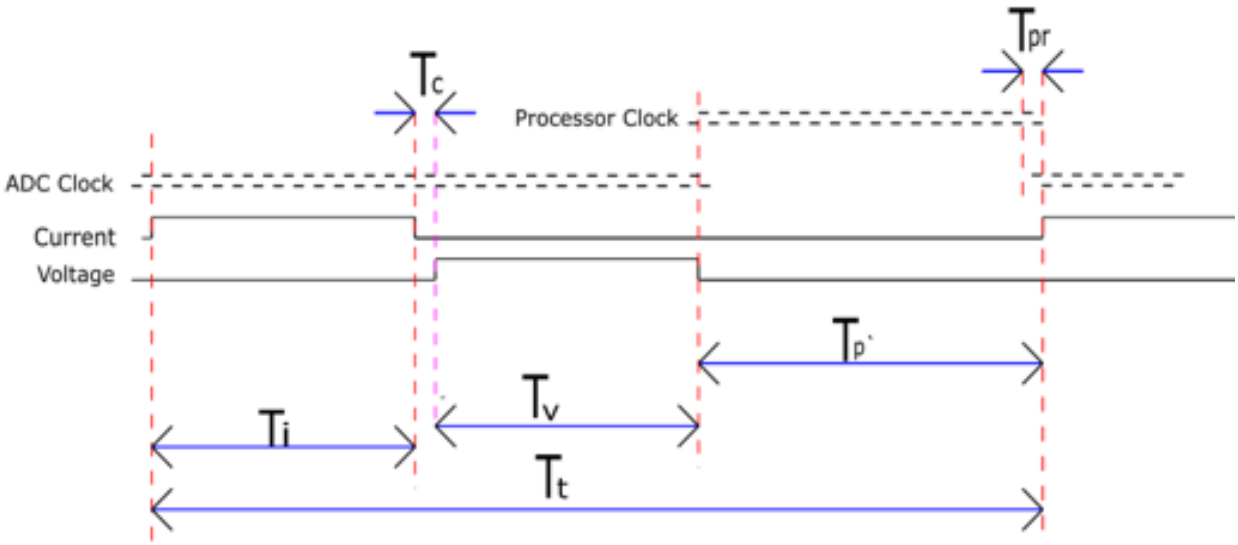

Figure 3.9: Timing diagram of sampling process.

From the timing diagram shown in Figure 3.9;

T_i = time taken to sample current signal

T_v = time taken to sample voltage signal

Tp' = time taken to process one pair of current and voltage signals

T_c = time taken by ADC to reset and be ready for the next sample

$T_{pr} = \frac{1}{16MHz} = 0.0625\ \mu s$ = time taken by one processor clock cycle.

T_t = Total time taken to sample one pair of current and voltage signals and process them.

NB:

$$T_t = 500\,\mu s, T_i = T_v = 112\,\mu s, T_c = \frac{1}{125000} = 8\mu s$$

$$T_t = 500\,\mu s - 232\,\mu s = 268\,\mu s$$

3.3.9 Computation of voltage, current, power, pf and electrical energy

(a) Voltage and current

The ADCs in the microcontroller continuously sampled the analogue voltage $v(t)$ and current $i(t)$ at a constant frequency $F_s = 2kHz$ to obtain instantaneous digital data values (V_{i_k} and I_{i_k}). The sampled data was processed and saved before taking the next set of

sample values. Saving raw values was not desirable since it required a large memory space.

Computations of the RMS values of voltage and current were based on equations 2.24 and 2.25, respectively. Each sampled data value was squared and added to the preceding sum of the squared values for a total of N = 10,000 samples. The averages of the squares (variables D and E in Figures 3.7a and 3.7b) and their square roots were computed to obtain the RMS values for the voltage and current, respectively:

$$V = \left(\frac{1}{N}\left(v_{i_1}{}^2 + v_{i_2}{}^2 + v_{i_3}{}^2 + \ldots\ldots\ldots + v_{i_N}{}^2\right)\right)^{\frac{1}{2}} \quad (2.24)$$

$$I = \left(\frac{1}{N}\left(i_{i_1}{}^2 + i_{i_2}{}^2 + i_{i_3}{}^2 + \ldots\ldots\ldots + i_{i_N}{}^2\right)\right)^{\frac{1}{2}} \quad (2)$$

(b) Power

After every sample, the instantaneous values of current and voltage were multiplied to give the instantaneous power which was added to the stored sum (only the new sum of the instantaneous power was stored to save memory space). In reference to Figure 3.7, the new sum was stored as a variable C and this continued until 10,000 samples had been taken. The final value in the memory gave the total power consumed during the 10,000 samples. The computation of average power was based on equations 2.26:

$$P_{average} = \frac{1}{N}\left(V_{i_1} I_{i_1} + V_{i_2} I_{i_2} + \ldots\ldots + V_{i_N} I_{i_N}\right) \quad (2.26)$$

(c) Apparent power and power factor

The computation of apparent power was based on equation 8 (product of the RMS values of voltage and current) while the power factor was based on equation 2.9. As demonstrated by the power triangle in Figure 2.6, the power factor was obtained from the results of the average power (active power) and the apparent power;

$$pf = \frac{Active\ Power}{\text{Apparent Power}} = cos\Phi \quad (2.27)$$

(d) Electrical energy

Computation of electrical energy was based on equation 2.17 and obtained as the average power multiplied by the time for the 10,000 samples (0.5ms/sample×10,000 samples = 5seconds). The electrical energy consumed by the load in 5 seconds was computed and stored as variable G. The electrical energy was expressed in kWh (power in kW and time in hours);

$$Energy = \frac{P_{average} \times 5 seconds}{3600 \times 1000} kWhrs$$

(2.28)

This was repeated and the cumulative units stored in EEPROM until variable G was equal or greater than 0.01 kWh. This was followed by incrementing the electrical energy units by 0.01 kWh and storing the result as variable H. The same value was subtracted from G to avoid a double entry in the following count. The new value of electrical energy was stored in the EEPROM until it was next incremented. After incrementing H by 0.01 kWh, an LED blinked once as a sign of a consumption of 0.01 units. Every time H was incremented by 0.01 kWh, the LCD displayed the values of current, voltage, power consumed, pf and the cumulated electrical energy.

(e) Testing the prototype AMR meter

The experimental set-up shown in Figure 3.10 was used to measure the initial values of voltage and current.

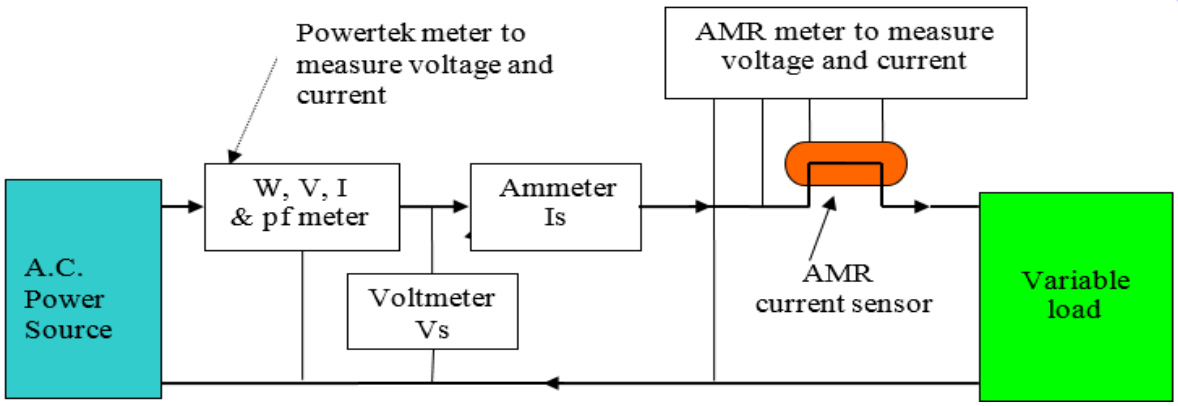

Figure 3.10: Measurement of voltage and current using AMR meter.

Electrical loads were connected in series with the ammeters and in parallel with the voltmeters. Three sets of data were recorded using (a) 240V 100W bulbs (b) 240V 1.2M × 36W fluorescent fittings and (c) a parallel combination of loads in (a) and (b). The results were tabulated in Tables D-1 (a), D-1 (b) and D-1 (c) in Appendix D.

All the ammeters recorded good results but some hardware correction had to be carried out on the AMR meter to improve its accuracy on the voltage readings.

3.4 Determination of performance of AMR energy meter

The laboratory set-up for measuring the electrical energy is shown in Figure 3.11.

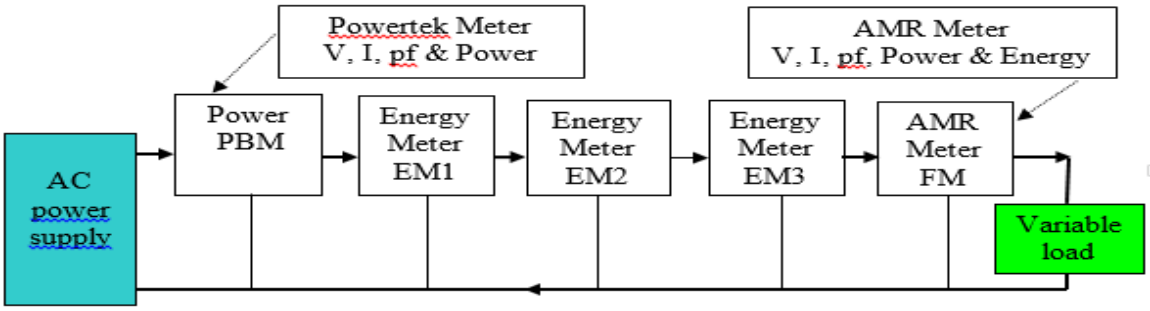

Figure 3.11: Electrical energy measurement using five different meters

The Powertek and AMR meters measured the voltage, current, 'real-time' power consumption as well as the electrical energy. Other ammeters and voltmeters (not shown in the diagram) were also connected to measure current and voltage. Three electrical energy meters (EM1, EM2 and EM3) commonly used by power utility companies like Kenya Power were connected to measure the electrical energy for comparison of performance. The meters are described below:

i. EM1: Single Phase Static Meter Class 1.0 EM101-1 5(100) A 240V 50 Hz
ii. EM2: Single Phase Static Meter Class 1.0 DDS9999 10(40) A 220V 50 Hz
iii. EM3: Electric Watt-hour Meter Class 2.0 20(100) A 220V 50Hz Model 28

Since the Powertek meter could not measure electrical energy directly, its average power consumption multiplied by time (5 minutes) was recorded as the electrical energy consumed within the recorded time. An electronic timer was used to record the time.

3.4.1 Pilot data

Three electrical loads were selected for pilot data collection and test-runs carried out for 5 minutes each and replicated four times with 5 minutes between test-runs. The test-run was repeated if there was a major voltage fluctuation within the testing period. Table F in Appendix F shows the loads (in watts) which were used for the test-runs while Tables F-1 (a), (b) and (c) show the readings which were recorded for current, voltage, pf, power and electrical energy. Tables of data analysis on the pilot data are presented in various tables in Appendix F.

3.4.2 Main data collection

Experience acquired during the pilot data collection revealed that experiments for each load took about one hour and required a lot of concentration because there were several sets of data to be recorded from the instruments. The time for the experiments was therefore reduced from

20 to 15 minutes. Table E in Appendix E shows the loads which were used for those experiments while Tables E-1 (a) through (e) show the instrument readings which were recorded for current, voltage, pf, power and electrical energy.

3.4.3 Data analysis of AMR energy meter

The AMR meter was designed to display current, supply voltage, pf, real power and electrical energy. It was therefore necessary to analyze all the data recorded from all the instruments to make a comprehensive analysis of the performance. The analysis was carried out using Statistical Analysis of Systems (SAS, 2001) and EXCEL Spreadsheet. The loads used for the collection of the main and pilot data are given in the Appendices - Tables E and F, respectively.

Each experiment was conducted for 5 minutes using the loads described in the tables and data on current, supply voltage, pf, power and electrical energy recorded. The readings were recorded from the start (zero time with energy meters not running) and after 5 minutes of the experiment. Those experiments were then repeated until all the test-runs were completed. A time of about 5 minutes was allowed for recording the data and preparation for the next experiment.

3.4.4 Meter calibration

Accurate measurements of current and voltage were crucial in the measurement of electrical energy. To test the AMR meter without an actual load, varying voltages were provided by a resistance chain which was designed to have an approximate successive doubling of resistance of ten steps from the lowest to the highest. Jumpers were connected across the resistors for normal meter operation (to give 240mV for a supply voltage of 240V). By opening the jumpers, it was possible to obtain scaled down output voltages of about 100 down to 50.5% of the supply voltage required for sampling. The results are shown in Appendix G. A test-run of 15 minutes was performed on a selected load of 8×100W incandescent bulbs and the electrical energy and number of blinks of the meter's LED were recorded. This was done to obtain the meter's constant in kWh/blink.

CHAPTER FOUR
RESULTS AND DISCUSSIONS

4.1 Introduction

This chapter presents the results of the relationship between the output voltage of the AMR sensor
and current in tables and graphs. The results are analysed and implication of its suitability in electrical energy metering discussed. The designed and fabricated electrical energy meter is also presented together with other energy meters for experimental comparison. Measurements of load current (same as sensor current), supply voltage, power factor, power and electrical energy displayed on AMR meter's LCD yielded results which are presented in tables and graphs in this chapter and Appendices D through H. The results were analysed and discussed to assess their accuracy. The performance of the AMR energy meter against selected domestic energy meters commonly used by power utility firms have also been presented and discussed in this section and in the Appendices.

4.2 Relationship between AMR sensor output voltage and current

Electrical loads (described in Table 3.1) were varied to obtain different currents and output voltages which were recorded as in Table 4.1. These results were obtained from the experimental set-up of Figure 3.1 and presented in Figures 4.1 and 4.2 to assess the suitability of the current sensor in the design of the meter.

Table 4.1 Output voltages and currents for various loads.

Electrical loads	Current (A)	Output voltage (V)
L1	0.373	0.038
L2	0.836	0.085

L3	1.487	0.149
L4	1.88	0.188
L5	2.28	0.227
L6	2.67	0.267
L7	3.41	0.341
L8	3.87	0.386
L9	4.19	0.419
L10	4.85	0.486
L11	5.55	0.55

Figure 4.1 shows the relationship between the output voltage of the sensor and the current flowing through it.

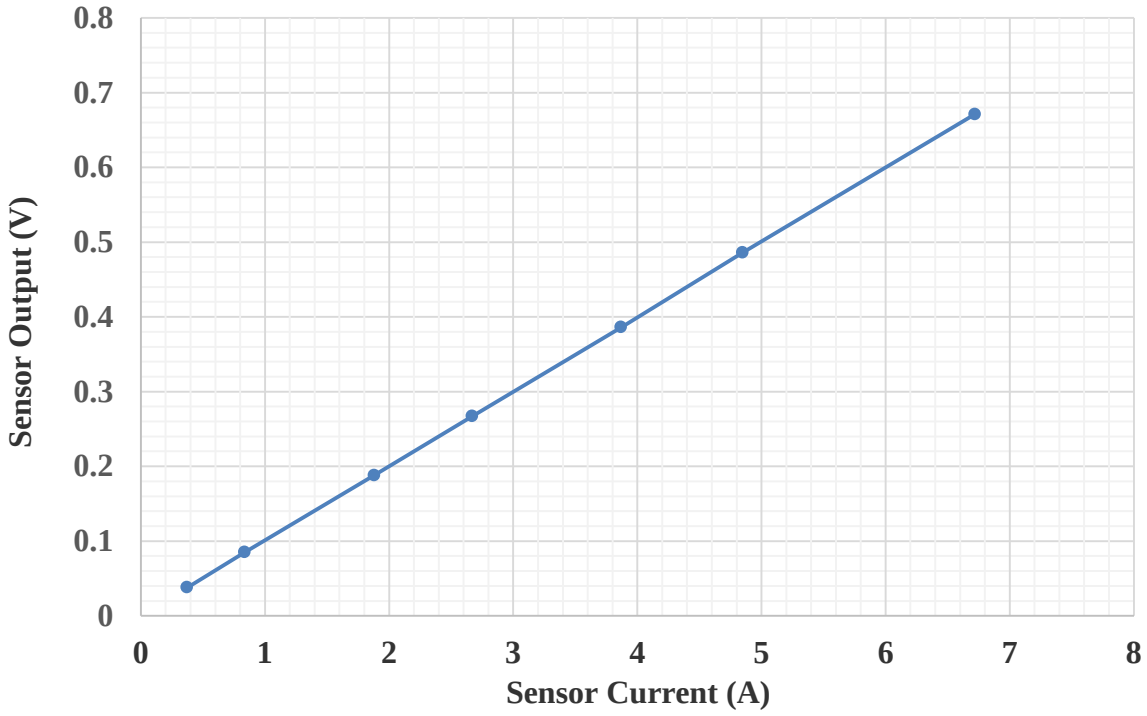

Figure 4.1: Relationship between sensor output voltage and current.

Figure 4.1 shows a linear relationship between the sensor output voltage and its input current which compares closely with the theoretical straight line. These results confirmed the manufacturer's claim that the sensor output voltages are 10% of the input current values whose characteristic is desirable for current sensors. To test for linearity, linear regression analysis was performed on the data and the results presented in Figure 4.2. The Summary and ANOVA Table are given in Appendix C.

The regression line is generally given by the expression, $y = a + bx$ which compares with the equation of the sensor output voltage, $Vout = a + bI$ where; a is the $Vout$-intercept, b is the slope and I is the current flowing through the sensor. From the ANOVA Table in Appendix C, $a = 0.000600893$ and $b = 0.099821316$ (as obtained from the coefficients column). In this case, the Regression line is given by: $V_{out} = 0.000600893 + 0.099821316\ I$ volts, where $a = 0.000600893$ is the $Vout$-intercept and $b = 0.099821316$ is the slope of the regression line.

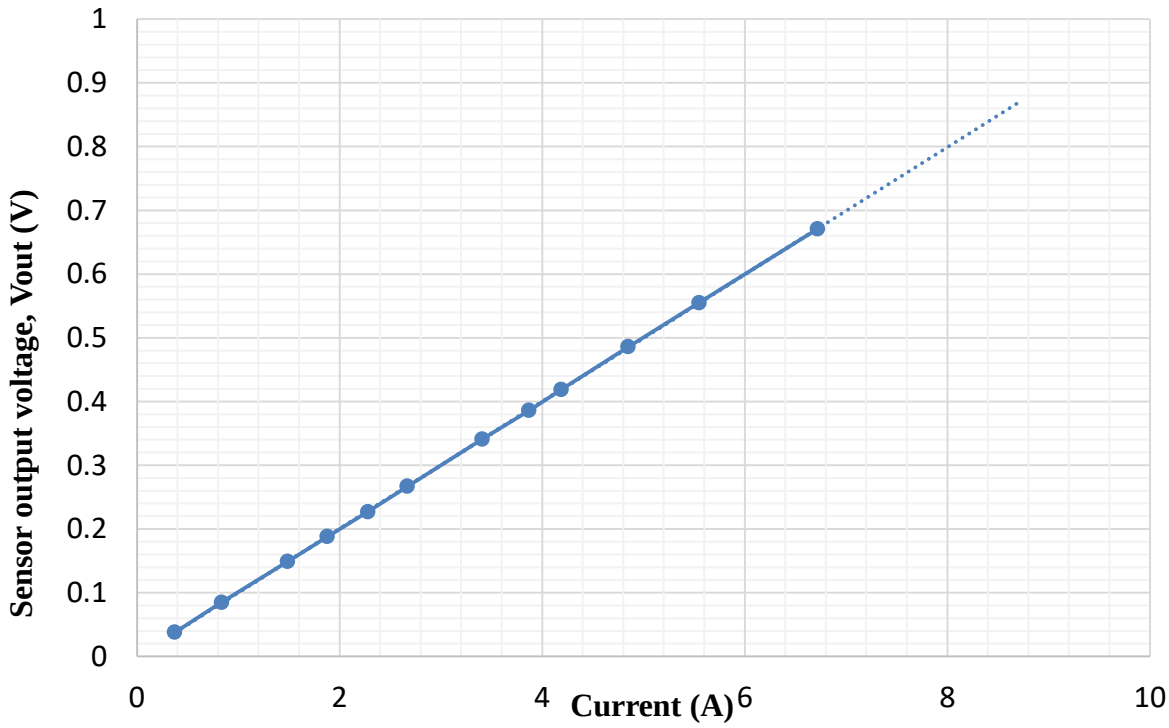

Figure 4.2: Linear regression on sensor current and output voltage.

The sensor output voltages for any current within the sensor current rating may be predicted using this formula as illustrated below:

For a current of 10A; $V_{out} = 0.000600893 + 0.099821316 \times 10 = 0.998814053\ V$

For a current of 25A; $V_{out} = 0.000600893 + 0.099821316 \times 25 = 2.496133793\ V$

These figures may, for all practical purposes, be approximated to 1 V and 2.5 V respectively and confirms the Manufacturer's claim.

From the summary of the regression statistics in Appendix C, Multiple R (square root of R Square) is 0.999993708. This figure is a measure of how the data clusters around the regression line, and the closer it is to unity, the better the data. In this case, Multiple R was very close to unity implying that the data clustered closely around the regression line. From the two graphs and the results in Appendix B, the sensor was considered to be suitable for electrical energy metering.

Hou and Yu (2011) designed an electrical energy meter using a resistive shunt current sensor and a potential divider for the voltage signal channel. Shahrara (2011) and Nayak (2013) implemented energy meter designs with Hall-effect current sensors and also obtained meter voltage signals
through potential divider methods. Hou and Yu (2011) also implemented a digital energy meter using a current transformer. Most design methods utilize traditional current sensors but vary their designs through digital processing and display, centralized data transmission and billing (Zig-bee). Though manufacturers produce good meter results which compare closely to the performance characteristics shown in Table 2.1, they repeat the applications of these traditional sensors without exploring the use of other sensors.

4.3 Designed and fabricated electrical energy meter

The fabricated meter is shown in Plate 4.1 and its LCD display in Plate 4.2

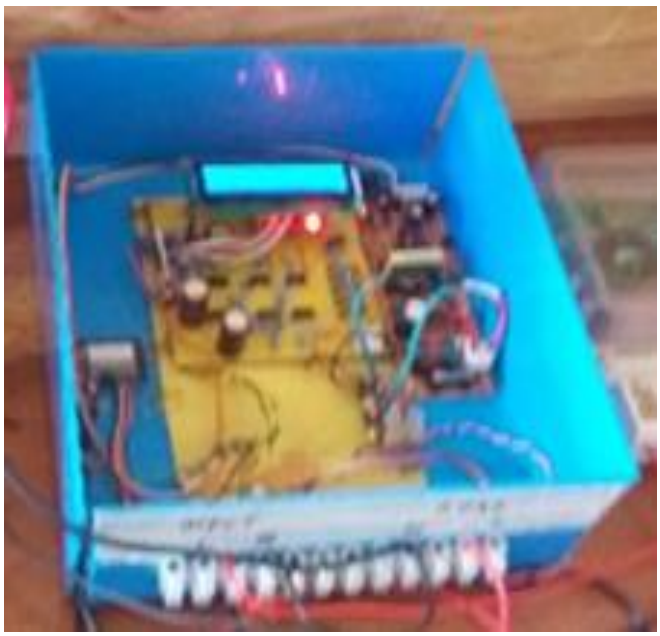

Plate 4.1: Fabricated electrical energy meter

Plate 4.2: LCD display

Plate 4.1 shows the fabricated energy meter with some interconnection leads for experimental work and Plate 4.2 shows a practical display of voltage, current, power factor, power consumption and cumulated electrical energy over some time. Experiments were set up and these readings together with those of other meters recorded for analysis.

4.4 Performance of AMR electrical energy meter on 5 loads

The analysis of the performance of the AMR meter was based on data collected from ammeters, voltmeters, pf meters, power and electrical energy meters on five different loads. The results obtained were recorded in Tables E-1 (a) through (e) in Appendix E. The AMR meter was designed to display the five variables and therefore it was important to analyse all the variables it displayed. The data collected from tests on 5 loads each taking 15 minutes was analyzed in detail as shown in this section. Data analysis on readings from the meters was carried out using EXCEL and SAS, 2001 software.

4.4.1 Analysis of current

The analysis of current was based on measurements from 3 ammeters (I1, IBM and IFM) tabulated in Tables E-1 (a) through (e). Table 4.2 summarizes t-Test outputs of analysed data for 5 loads. It was observed from the table that the means of the 2^{nd}, 5^{th} and 6^{th} columns did not share same letters in their respective columns implying that the means of the currents were significantly different. In the 3^{rd} and 4^{th} columns some means shared same letters which implied that they were not significantly different. In this case, the means for ammeters IBM and IFM in the 3^{rd} and 4^{th} columns were the same (4.4433^{b} and 7.0467^{b}) implying that the two meter readings were not significantly different. However, the current mean values not followed by the same letters in the same columns were significantly different.

Table 4.2 Mean currents

Ammeters	**Electrical Loads**				
	L1	**L2**	**L3**	**L4**	**L5**
IBM	5.6900^{a}	4.4433^{b}	7.0467^{b}	3.3350^{a}	6.1567^{b}
I1	5.6567^{b}	4.5533^{a}	7.2333^{a}	3.3333^{b}	6.1733^{a}
IFM	5.6033^{c}	4.4433^{b}	7.0467^{b}	3.3067^{c}	6.0733^{c}
LSD	0.0005	0.0003	0.0030	0.0020	0.0001

NB: Means followed by the same letter in the respective columns are not significantly different at 0.05 level of significance and LSD.

It was observed from the ANOVA of currents in Table E-2 (a) (ii) of Appendix E-2 revealed that R-squares were close to unity for all the 5 loads. It was deduced from R-square values that correlation coefficients were also close to unity implying that the data clustered around the overall mean value. Moreover, it was observed that the p-values in all the rows were lower than 0.05 level of significance. This implied that the differences between the means were significant. This confirmed the results in Table 4.5 in which some mean currents in the same columns did not share same letters. To compare the performance of the ammeters, the data in Table 4.2 was plotted in Figure 4.3 and error bars inserted.

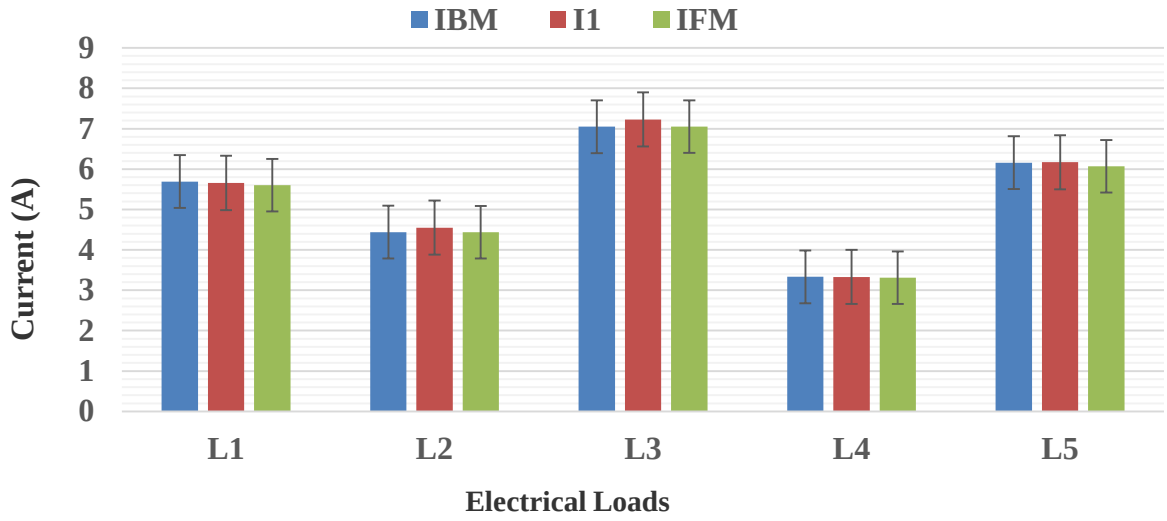

Figure 4.3: Mean currents against electrical loads using three ammeters.

The error bars overlapped for all the currents measured by the three ammeters on different loads implying that their readings were not significantly different and that the AMR meter performed competitively with the other ammeters.

4.4.2 Analysis of voltage

The analysis of voltage was based on three measurements from V1, VBM and VFM voltmeters presented in Tables E-1 (a) through (e). Summarized t-Test outputs of analysed data for 5 loads are given in Table 4.3**.** It was observed that the mean voltages in the 2nd column shared the same letters. This implied that the measured mean voltages by the three voltmeters were not significantly different and the instruments had similar performance in this aspect. In 3rd, 4th and 6th columns, some voltage means shared same letters which implied that differences between means were not significantly different.

Table 4.3 Mean voltages.

Voltmeters	**Electrical Loads**				
	L1	**L2**	**L3**	**L4**	**L5**
VBM	226.6667[a]	231.6667[a]	229.6667[a]	236.0000[a]	232.6667[a]
V1	227.0000[a]	230.3333[b]	227.6667[b]	233.3333[c]	230.3333[b]
VFM	227.0000[a]	231.6667[a]	229.3333[a]	235.0000[b]	232.3333[a]
LSD	0.7901	0.0123	0.0037	0.0015	0.0223

NB: Means followed by the same letter in the respective columns are not significantly different at 0.05 level of significance and LSD.

It was also observed from Table 4.3 that voltmeters VBM and VFM shared same letters in all the columns except in the 5th column. This implied that there was no significant difference between the mean voltages of the two voltmeters in the 4 load tests. However, there was a significant difference between the mean voltages of those 2 voltmeters and voltmeter V1 in each test.

In scrutiny of the statistical results in the summary of ANOVA Table E-3 (a) (ii), it was observed that R-squares in all the rows (except row 1) were almost unity. Since the R-squares were large, it implied that the correlation coefficients for the 4 tests were also close to unity and that the data clustered about the overall mean. Except in row 1, p-values in all the other rows were lower than the significance level of 0.05. This implied that the differences between some of the mean voltages were significantly different. In this case, the mean voltages of voltmeters VBM and VFM were significantly different from the mean voltages of voltmeter V1 in all the

loads except for load L1. The p-value in row 1 was larger than the significance level of 0.05 which implied that the means were not significantly different.

To compare the performance of the voltmeters, the data in Table 4.3 was plotted as in Figure 4.4 and error bars inserted. The error bars of voltmeters VBM and VFM overlapped on all the 5 load tests.

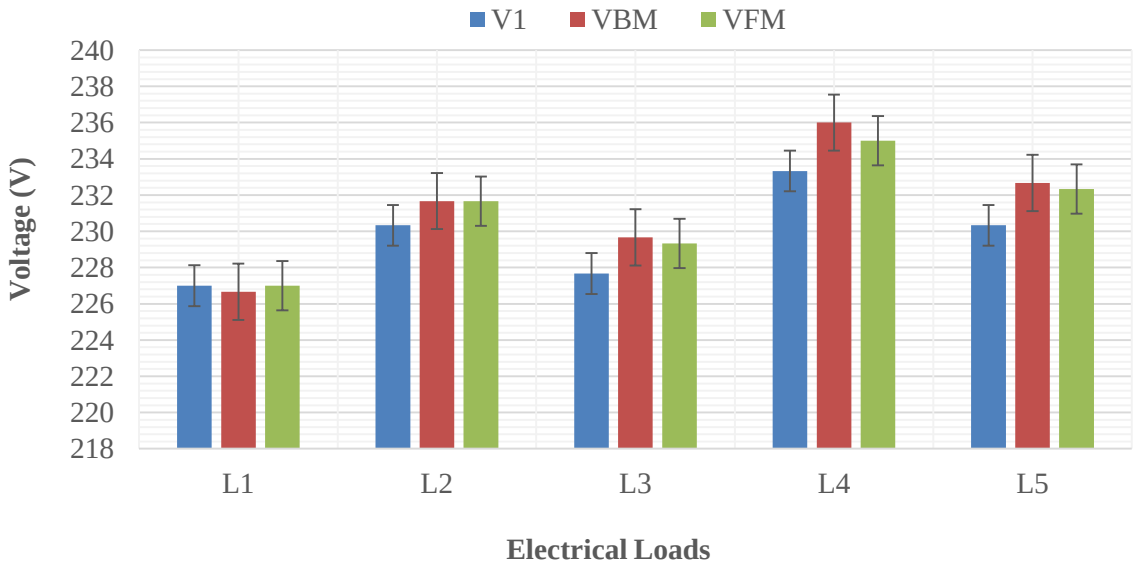

Figure 4.4: Voltage versus Electrical Loads

This implied that the mean voltages of the 2 voltmeters were not significantly different in all the tests. However, there was a significant difference between means of voltmeter V1 and the other 2 voltmeters in most of the tests.

4.4.3 Analysis of power factor (pf)

The analysis of power factors (pf**)** was based on 2 pf meter readings (pfBM and pfFM) tabulated in Tables E-1(a) through (e). Table 4.4 shows summarized t-Test outputs of analysed data for 5 loads.

Table 4.4 Mean power factors.

Power factor	**Electrical Loads**				
meters	**L1**	**L2**	**L3**	**L4**	**L5**
pfBM	1.0000[a]	0.9400[a]	0.9840[b]	1.0000[a]	1.0000[a]
pfFM	1.0000[a]	0.9600[a]	0.9900[a]	1.0000[a]	1.0000[a]

LSD	0.0000’	0.0001	0.0001	0.0000’	0.0000’

NB: Means of pf in the same column followed by the same letter are not significantly different at 0.05 level of significance and LSD.

It was observed from the Table that the means shared the same letters in their respective columns except in the 4th column. This implied that the mean pfs that shared the same letters in the same columns were not significantly different and the means in the 4th column were significantly different. Both meters indicated pf of unity for loads L1, L4 and L5 which was expected since the loads were resistive. The means were therefore not significantly different at 0.05 level of significance.

It was observed from the ANOVA results of pf in Table E-4 (a) (ii) in Appendix E-4 that R-squares in rows 1, 4 and 5 were zero. This was expected because the difference between the means was zero. R-squares in rows 2 and 3 were unity and this was a good indication that the data clustered very close to the overall mean. For loads L1, L4 and L5, the pf was unity on both meters. Since there was no difference in the readings, computations for variables in columns 2, 3 and 4 yielded “0” as the output. Divisions involving “0” in the denominator could only give an infinitely high value, hence the dots (.) for the LSD and F Values. The p-values of row 2 and 3 were lower than 0.05 level of significance implying that the means of the 2 pf were significantly different.

To compare the performance of the power factor meters, the data in Table 4.4 was plotted in Figure 4.5 and error bars inserted.

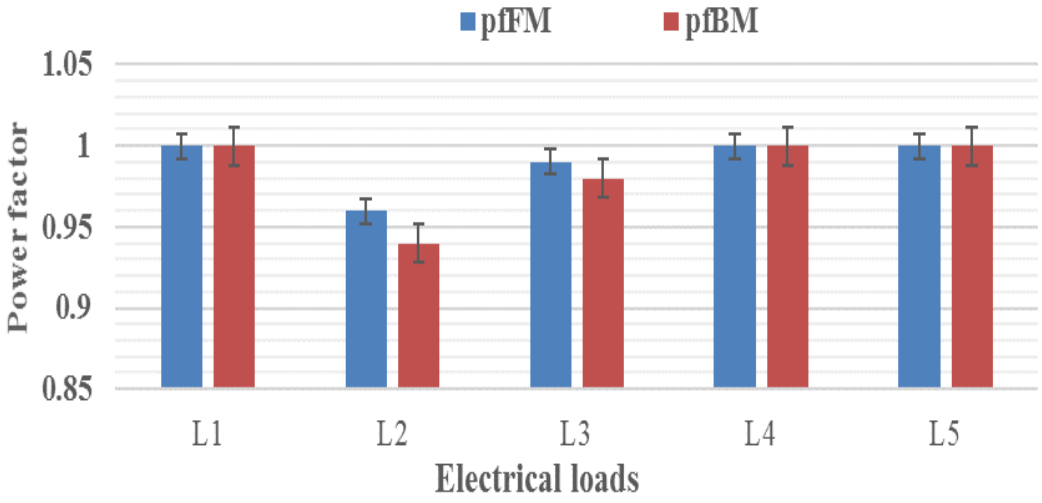

Figure 4.5: Power factor versus electrical loads.

It was observed that the error bars overlapped for all the loads except L2 which could be due to human error during measurement.

4.4.4 Analysis of power

The analysis of power was based on two meter readings (PBM and PFM) presented in Tables E-1 (a) through (e). Table 4.5 shows t-Test outputs of analysed data for five loads. In this table, the mean values of power in the 2nd column shared the same letters. This implied that the means were not significantly different at 0.05 level of significance. In the other columns, the means did not share same letters in their respective columns. This implied that the means were significantly different. The difference between the readings of the 2 power meters was not significant and therefore the wattmeters had similar performance.

Table 4.5 Means of power

Wattmeters	**Electrical Loads**				
	L1	**L2**	**L3**	**L4**	**L5**
PBM	1309.6667[a]	994.3333[a]	1612.0000[a]	792.6667[a]	1436.6667[a]
PFM	1280.0000[b]	1002.0000[a]	1606.6667[b]	778.6667[b]	1410.0000[b]
LSD	0.0009	0.2809	0.0153	0.0117	0.0011

NB: Means followed by the same letter in the same column are not significantly different at 0.05 level of significance and LSD.

The ANOVA summary in Table E-5 (a) (ii) shows that R-square in each row is close to unity. Multiple-R (correlation coefficient) values were close to unity which was a good indication that the data clustered closely to the overall mean. Also, the p-value in row 2 was higher than 0.05 level of significance. This implied that the means were not significantly different. The 2 power meters registered readings which were not significantly different. The p-values in the other rows were lower than the significance level of 0.05. This implied that some of the means were significantly different.

To compare the performance of the power meters, the data in Table 4.5 was plotted in Figure 4.6 and error bars inserted.

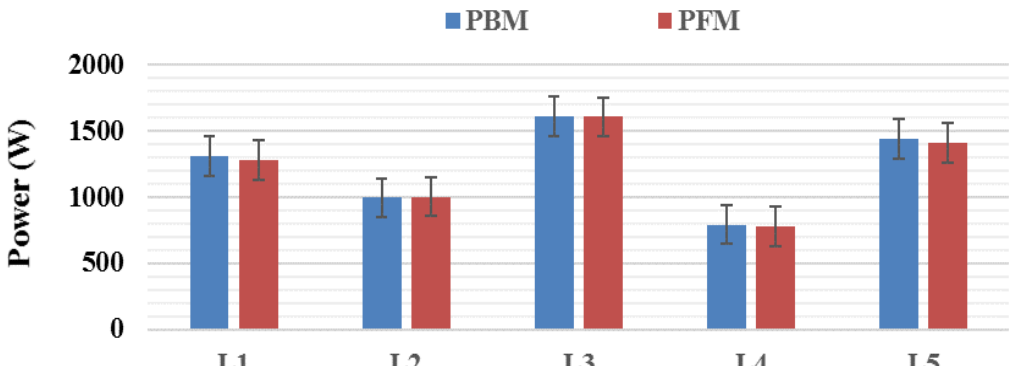

Figure 4.6: Power measured with two wattmeters on different loads

It was observed from Figure 4.6 that the error bars overlapped for all the loads implying that the mean powers recorded by the two wattmeters were not significantly different.

4.4.5 Analysis of electrical energy

The analysis of electrical energy was based on 5 meter readings in Tables E-1 (a) through (e). Table 4.6 shows a summary of the t-Test outputs for loads L1, L2, L3, L4 and L5.

Table 4.6 Means of electrical energy consumed

Energy meters	**Electrical Loads**				
	L1	**L2**	**L3**	**L4**	**L5**
EBM	0.1091^{b}	0.0829^{c}	0.1343^{b}	0.0661^{a}	0.1197^{a}
EFM	0.1100^{ab}	0.0933^{b}	0.1433^{ab}	0.0700^{a}	0.1233^{a}
EM1	0.1067^{b}	0.0867^{bc}	0.1567^{a}	0.0667^{a}	0.1233^{a}
EM3	0.1167^{a}	0.0967^{a}	0.1567^{a}	0.0700^{a}	0.1333^{a}
LSD	0.0481	0.0117	0.0358	0.6585	0.3560

NB: Means followed by the same letter in the respective columns are not significantly different at 0.05 level of significance and LSD.

It was observed from Table 4.6 that in the 4^{th} and 5^{th} columns, all the means shared the same letters. This implied that the means were not significantly different and the energy consumptions registered by the 4 meters were not significantly different. In the other 3 columns, some means shared same letters and therefore the electrical energy means were not significantly different. However, some means in the same columns did not share same letters and they were therefore significantly different.

In column 2, means of EBM and EM1 shared same letters and were therefore not significantly different. However, the means of EFM and EM3 did not share same letters and were therefore significantly different. In column 3 (load L2), the means did not share same letters and therefore

the means were significantly different. In column 4 (load L3), means of EM1 and EM3 shared same letters and therefore they were not significantly different. Also, the means of EM1 and EM3 in column 4 did not share same letters with the other meters and their electrical energy means were therefore significantly different.

It was observed from the statistical results in Table E-6 (a) (ii) in Appendix E-6 that R-squares in 4 out of the 5 rows were above 0.85 and therefore close to unity. Since Multiple-R (correlation coefficient) values were close to unity, this was a good indication that the data clustered closely to the overall mean. Multiple R value for the other row was 0.73 which implied that the data clustered less closely to the overall mean.

The p-values for loads L1, L2 and L3 were lower than the significance level of 0.05. This implied that the differences between the means were significantly different. This was in agreement with the results in Table 4.6 where it shows that the means did not share same letters for loads L1, L2 and L3. The p-values for loads L4 and L5 were higher than the significance level of 0.05. This implied that the differences between the means were not significantly different. This was in agreement with the results in Table 4.6 which showed that the means for loads L4 and L5 shared same letters. This implied that the means were significantly different. In this case, the differences between some of the means for loads L1, L2 and L3 were significantly different.

To compare the performance of the meters in the measurement of electrical energy, the data in Table 4.6 was plotted in Figure 4.7 and standard error bars included.

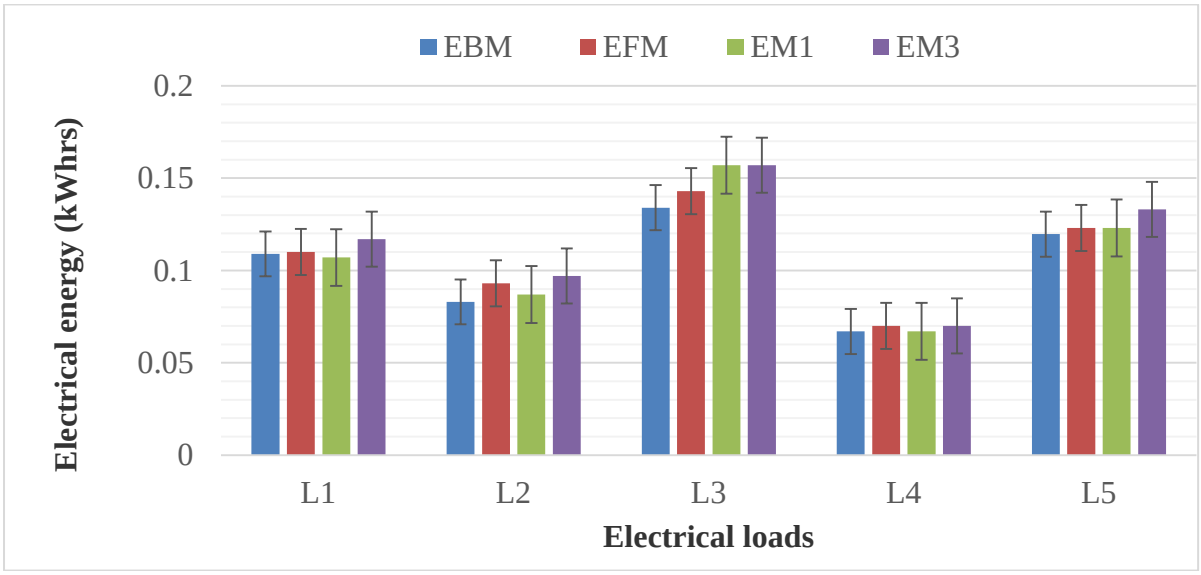

Figure 4.7: Electrical Energy versus Electrical Loads.

It was observed that the error bars overlapped for all the 5 loads implying that the means of the electrical energy were not significantly different. This was an indication that the performance of each meter was not significantly different. Since the error bars of all the meters overlapped, it implied that the performance of the AMR electrical energy meter (EFM) was not significantly different.

4.4.6 Comparison of cumulated data from 5 meters

It is important to note that the data from meter EM2 was not used in data analysis of the other meters because it has a single decimal point display and could not output most of the consumed electrical energy between 0 and 0.1 kWh like the other meters. The cumulative electrical energy (kWh) consumed in 75 minutes (15 minutes for each load) from the 5 meters for the 5 electrical loads is shown in Table G (a) in Appendix G. This data was obtained from Tables EE-1 (a) through (e) which are extracts from Tables E-1 (a) through (e).

To compare the performance of the meters, the data was plotted in Figure 4.8 and error bars inserted.

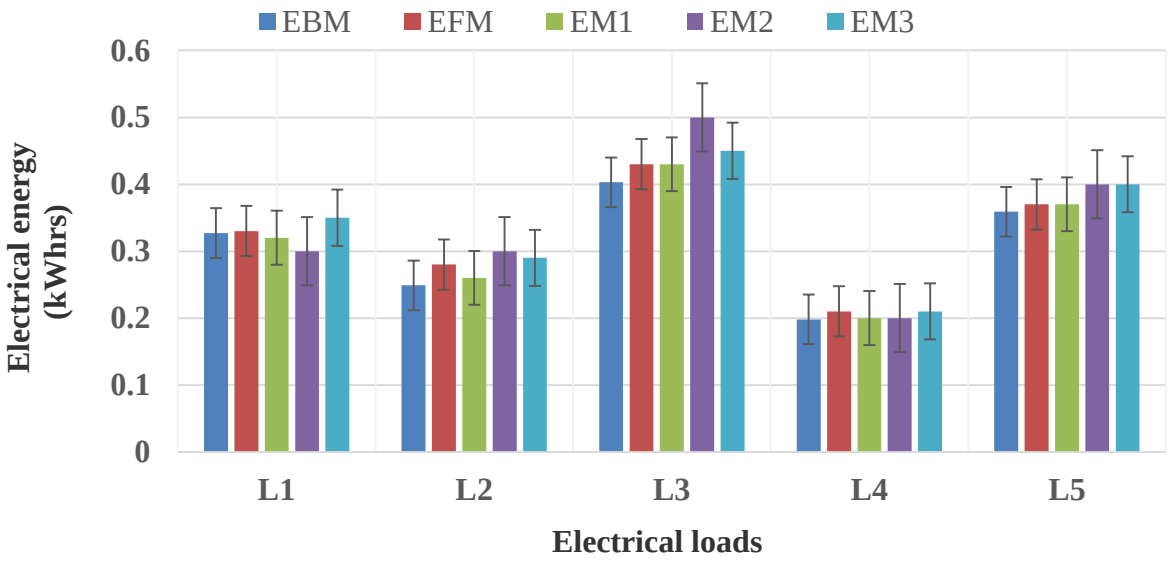

Figure 4.8: Cumulative electrical energy versus electrical loads.

It was observed from Figure 4.8 that the error bars on data of the five electrical energy meters overlapped implying that all the meters registered kWh units which were not significantly

different. It was noted that over a long time, the performances of the single decimal point meter (EM2) and the other meters were not significantly different.

Electrical energy could also be obtained through manual multiplications of voltage, current, power factor (equation 5) and time recorded from various meters and timer during the test-runs. These calculations were carried out and recorded in Tables EE-1 (a) through (e) for comparison with those recorded from the power meters (EBM and EFM). It was observed from Tables EE-1 (a) through (e) that the calculated figures in columns for EBM and EFM were not significantly different.

4.5 Performance of electrical energy meter on 3 loads

The performance of the energy meter was based on measurements of current, voltage, power, power factor and electrical energy. An analysis was carried out on the 5 variables in detail in section 4.4. A further analysis (less detailed) was carried out based on test-runs for 3 loads that took 20 minutes each. The analysis is explained in section 4.5.1 through 4.5.5.

4.5.1 Analysis of current

The analysis was based on measurements of current using 4 ammeters on 3 electrical loads for 20 minutes each. The means of currents and a comparison of means using bar graphs are shown in Table 4.7 and Figure 4.9 respectively.

Table 4.7 Means of currents

Ammeters	**Electrical loads**		
	L1	**L2**	**L3**
I1	1.7350[c]	3.6600[a]	6.7600[a]
IBM	1.7730L1[a]	3.6250[b]	6.7500[a]
IFM	1.7500[b]	3.5750[c]	[6].6400[b]
I4	1.6850[d]	3.6550[a]	6.7600[a]

NB: Means followed by the same letter in the respective columns are not significantly different at 0.05 level of significance and LSD of 0.0001.

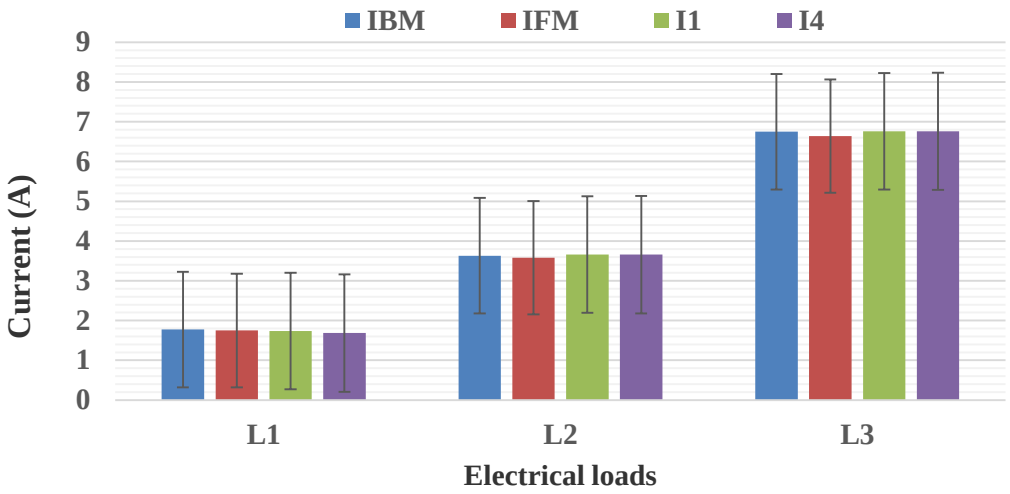

Figure 4.9: Current against electrical loads

It was observed from Table 4.7 that the means of the 2nd, 3rd and 4th columns did not share same superscript letters in their respective columns. This implied that the means of the currents were significantly different. In the 2nd and 4th columns some means shared same letters which implied that they were not significantly different. From the ANOVA table (Table F-2 (a)), the R-square values were 0.97 for the 3 loads. This implies that the data clustered closely around the overall mean. It was also observed that the p-values were lower than 0.05 level of significance. This implied that the differences between the means were significant. This confirmed the results in Table 4.7 in which some mean currents in the same columns did not share same letters.

To compare the performance of the ammeters, the data in Table 4.7 was plotted in Figure 4.9 and error bars inserted. It was observed that all the error bars overlapped implying that the differences between the means were not significantly different.

4.5.2 Analysis of voltage

The analysis of voltage was based on three measurements from voltmeters V1, VBM and VFM presented in Table 4.8. It was observed that the mean voltages in the 3rd column shared the same letters. This implied that the measured voltages by the three voltmeters were not significantly different and that the instruments had similar performance in this aspect. In the 2nd column, some means shared the same superscript letters which implied that the means were not significantly different. In the 4th column, the means did not share the same letters which implied that the means were significantly different

Table 4.8 Means of voltages

Voltmeters	Electrical Loads		
	L1	L2	L3
VBM	230.5000[a]	227.5000[a]	227.5000[ab]
V1	229.2500[b]	226.5000[a]	226.5000[b]
VFM	229.2500[b]	227.5000[a]	228.2500[a]
LSD	0.0012	0.0421	0.095

NB: Means followed by the same letter in the same column are not significantly different at 0.05 level of significance and LSD.

It was observed from the statistical results in the summary of ANOVA Table F-3 (a), that R-squares in all the rows were close to unity which implied that the data clustered around the overall mean. To compare the performance of the voltmeters, the data in Table 4.8 was plotted in Figure 4.9 and error bars inserted. It was observed that all the 3 error bars overlapped implying that the differences between their means were not significantly different. It was also observed that the error bars of the laboratory meter (VBM) and the fabricated meter (VFM) overlapped in all the three load tests.

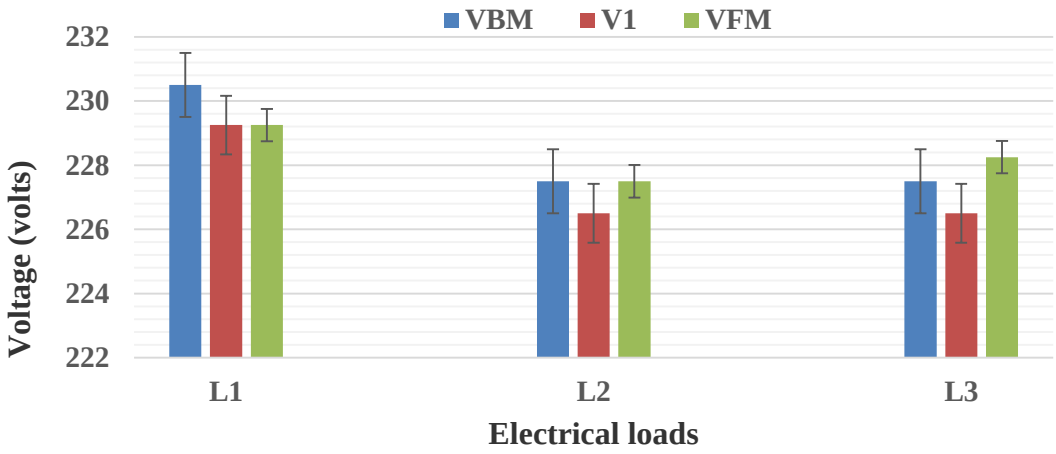

Figure 4.10: Voltages against different loads

4.5.3 Analysis of power factor (pf)

It was observed from Table 4.9 that in the 2nd and 4th columns, the superscript letters following the means were all different. This implied that the differences between the means were significantly different. In the 3rd column, the means shared the same letters and implied that the means were not significantly different. The means were therefore not significantly different at 0.05 level of significance. R-squares in row 1 was unity and this was a good indication that the data clustered very closely to the overall mean. R-squares in rows 2 and 3 for respective loads

L2 and L3 were 0.6667which implied that the data was not as closely clustered around the overall mean as for load L1 in column 1.

Table 4.9 Means of pf

pf meters	**Electrical Loads**		
	L1	**L2**	**L3**
pfFM	0.5825[a]	0.9400[a]	0.9900[a]
pfBM	0.5150[b]	0.9250[a]	0.9850[b]
LSD	0.0001	0.1817	0.1817

Means followed by the same letter in the same column are not significantly different at 0.05 level of significance and LSD of 0.0001, 0.1817and 0.1817.

To compare the performance of the power factor meters, the data in Table 4.9 was plotted in Figure 4.11 and error bars inserted. It was observed that the error bars overlapped in all the cases implying that the means were not significantly different.

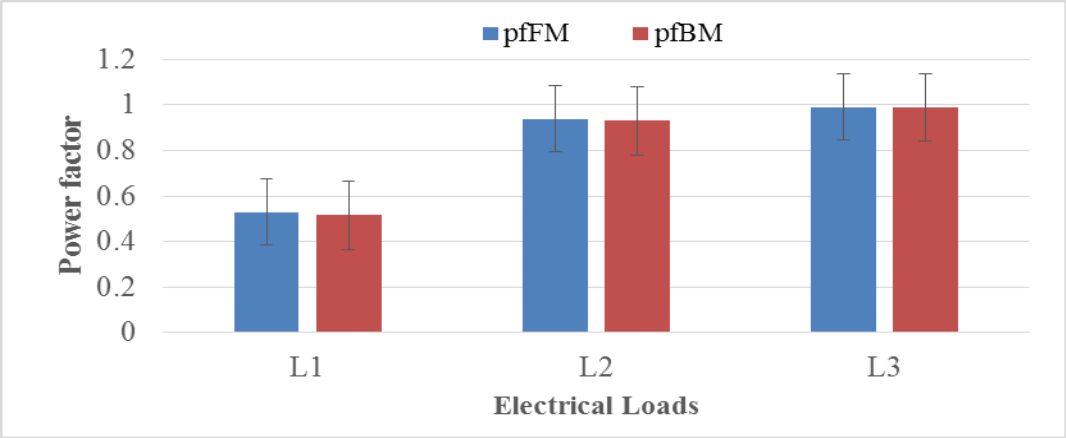

Figure 4.11: Power factor against different loads

4.5.4 Analysis of power

The analysis of power was based on two meter readings (PBM and PFM) whose means are presented in Table 4.10.

Table 4.10 Means of power

Power meters	**Electrical loads**		
	L1	L2	L3
PFM	233[a]	768.25[a]	1500[b]

PBM	211.25[b]	759.25[b]	5110[a]
LSD	0.0001	0.0193	0.0498

NB: Means followed by the same letter in the same column are not significantly different at 0.05 level of significance and LSD.

From the t-Test outputs of analysed data for the 3 loads, the mean values of power in the 3 columns did not share the same superscript letters. This implied that the means were significantly different at 0.05 level of significance.

To compare the performance of the two meters, the means were plotted in Figure 4.12 and error bars inserted. It was observed that all the error bars overlapped. This implied that there was no significant difference between the means of the two power meter readings.

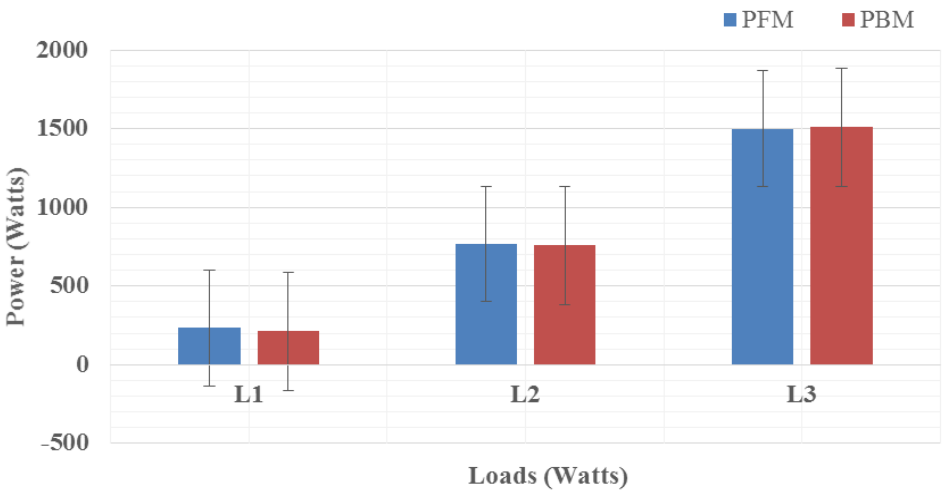

Figure 4.12: Mean power against different loads

4.5.5 Analysis of electrical energy

It was observed from the 1st column that the means shared the same superscript letters implying that the means were not significantly different. In the 3rd and 4th columns, some means shared the same letters implying that the means were not significantly different. Some did not share the same letters which implied that the means were significantly different.

Table 4.11 Means of electrical energy

Energy meters	Electrical Loads		
	L1	**L2**	**L3**
EFM	0.02[b]	0.07[a]	0.14[a]
EBM	0.018[a]	0.063[b]	0.126[ab]
EM1	0.02[a]	0.063[b]	0.125[b]
EM3	0.0175[a]	0.073[a]	0.138[ab]
LSD	0.0001	0.0193	0.0498

NB: Means followed by the same letter in the same column are not significantly different at 0.05 level of significance and LSD.

To compare the performance of the meters, the data was plotted in Figure 4.13 and standard error bars inserted.

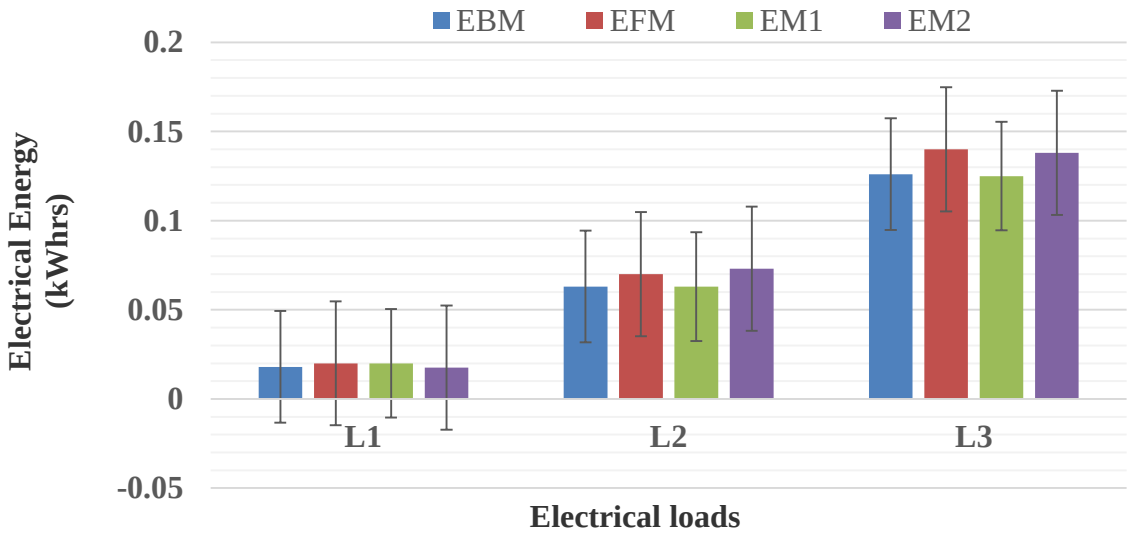

Figure 4.13: Electrical energy against loads

It was observed that all the error bars overlapped implying that the means of the electrical energy were not significantly different. Since all the error bars overlapped, it implied that the performance of the AMR electrical energy meter (EFM) was not significantly different from the other meters.

4.5.6 Comparison of cumulated data from 5 meters

It should be noted that the data from meter EM2 was not used in data analysis of the other meters because it has a single decimal point display and could not output most of the consumed electrical energy between 0 and 0.1 kWh like the other meters. The cumulative electrical energy

(kWh) consumed in 60 minutes (20 minutes for each load) from the 5 meters for the 3 electrical loads is shown in Table G (b) in Appendix G. This data was obtained from Tables FE-1 (a), (b) and (c) which are extracts from Tables F-1 (a), (b) and (c).

To compare the performance of the meters, the data was plotted in Figure 4.14 and error bars inserted. It was observed from Figure 4.14 that the error bars on data of the five electrical energy meters overlapped implying that all the meters registered kWh units which were not significantly different.

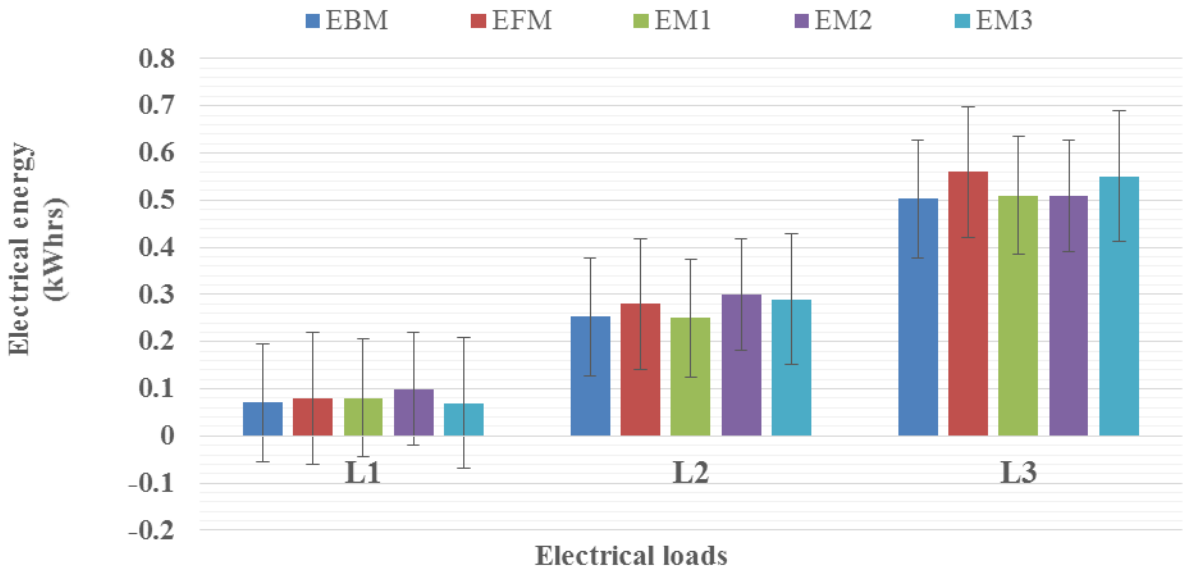

Figure 4.14: Electrical energy against electrical loads over 20 minutes each.

It was observed that over a long time (60 minutes), the performances of the single decimal point meter (EM2) and the other meters were not significantly different.

Electrical energy was also obtained through manual multiplications of voltage, current, power factor (equation 2.5) and time recorded from various meters and timer during the test-runs. These calculations were carried out and recorded in Tables FE-1 (a), (b) and (c) for comparison with those recorded from the power meters (EBM and EFM). It was observed from the Tables that calculated figures in columns for EBM and EFM were not significantly different.

4.5.7 Calibration and meter constant

Calibration was carried out to assess the accuracy of the AMR meter. The voltage channel was calibrated using successive approximation technique and results tabulated in Table H (b) in the Appendix where output voltages are expressed as percentages of supply voltage. For any supply voltage, the output voltages would be in the percentages shown in Table H (b). The output

voltages are available if, starting with all jumpers closed, jumpers J10, J9, J8 and so on are opened progressively one at a time up to J1. Using these output voltages, and a selected load, the registered kWh units would be compared with those of a calibrating instrument to assess the accuracy of the fabricated energy meter.

The number of blinks for three loads were recorded as in Tables F-1 (a), (b) and (c) from which the meter constant was 0.01 kWh/blink (0.14 kWh/14 blinks). Test runs over 15 minutes for loads L1 and L4 confirmed the meter constant. The meter electrical energy readings from the AMR and Powertek meters were 0.21 and 0.198 kWh (average of 0.204 kWh) respectively and the LED blinked 20 times giving a meter constant of 0.204/20 kWh/blink (0.01 kWh/blink). From the voltage and current readings, the electrical energy consumed in 15 minutes (V×I×pf×time) were 0.1947 and 0.1977 kWh respectively for the AMR and Powertek meters. The average meter constant was averaged to 0.01 kWh/blink. The AMR meter was calibrated by counting the number of pulses, converting them to kWh and finally comparing the result with that recorded by a standard electrical energy meter.

CHAPTER FIVE
CONCLUSIONS AND RECOMMENDATIONS

5.1 Conclusions

Regression analysis of the analyzed data demonstrated that a linear relationship existed between the AMR sensor output voltage and its input current. Hence, the AMR sensor was found suitable for current sensing and metering electrical energy since it can be used to accurately estimate the output voltage for any current within its rating. The meter was designed and fabricated based on the sensor and the supply voltage. The voltage and current signal conditioning circuits formed the basis of the design hardware. Etching the PCB was successful and components soldered to the board. The software was finally installed to complete the meter.

The AMR meter displayed on LCD accurate results of supply voltage, load current, power factor, 'real-time' power consumption and electrical energy consumed for various electrical loads. This confirmed that the hardware design, written C-code, sampling, signal conditioning and processing performed various tasks correctly to finally display accurate variables on the LCD. Statistical data analysis revealed that all the meters had similar results and that the AMR meter performed well against the other meters.

Statistical results were used to determine the performance of the meters from the electrical energy data (EBM, EFM, EM1 and EM3) and showed that their performance was not significantly different. The results from the bar graphs plotted using the cumulated data from the 5 electrical energy meters (including EM2) revealed that all the error bars overlapped in all the experiments and that their performances were not significantly different. Since the meters are usually read after a long time (usually one month), consumer billing would not matter if the meters had single or double decimal point displays.

5.2 Recommendations

5.2.1 Calibrations

All the experiments were carried out within uncontrolled laboratory power supply conditions, often with small voltage fluctuations due to external electrical loads. Although the laboratory meters used to carry out the measurements had been calibrated in the laboratory by agents of Kenya Bureau of Standards (KEBS), further calibration should be carried out using standard electrical energy meter calibration equipment. The performance of the AMR meter should be

studied further, evaluated and calibrated to ensure that it meets the ±1% accuracy for Class 1 instruments before it is considered for the market.

5.2.2 Meter reliability

A good assessment of reliability of an equipment is a function of individual component reliabilities and operation life time. Reliability testing and assessment may be very difficult to carry out on a proto-type equipment like the fabricated energy meter. Time-testing may sometimes be the only way to test for reliability. However, its reliability is expected to be high because the choice of the components took care of high power rating of resistors used (0.5W) and a reliable time-tested power supply. It would require the equipment to be time-tested to assess the reliability and may not be easy to carry out. The reliabilities of the OPAMPS and the AMR sensor would depend on the manufacturers but reliability engineers may give a better assessment of the overall reliability. It is recommended that further study be carried out to assess its reliability.

5.2.3 Suitability of AMR current sensor in electrical energy metering

Tests carried out on the AMR current sensor showed that there was a substantial error at low input currents (about 6% at 0.5A) which declined to within 1% at about 1.8A. However, the error remained within ±1% at current values above 1.8A. The meter should therefore be studied further to investigate how this error could be reduced at low currents.

REFERENCES

Al-Omary, A., El-Medany, W., & Al-Irhayim, S. (2011). Design and implementation of secure low cost automatic meter reading system using GPRS technology. International Conference on Telecommunication Technology and Applications, Proceedings of CSIT, 5, 138-143

Ambedkar, P. B., & Vadirajacharya, K. (2017). Automatic Meter Reading using Wireless Zigbee Based System. *International Journal of Scientific Engineering and Technology Research*, *6*(17), 3384-3387. https://www.ijsetr.com

Arun, S., & Naidu, S. (2012). Hybrid automatic meter reading system. *International Journal of Advanced Research in Computer Science and Software Engineering*, *2*(7), 361-365. http://www.ijarcsse.com

Ashiquzzaman, M., Afroze, N., & Abdullah, T. M. (2012). Design and implementation of wireless digital energy meter using microcontroller. *Global Journal of Researches in Engineering, Electrical and Electronics Engineering*, *12*(2), 30-35. https://www.academia.edu

Azasoo, J. Q. (2012). *Design of a GSM-based smart metering system* [Master's thesis, Kwame Nkrumah University of Science and Technology]. Kumasi, Ghana, 12-15

Bell, F. W. (2003). NT series magneto-resistive current sensors for peak currents up to 150A. https://www.fwbell.com

Beştepe, F. (2004). *Microcontroller-based multiport communication system for digital electricity meters* [Master's thesis, Middle East Technical University]. Beirut, Lebanon, 23-24.

Chaluvadi, V. N. H. (2008). *Accelerated life testing of electronic revenue meters* [Master's thesis, Clemson University]. Greenville, SC, 104-106

Chattopadhyay, S. (2005). *Designing energy meters with the PIC16F873A*. Application Note AN939, Microchip Technology In. http://application-notes.digchipcom

Collins, A. (1999). Solid state solutions for electricity metrology, metering and tariffs for energy supply. IEEE Symposium. https://doi.org/10.462/vr.1999.148

Collins, A., & Koon, W. (1999). A tamper-resistant watt-hour energy meter based on the AD7751 and two current sensors. Analog Electronics Application Note AN-563 (3). https://www.analog.com

Daigle, P. (1999). All-electronic power and energy meters. Analog Devices Inc. https://www.analog.com

Drafts, B. (2004). Methods of current measurement. Pacific Scientific-OECO. https://www.oeco.com

Elliot, S. R. (1990). *Physics of amorphous materials* (2nd ed.). Longman Scientific & Technical. 1-22

Enrique, G. V., Diego, R. M., Sergio, I. R. A., Jaime, S. M., Susana, C., Ricardo, F., & Paulo, F. (2017). Electronic energy meter based on a tunnel magneto-resistive effect (TMR) current sensor. *Materials*, *10*(10), 1134.

Friedrich, A. P., & Kunze, J. (2022). Universal magneto-resistive current sensor for automotive applications. *Sensitec*, *6*, 6330. https://www.researchgate.net

Glória, A. D. M. (2010). *A ZigBee automatic meter reading system* [Master's thesis, Instituto Superior Técnico, Universidade Técnica de Lisboa]. Lisbon, Portugal, 22-24. https://fenix.tecnico.ulisboa.pt

Haque, M., Hossain, K., Ali, M., & Sheikh, R. I. (2011). Microcontroller based single phase digital prepaid energy meter for improved metering and billing system. *International Journal of Power Electronics and Drive System, 1*(2), 139-147.

Hauser, H., Stangl, G., Janiba, M., & Giouroudi, I. (2006). Measurements, technology and layout of sensitive anisotropic magneto-resistive sensors. *Journal of Electrical Engineering, 57*(8) 171-174

Horowitz, P., & Hill, W. (1989). *The art of electronics* (2nd ed.). Cambridge University Press, 1007

Hou, F., & Yu, P. (2011). Implementation of a single-phase electronic watt-hour meter using the MSP430AFE2xx. Application Report, 2011-2023.

Hribik, J., Fuchs, P., Hruškovic, M., Michálek, R., & Lojko, B. (2004). Digital power and energy measurement. *Measurement Science Review*, *4*(3), 17-21.

Hübschmann, S., & Schneider, M. (1996). Magneto-resistive sensors: Principles of operation and applications. *Application Magazine*, *20*(1).

John, Q. (2012). *Customer perception and acceptability on the use of prepaid metering system in Accra west region of electricity company of Ghana* [Master's thesis, Kwame Nkrumah University of Science and Technology]. Ghana, 11-13. https://www.academia.edu

Jones, E. B. (1987). *Jones' instrument technology: Electrical and radiation measurements*. Butterworth & Co, UK, 38-40. https://books.google.co.ke

Kamilaris, A. (2012). *Enabling smart homes using web technologies* [Doctoral dissertation, University of Cyprus]. Cyprus, 49-52. https://superworld.cyens.org.cy

Kaplan, R. (2002). *Tapping the potential of electronic energy metering*. Analogue and Power Vision Supplement. https://www.analog.com

Kelly, D. A. (2011). *Disaggregating smart meter readings using device signatures* [Master's thesis, Imperial College]. London, 7-17. https://jack-kelly.com

Kittel, C. (1986). *Introduction to solid state physics* (6th ed.). John Wiley & Sons, New York, 423-459

Koon, W. (1999). Current sensing for energy metering. http://www.analog.com/energymeter

Liikkanen, L. A., & Nieminen, T. (2009). Comparison of end-user electric power meters for accuracy. *Helsinki Institute for Information Technology (HIIT) Technical Reports*, *1*, 4-13.

Mason, H. (2003). Basic introduction to the use of magneto-resistive sensors. *Application Note*, *7*(1).

McCurrie, R. A. (1994). *Ferromagnetic materials: Structure and properties*. Cambridge University Press.

Megraw, K., Mumm, D., Roodem, S., & Yockey, S. (2002). Theories and modelling of the kilowatt-hour meter. *Physics*, *222*(1), 10-15.

Muñoz, D.R., Pérez, D.M., Moreno, J.S., Berga, S.C., & Montero, S.C. (2009). Design and experimental verification of a smart sensor to measure the energy and power consumption in a one-phase AC line. *Measurement*, *42*(3), 412-419.

Nayak, P. (2013). *Implementation of single phase watt hour meter using LPC2148* [Master's thesis, National Institute of Technology Rourkela]. Rourkela, India, 19-20

Pinto, J. G. O., & Afonso, J. L. (2006). Development of a low cost digital energy meter. *Proceedings of the 3rd International Conference on Hands-on Science – Science Education and Sustainable Development*, University of Minho, Braga, Portugal, 257-261

Raposo, V., Garcia, D., Montero, O., Flores, A. G., & Iniguez, J. I. (2004). Analysis of the frequency dependence of the magneto-impedance in current annealed amorphous wires. *Journal of Optoelectronics and Advanced Materials*, *6*(2), 575-580.

Ripka, P. (2004). Current sensors using magnetic materials. *Journal of Optoelectronics and Advanced Materials*, *6*(2), 587-592.

Ripka, P., Tondra, M., Stokes, J., & Beech, R. (1998). AC-driven AMR and GMR magneto-resistors. Eurosensors XII Proceedings, 967-969.

Seal, B., & McGranaghan, M. (2010). Accuracy of digital electricity meters. Electric Power Research Institute (EPRI), Inc. https://www.epri.com

Seppälä, A. (1996). *Load research and load estimation in electricity distribution* [Doctoral dissertation, Helsinki University of Technology]. Espoo, Finland, 12-17 https://publications.vtt.fi/pdf/publications/1996//p289.pdf

Shahrara, R. (2011). *Design and implementation of a microcontroller based wireless energy meter* [Master's thesis, Eastern Mediterranean University]. Gazimağusa, North Cyprus, 21-22

Shomuyiwa, D. A., & Ilevbare, J. O. (2013). Design and implementation of remotely-monitored single phase smart energy meter via short message service (SMS). *International Journal of Computer Applications*, *74*(9), 14-22.

Srividyadevi, P., Pusphalatha, D. V., & Sharma, P. M. (2010). Measurement of power and energy using Arduino. *Research Journal of Engineering Sciences*, *2*(10), 10-15.

Veerabadhra, G. R. V. K. (2011). *Agent based economic framework for resource distribution in household smart grid* [Master's thesis, Delft University of Technology]. Netherlands.

Volokhin, V., & Diahovchenko, I. (2017). Peculiarities of current sensors used in contemporary electric energy metering devices. *Energetika*, *63*(1), 8-15. https://doi.org/10.6001/energetika.v63i1.3504

Xu, Y., & Lorenz, R. D. (2002). *Design of integrated shunt current sensors for IPEM* [Master's thesis, University of Wisconsin]. Madison, USA.

Yan, S., Zhou, Z., Yang, Y., Leng, O., & Zhao, W. (2022). Developments and applications of tunneling magneto-resistance sensors. *Tsinghua Science and Technology*, 27(3), 443-454.
http:www.ijcaonline.org

Ziegler, S., Robert, C., Woodward, H., Ho-Ching, I., & Lawrence, J. B. (2009). Current sensing techniques. *IEEE Sensors Journal*, *9*(4), 354-376. https://ieeexplore.ieee.org

APPENDICES

Appendix A: Preparations for Experiments and Data Collection

Plate A-1: Student sets up laboratory instruments to carry out experiments

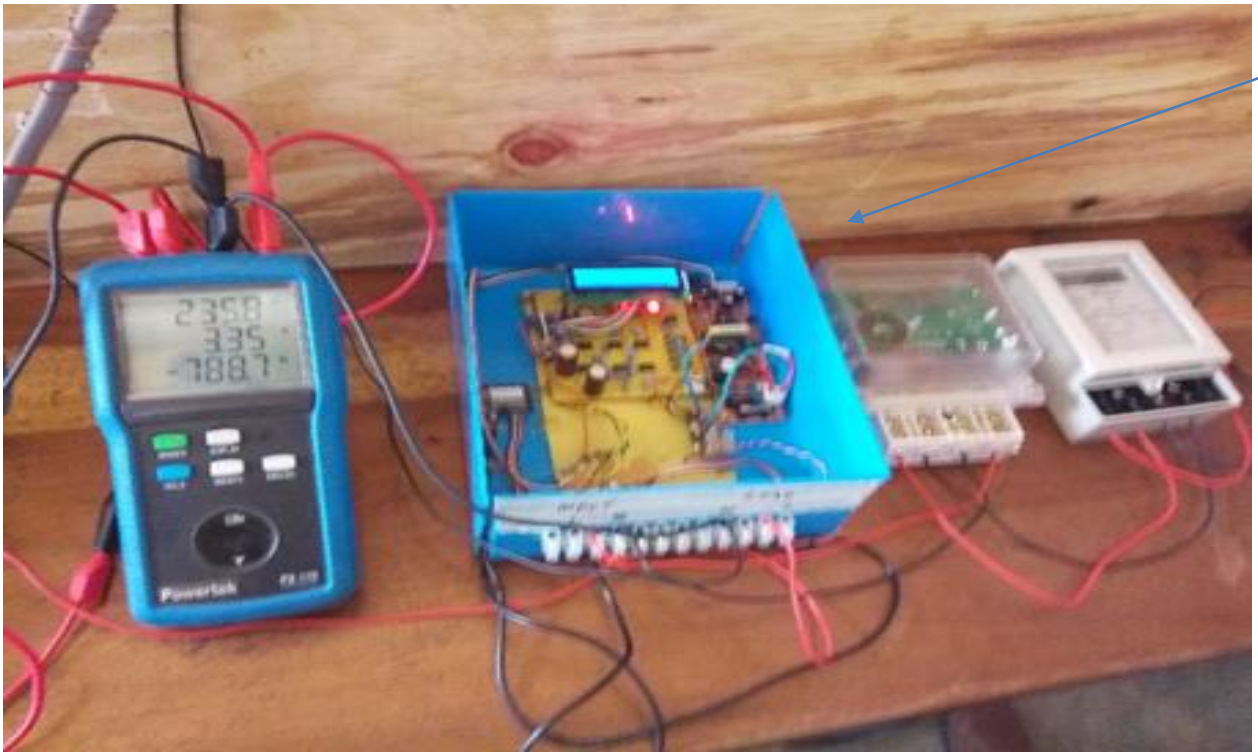

Plate A-2: Four desk-top instruments connected to record data

Plate A-3: Vertically-mounted energy meter and other instruments for data collection

Plate A-4: Fabricated energy meter displaying voltage, current, pf, ‘real’ power consumed and cumulated electrical energy

Plate A-5: 240V 100W bulbs and 1.2M × 36W fluorescent fittings connected in parallel for data collection

Appendix B: Microcontroller C-Code for AMR Energy Meter

```
#include<EEPROM.h>
 #include <LiquidCrystal.h>
constintrs = 14, en = 16, d4 = 10, d5 = 9, d6 = 8, d7 = 7;
LiquidCrystallcd(rs, en, d4, d5, d6, d7);

float b, a,d,e,f=0;
floatg,h,i,j;
float count;
float   Energy;

// the setup routine runs once when you press reset:
void setup() {
lcd.begin(20, 4);
  // initialize serial communication at 9600 bits per second:
Serial.begin(9600);
count =  EEPROM.get(0,f);
}

// the loop routine runs over and over again forever:
void loop() {

for(int x=0;x<10000;x++){
intsensorValue = analogRead(A2);
int sensorValue1 = analogRead(A1);
  a =((sensorValue 0.00488)-2.31);
  e= ((sensorValue1 0.00488)-2.31)/5.75;
  b+=(a a);
  d+=(e e);
g+= a e;
  }
float c = sqrt(b/10000) 10;
float f = sqrt(d/10000) 1000;
float h= (c f);
```

```
floatpf = g/(c f);
   Energy += (g/3600000);
if(Energy>=0.001){
count +=0.001;
EEPROM.put(0,count);
    Energy -=0.001;
   }
lcd.clear();
lcd.setCursor(0,0);
lcd.print(c,3);
lcd.print("A");
lcd.setCursor(14,0);
lcd.print(f,0);
lcd.print("V");
lcd.setCursor(0,1);
lcd.print(h/1000,3);
lcd.print("kVA");
lcd.setCursor(0,2);
lcd.print(g/1000,3);
lcd.print("kW");
lcd.setCursor(14,2);
lcd.print(pf,2);
lcd.print("pf");
lcd.setCursor(0,3);
lcd.print(count,3);
lcd.print("kWh");
  b=0;
  d=0;
  g=0;
}
```

Appendix C: Table of Regression Statistics from EXCEL

SUMMARY OUTPUT

Regression Statistics	
Multiple R	0.9999937
R Square	0.9999874
Adjusted R Square	0.9999862
Standard Error	0.0007213
Observations	12

ANOVA

	df	*SS*	*MS*	*F*	*Significance F*
Regression	1	0.413381465	0.41338146	794644.35	7.76625E-26
Residual	10	5.20209E-06	5.2021E-07		
Total	11	0.413386667			

	Coefficients	*Standard Error*	*t Stat*	*P-value*	*Lower 95%*	*Upper 95%*
Intercept	0.000600893	0.000412142	1.45797607	0.17552586	-0.000317416	0.0015192
X Variable 1	0.099821316	0.000111979	891.428264	7.7663E-26	0.099571811	0.1000708

Appendix D: Experimental Results And Statistical Data Analysis

Table D-1 (a): Effects of varying load on current and voltage

Load: 240V 100W incandescent bulbs connected in parallel

Electrical loads	**Current (A)**					**Voltage (V)**		
(W)	I1	I2	IBM	IFM	I5	V1	VBM	FM
100	0.42	0.415	0.422	0.45	0.428	232	235	228
200	0.81	0.808	0.82	0.85	0.825	232	235	228
300	1.2	1.2	1.227	1.25	1.22	230	232	227
400	1.63	1.63	1.66	1.68	1.654	230	232	227
500	2.04	2.04	2.07	2.08	2.03	230	233	228
600	2.45	2.45	2.48	2.49	2.48	231	233	228
700	2.85	2.85	2.9	2.9	2.88	222	231	226
800	3.21	3.21	3.25	3.23	3.24	222	225	219
900	3.62	3.62	3.67	3.64	3.66	225	226	222
1000	4.04	4.04	4.08	4.06	4.05	228	230	225
1200	4.83	4.81	4.88	4.85	4.85	224	227	221
1400	5.67	5.65	5.74	5.68	5.69	225	228	223
1600	6.48	6.46	6.54	6.49	6.49	226	229	224

Table D-1 (b): Effects of varying load on current and voltage

Load: 1.2M × 36W fluorescent fittings

Electrical loads	**Current (A)**					**Voltage (V)**		
(W)	I1	I2	IBM	IFM	I5	V1	VBM	VFM
36W	0.38	0.38	0.39	0.46	0.34	230	233	227
72W	0.76	0.76	0.78	0.83	0.72	231	233	228
108W	1.12	1.12	1.14	1.2	1.07	232	233	228
144W	1.45	1.45	1.49	1.54	1.44	230	232	228
180W	1.81	1.81	1.89	1.78	1.77	233	234	229

Table D-1 (c): Effect of varying load on current and voltage

Load: 240V 100W and 1.2M × 36W fluorescent fittings

Electrical loads (W)		**Current (A)**					**Voltage (V)**		
1.2M×36W Fluorescents	100W Bulbs	I1	I2	IBM	IFM	I5	V1	VBM	VFM
72	200	1.38	1.38	1.38	1.45	1.38	230	231	226
108	300	2.07	2.07	2.05	2.1	2.05	231	232	227
144	400	2.76	2.76	2.73	2.77	2.75	230	231	225
180	500	3.41	3.41	3.39	3.41	3.42	230	231	226
180	700	3.76	3.76	3.73	3.74	3.75	228	230	224
180	900	4.85	4.84	4.84	4.83	4.86	227	229	224
180	1100	5.59	5.57	5.57	5.55	5.59	225	227	222
180	1300	6.31	6.33	6.33	6.31	6.35	224	226	221
180	1500	6.77	6.75	6.76	6.72	6 .79	227	229	224

Appendix E: Measurements of current, voltage, pf, power and electrical energy for selected electrical loads over 15 minutes

Table E: Electrical loads

Electrical loads	Description
L1	14 100 Watt bulbs
L2	5 36W 4ft fluorescent lights plus 8 100 Watt bulbs
L3	5 36W 4ft fluorescent lights plus 15 100 Watt bulbs
L4	8 100 Watt bulbs
L5	15 100 Watt bulbs

Table E-1 (a): Load L1

Time (mins)	**Current (A)**			**Voltage (V)**			**Power factor**		**Power (w)**		**Electrical Energy (kWh)**				
	I1	IBM	IFM	V1	VBM	VFM	pfBM	pfFM	PBM	PFM	EBM	EFM	EM1	EM2	EM3
0	5.66	5.69	5.61	227	228	228	1	1	1301	1200	0	0	0	0	0
5	5.66	5.69	5.61	227	226	227	1	1	1311	1200	0.109	0.11	0.11	0.1	0.11
5	5.65	5.69	5.61	227	226	227	1	1	1310	1200	0.109	0.11	0.11	0.1	0.12
5	5.65	5.69	5.61	227	228	227	1	1	1308	1200	0.109	0.11	0.11	0.1	0.12

Table E-1 (b): Load L2

Time (mins)	**Current (A)**			**Voltage (V)**			**Power factor**		**Power (w)**		**Electrical Energy (kWh)**				
	I1	IBM	IFM	V1	VBM	VFM	pfBM	pfFM	PBM	PFM	EBM	EFM	EM1	EM2	EM3
0	4.54	4.5	4.45	228	230	230	0.94	0.96	984	991	0	0	0	0	0
5	4.58	4.52	4.46	231	231	233	0.94	0.96	1002	1020	0.084	0.1	0.09	0.1	0.1
5	4.55	4.51	4.43	230	232	231	0.94	0.96	990	991	0.083	0.09	0.08	0.1	0.09
5	4.53	4.49	4.44	230	232	231	0.94	0.96	991	995	0.083	0.09	0.09	0.1	0.1

Table E-1 (c): Load L3

Time (mins)	Current (A)			Voltage (V)			Power factor		Power (w)		Electrical Energy (kWh)				
	I1	IBM	IFM	V1	VBM	VFM	pfBM	pfFM	PBM	PFM	EBM	EFM	EM1	EM2	EM3
0	7.2	7.15	7.04	227	229	229	0.98	0.99	1609	1610	0	0	0	0	0
5	7.2	7.15	7.0	226	228	227	0.98	0.99	1586	1580	0.132	0.15	0.14	0.2	0.15
5	7.26	7.19	7.01	229	231	231	0.98	0.99	1626	1620	0.136	0.14	0.14	0.1	0.15
5	7.24	7.18	7.08	228	230	230	0.98	0.99	1624	1620	0.135	0.14	0.14	0.2	0.17

Table E-1 (d): Load L4

Time (mins)	Current (A)			Voltage (V)			Power factor		Power (w)		Electrical Energy (kWh)				
	I1	IBM	IFM	V1	VBM	VFM	pfBM	pfFM	PBM	PFM	EBM	EFM	EM1	EM2	EM3
0	3.34	3.36	3.31	234	236	236	1	1	800	789	0	0	0	0	0
5	3.32	3.33	3.26	231	234	233	1	1	785	769	0.065	0.07	0.07	0.1	0.07
5	3.33	3.34	3.30	235	236	234	1	1	788	773	0.066	0.06	0.06	0	0.07
5	3.35	3.38	3.33	236	239	228	1	1	805	794	0.067	0.08	0.07	0.1	0.07

Table E-1 (e): Load L5

Time (mins)	Current (A)			Voltage (V)			Power factor		Power (w)		Electrical Energy (kWh)				
	I1	IBM	IFM	V1	VBM	VFM	pfBM	pfFM	PBM	PFM	EBM	EFM	EM1	EM2	EM3
0	6.19	6.18	6.08	232	234	233	1	1	1435	1420	0	0	0	0	0
5	6.17	6.15	6.06	230	233	232	1	1	1428	1400	0.119	0.14	0.14	0.2	0.15
5	6.18	6.16	6.08	230	233	232	1	1	1437	1410	0.12	0.12	0.11	0.1	0.13
5	6.17	6.16	6.08	231	232	233	1	1	1445	1420	0.12	0.11	0.12	0.1	0.12

Appendix E-2: Analysis of Current

Table E-2 (a) (i): ANOVA outputs of current

Class	Levels		Values	
Rep	3	5	10	15
Error	3	I1	IBM	IFM
Number of observations:	9			

Table E-2 (a) (ii): ANOVA summary of currents measured on five different loads.

Load	R-Square	Coeff Var	Root MSE	Mean Current	F Value	LSD
L1	0.977401	0.144513	0.008165	5.650000	86.00	<.0005
L2	0.984848	0.223214	0.010000	4.480000	121.00	<.0003
L3	0.947124	0.447299	0.031798	7.108889	34.46	<.0030
L4	0.976190	0.173378	0.005774	3.330000	43.00	<.0020
L**5**	0.993695	0.085916	0.005270	6.134444	310.00	<.0001

Table E-2 (b): Dependent variable - L1

Source	DF	Sum of Squares	Mean Square	F Value	Pr > F
Model	4	0.01153333	0.00288333	43.25	0.0015
Error	4	0.00026667	0.00006667		
Corrected Total	8	0.01180000			

R-Square	Coeff Var	Root MSE	L1 Mean
0.977401	0.144513	0.008165	5.65000

Source	DF	Anova SS	Mean Square	F Value	Pr > F
Rep	2	0.00006667	0.00003333	0.50	<.6400
Variety	2	0.01146667	0.00573333	86.00	<.0005

Table E-2 (c): Dependent variable – L2

Source	DF	Sum of Squares	Mean Square	F Value	Pr > F
Model	4	0.02600000	0.00650000	65.00	<.0007
Error	4	0.00040000	0.00010000		
Corrected Total	8	0.02640000			

R-Square	Coeff Var	Root MSE	L2 Mean
0.984848	0.223214	0.010000	4.480000

Source	DF	Anova SS	Mean Square	F Value	Pr > F
Rep	2	0.00180000	0.00090000	9.00	<.0331
Variety	2	0.02420000	0.01210000	121.00	<.0003

Table E-2 (d): Dependent variable – L

Source	DF	Sum of Squares	Mean Square	F Value	Pr > F
Model	4	0.07244444	0.01811111	17.91	<.0081
Error	4	0.00404444	0.00101111		
Corrected Total	8	0.07648889			

R-Square	Coeff Var	Root MSE	L3 Mean
0.947124	0.447299	0.031798	7.10888

Source	DF	Anova SS	Mean Square	F Value	Pr > F
Rep	2	0.00275556	0.00137778	4 1.36	<.3538
Variety	2	0.06968889	0.03484444	34.46	<.0030

Table E-2 (e): Dependent variable – L4

Source	DF	Sum of Squares	Mean Square	F Value	Pr > F
Model	4	0.00546667	0.00136667	41.00	<.0017
Error	4	0.00013333	0.00003333		
Corrected Total	8	0.00560000			

R-Square	Coeff Var	Root MSE	L4 Mean
0.976190	0.173378	0.005774	3.330000

Source	DF	Anova SS	Mean Square	F Value	Pr > F
Rep	2	0.00260000	0.00130000	39.00	<.0024
Variety	2	0.00286667	0.00143333	43.00	<.0020

Table E-2 (f): Dependent variable – L5

Source	DF	Sum of Squares	Mean Square	F Value	Pr > F
Model	4	0.01751111	0.00437778	157.60	<.0001
Error	4	0.00011111	0.00002778		
Corrected Total	8	0.01762222			

R-Square	Coeff Var	Root MSE	L5 Mean
0.993695	0.085916	0.005270	6.134444

Source	DF	Anova SS	Mean Square	F Value	Pr > F
Rep	2	0.00028889	0.00014444	5.20	<.0772
Variety	2	0.01722222	0.00861111	310.00	<.0001

Table E-2 (g): t-Test (LSD) for L1

Alpha	0.05
Error Degrees of Freedom	4
Error Mean Square	0.000067
Critical Value of t	2.77645
Least Significant Difference	0.0185

t-Grouping	Mean (Amps)	N	Current
A	5.690000	3	IBM
B	5.656667	3	I1
C	5.603333	3	IFM

NB: Means with the same letter in the same column are not significantly different

Table E-2 (h): t-Test (LSD) for L2

Alpha	0.05
Error Degrees of Freedom	4
Error Mean Square	0.0001
Critical Value of t	2.77645
Least Significant Difference	0.0227

t-Grouping	Mean (Amps)	N	Current
B	4.443333	3	IBM
A	4.553333	3	I1
B	4.443333	3	IFM

NB: Means with the same letter in the same column are not significantly different

Table E-2 (i): t-Test (LSD) for L3

Alpha	0.05
Error Degrees of Freedom	4
Error Mean Square	0.001011
Critical Value of t	2.77645
Least Significant Difference	0.0721

t-Grouping	Mean (Amps)	N	Current
B	7.04667	3	IBM
A	7.23333	3	I1
B	7.04667	3	IFM

NB: Means with the same letter in the same column are not significantly different

Table E-2 (j): t-Test (LSD) for L4

Alpha	0.05
Error Degrees of Freedom	4
Error Mean Square	0.000033
Critical Value of t	2.77645
Least Significant Difference	0.0131

t-Grouping	Mean (Amps)	N	Current
A	3.350000	3	IBM
B	3.333333	3	I1
C	3.306667	3	IFM

NB: Means with the same letter in the same column are not significantly different

Table E-2 (k): t-Test (LSD) for L5

Alpha	0.05
Error Degrees of Freedom	4
Error Mean Square	0.000028
Critical Value of t	2.77645
Least Significant Difference	0.0119

t-Grouping	Mean (Amps)	N	Current
B	6.156667	3	IBM
A	6.173333	3	I1
B	6.073333	3	IFM

NB: Means with the same letter in the same column are not significantly different

Appendix E-3: Analysis of Voltage

Table E-3 (a) (i): ANOVA outputs of voltage

Class	Levels	Values		
Rep	3	5	10	15
Error	3	V1	VBM	VFM
Number of observations:	9			

Table E-3 (a) (ii): ANOVA summary of voltages for various loads

Load	**R-Square**	**Coeff Var**	**Root MSE**	**Mean Voltage**	**F Value**	**LSD**
L1	0.384615	0.293830	0.666667	226.8889	0.25	<.7901
L2	0.953488	0.144161	0.333333	231.2222	16.00	<.0123
L3	0.982143	0.145631	0.333333	228.8889	31.00	<.0037
L4	0.991379	0.141978	0.333333	234.7778	49.00	<.0015
L5	0.880184	0.516801	1.201850	232.5556	11.38	<.0223

Table E-3 (b): Dependent variable - L1

Source	**DF**	**Sum of Squares**	**Mean Square**	**F Value**	**Pr > F**
Model	4	1.11111111	0.27777778	0.63	<.6700
Error	4	1.77777778	0.44444444		
Corrected Total	8	2.88888889			

R-Square	Coeff Var	Root MSE	L1 Mean
0.384615	0.293830	0.666667	226.8889

Source	**DF**	**Anova SS**	**Mean Square**	**F Value**	**Pr > F**
Rep	2	0.88888889	0.44444444	1.00	<.4444
Variety	2	0.22222222	0.11111111	0.25	<.7901

Table E-3 (c): Dependent variable – L2

Source	DF	Sum of Squares	Mean Square	F Value	Pr > F
Model	4	9.11111111	2.27777778	20.50	<.0063
Error	4	0.44444444	0.11111111		
Corrected Total	8	9.55555556			

R-Square	Coeff Var	Root MSE	L2 Mean
0.953488	0.144161	0.333333	231.2222

Source	DF	Anova SS	Mean Square	F Value	Pr > F
Rep	2	5.55555556	2.77777778	25.00	<.0055
Voltage	2	3.55555556	1.77777778	16.00	<.0123

Table E-3 (d): Dependent variable - L3

Source	DF	Sum of Squares	Mean Square	F Value	Pr > F
Model	4	24.44444444	6.11111111	55.00	0.0009
Error	4	0.44444444	0.11111111		
Corrected Total	8	24.88888889			

R-Square	Coeff Var	Root MSE	L3 Mean
0.982143	0.145631	0.333333	228.8889

Source	DF	Anova SS	Mean Square	F Value	Pr > F
Rep	2	17.55555556	8.77777778	79.00	<.0006
Voltage	2	6.88888889	3.44444444	31.00	<.0037

Table E-3 (e): Dependent variable – L4

Source	DF	Sum of Squares	Mean Square	F Value	Pr > F
Model	4	51.11111111	12.77777778	115.00	0.0002
Error	4	0.44444444	0.11111111		
Corrected Total	8	51.55555556			

R-Square	Coeff Var	Root MSE	L4 Mean
0.991379	0.141978	0.333333	234.77

Source	DF	Anova SS	Mean Square	F Value	Pr > F
Rep	2	40.22222222	20.11111111	181.00	<.0001
Voltage	2	10.88888889	5.44444444	49.00	<.001

Table E-3 (f): Dependent variable – L5

Source	DF	Sum of Squares	Mean Square	F Value	Pr > F
Model	4	42.44444444	10.61111111	7.35	0.0396
Error	4	5.77777778	1.44444444		
Corrected Total	8	48.2222222			

R-Square	Coeff Var	Root MSE	L5 Mean
0.880184	0.516801	1.201850	232.5556

Source	DF	Anova SS	Mean Square	F Value	Pr > F
Rep	2	9.55555556	4.77777778	3.31	0.1420
Voltage	2	32.88888889	16.44444444	11.38	0.0223

Table E-3 (g): t-Test (LSD) for L1

Alpha	0.05
Error Degrees of Freedom	4
Error Mean Square	0.444444
Critical Value of t	2.77645
Least Significant Difference	1.5113

t-Grouping	Mean (Volts)	N	Voltage
A	226.6667	3	VBM
A	227.0000	3	V1
A	227.0000	3	VFM

NB: Means with the same letter in the same column are not significantly different

Table E-3 (h): t-Test (LSD) for L2

Alpha	0.05
Error Degrees of Freedom	4
Error Mean Square	0.111111
Critical Value of t	2.77645
Least Significant Difference	0.7557

t-Grouping	Mean (Volts)	N	Voltage
A	231.6667	3	VBM
B	230.3333	3	V1
A	231.6667	3	VFM

NB: Means with the same letter in the same column are not significantly different

Table E-3 (i): t-Test (LSD) for L3

Alpha	0.05
Error Degrees of Freedom	4
Error Mean Square	0.111111
Critical Value of t	2.77645
Least Significant Difference	0.7557

t-Grouping	Mean (Volts)	N	Voltage
A	229.6667	3	VBM
B	227.6667	3	V1
A	229.3333	3	VFM

NB: Means with the same letter in the same column are not significantly different

Table E-3 (j): t-Test (LSD) for L4

Alpha	0.05
Error Degrees of Freedom	4
Error Mean Square	0.111111
Critical Value of t	2.77645
Least Significant Difference	0.7557

t-Grouping	Mean (Volts)	N	Voltage
A	236.0000	3	VBM
C	233.3333	3	V1
B	235.0000	3	VFM

NB: Means with the same letter in the same column are not significantly different

Table E-3 (k): t-Test (LSD) for L5

Alpha	0.05
Error Degrees of Freedom	4
Error Mean Square	1.444444
Critical Value of t	2.77645
Least Significant Difference	0.7245

t-Grouping	Mean (Volts)	N	Voltage
A	235.0000	3	VBM
B	230.3333	3	V1
BA	232.3333	3	VFM

NB: Means with the same letter in the same column are not significantly different

Appendix E-4: Analysis of power factor

Table E-4 (a) (i: ANOVA outputs of power factor

Class	Levels	Values
Rep	3	5 10 15
Error	2	pfBM pfFM
Number of observations:	6	

Table E-4 (a) (ii): ANOVA summary of pfs

Load	R-Square	Coeff Var	Root MSE	Mean pf	F Value	LSD
L1	0	0	0	1	.	.
L2	1	0	0	0.95	Infinity	
<.0001						
L3	1	1.07024E-7	1.05419E-9	0.985	1.35E14	
<.0001						
L4	0	0	0	1	.	.
L5	0	0	0	1	.	.

Table E-4 (b): Dependent variable – L1

Source	DF	Sum of Squares	Mean Square	F Value	Pr > F
Model	3	0	0	.	.
Error	2	0	0		
Corrected Total	5	0			

R-Square	Coeff Var	Root MSE	L1 Mean
0.000000	0	0	1.000000

Source	DF	Anova SS	Mean Square	F Value	Pr > F
Rep	2	0	0	.	.
Power factor	1	0	0	.	

Table E-4 (c): Dependent variable – L2

Source	DF	Sum of Squares	Mean Square	Value	Pr > F
Model	3	0.0006	0.0002	Infty	<.0001
Error	2	0	0		
Corrected Total	5	0.0006			

	R-Square	Coeff Var	Root MSE	L2 Mean
	1	0	0	0.95

Source	DF	Anova SS	Mean Square	F Value	Pr > F
Rep	2	0	0	.	.
Power Factor	1	0.0006	0.0006	Infty	<.0001

Table E-4 (d): Dependent variable – L3

Source	DF	Squares	Square	F Value	Pr > F
Model	3	0.00015	0.00005	4.5E13	<.0001
Error	2	0	0		
Corrected Total	5	0.00015			

	R-Square	Coeff Var	Root MSE	L3 Mean
	1	1.07024E-7	1.05419E-9	0.985

Source	DF	Anova SS	Mean Square	F Value	Pr > F
Rep	2	0	0	0	0
Variety	1	0.00015	0.00015	1.35E14	<.0001

Table E-4 (e): Dependent variable - L4

Source	DF	Sum of Squares	Mean Square	F Value	Pr > F
Model	3	0	0	.	.
Error	2	0	0		
Corrected Total	5	0			

	R-Square	Coeff Var	Root MSE	L4 Mean
	0	0	0	1

Source	DF	Anova SS	Mean Square	F Value	Pr > F
Rep	2	0	0	.	.
Variety	1	0	0	.	.

Table E-4 (f): Dependent variable – L5

Source	DF	Sum of Squares	Mean Square	F Value	Pr > F
Model	3	0	0	.	.
Error	2	0	0		
Corrected Total	5	0			

R-Square	Coeff Var	Root MSE	L5 Mean
0	0	0	1

Source	DF	Anova SS	Mean Square	F Value	Pr > F
Rep	2	0	0	.	.
Power Factor	1	0	0	.	.

Table E-4 (g): t-Test (LSD) for L1

Alpha	0.05
Error Degrees of Freedom	2
Error Mean Square	0
Critical Value of t	4.30265
Least Significant Difference	0

t-Grouping	Mean	N	Power factor
A	1.0	3	pfBM
A	1.0	3	pfFM

NB: Means with the same letter in the same column are not significantly different

Table E-4 (h): t-Test (LSD) for L2

Alpha	0.05
Error Degrees of Freedom	2
Error Mean Square	0
Critical Value of t	4.30265
Least Significant Difference	0

t-Grouping	Mean	N	Power Factor
B	0.9400	3	pfBM
A	0.9600	3	pfFM

NB: Means with the same letter in the same column are not significantly different

Table E-4 (i): t-Test (LSD) for L3

Alpha	0.05
Error Degrees of Freedom	2
Error Mean Square	1.11E-18
Critical Value of t	4.30265
Least Significant Difference	37E-10

t-Grouping	Mean	N	Power Factor
B	0.98000000	3	pfBM
A	0.99000000	3	pfFM

NB: Means with the same letter in the same column are not significantly different

Table E-4 (j): t-Test (LSD) for L4

Alpha	0.05
Error Degrees of Freedom	2
Error Mean Square	0
Critical Value of t	4.30265
Least Significant Difference	0

t-Grouping	Mean	N	Power Factor
A	1.0	3	pfBM
A	1.0	3	pfFM

NB: Means with the same letter in the same column are not significantly different

Table E-4 (k): t-Test (LSD) for L5

Alpha	0.05
Error Degrees of Freedom	2
Error Mean Square	0
Critical Value of t	4.30265
Least Significant Difference	0

t Grouping	Mean	N	Power Factor
A	1.0	3	pfBM
A	1.0	3	pfFM

NB: Means with the same letter in the same column are not significantly different

Appendix E-5: Analysis of Power

Table E-5 (a) (i): ANOVA outputs of power

Class	Levels	Values
Rep	3	5 10 15
Error	2	PBM PFM
Number of observations:	6	

Table E-5 (a) (ii): ANOVA Summary of Power

Load	R-Square	Coeff Var	Root MSE	Mean Power	F Value	LSD
L1	0.998239	0.083418	1.080123	1294.833	1131.57	<.0009
L2	0.877267	0.642791	6.416126	998.1667	2.14	<.2809
L3	0.999373	0.050735	0.816497	1609.333	64.00	<.0153
L4	0.992111	0.238120	1.870829	785.6667	84.00	<.0117
L5	0.998347	0.075887	1.080123	1423.333	914.29	<.0011

Table E-5 (b): Dependent variable - L1

Source	DF	Sum of Squares	Mean Square	F Value	Pr > F
Model	3	1322.500000	440.833333	377.86	<.0026
Error	2	2.333333	1.166667		
Corrected Total	5	1324.833333			

R-Square	Coeff Var	Root MSE	L1 Mean
0.998239	0.083418	1.080123	1294.833

Source	DF	Anova SS	Mean Square	F Value	Pr > F
Rep	2	2.333333	1.166667	1.00	<.5000
Variety	1	1320.166667	1320.166667	1131.57	<.0009

Table E-5 (c): Dependent variable - L2

Source	DF	Sum of Squares	Mean Square	F Value	Pr > F
Model	3	588.5000000	196.1666667	4.77	<.1783
Error	2	82.3333333	41.1666667		
Corrected Total	5	670.8333333			

R-Square	Coeff Var	Root MSE	L2 Mean
0.877267	0.642791	6.416126	998.1667

Source	DF	Anova SS	Mean Square	F Value	Pr > F
Rep	2	500.3333333	250.1666667	6.08	<.1413
Variety	1	88.1666667	88.1666667	2.14	<.2809

Table E-5 (d): Dependent variable – L3

Source	DF	Sum of Squares	Mean Square	F Value	Pr > F
Model	3	2124.000000	708.000000	1062.00	<.0009
Error	2	1.333333	0.666667		
Corrected Total	5	2125.333333			

R-Square	Coeff Var	Root MSE	L3 Mean
0.999373	0.050735	0.816497	1609.333

Source	DF	Anova SS	Mean Square	F Value	Pr > F
Rep	2	2081.333333	1040.666667	1561.00	<.0006
Variety	1	42.666667	42.666667	64.00	<.015

Table E-5 (e): Dependent variable - L4

Source	DF	Sum of Squares	Mean Square	F Value	Pr > F
Model	3	880.3333333	293.4444444	83.84	<.0118
Error	2	7.0000000	3.5000000		
Corrected Total	5	887.3333333			

R-Square	Coeff Var	Root MSE	L4 Mean
0.992111	0.238120	1.870829	785.6667

Source	DF	Anova SS	Mean Square	F Value	Pr >
Rep	2	586.3333333	293.1666667	83.76	<.0118
Variety	1	294.0000000	294.0000000	84.00	<.0117

Table E-5 (f): Dependent variable - L5

Source	DF	Sum of Squares	Mean Square	F Value	Pr > F
Model	3	1409.000000	469.666667	402.57	<.0025
Error	2	2.333333	1.166667		
Corrected Total	5	1411.333333			

R-Square	Coeff Var	Root MSE	L5 Mean
0.998347	0.075887	1.080123	1423.333

Source	DF	Anova SS	Mean Square	F Value	Pr > F
Rep	2	342.333333	171.166667	146.71	<.0068
Variety	1	1066.666667	1066.666667	914.29	<.0011

Table E-5 (h): t-Test (LSD) for L1

Alpha	0.05
Error Degrees of Freedom	2
Error Mean Square	1.166667
Critical Value of t	4.30265
Least Significant Difference	3.7946

t-Grouping	Mean (Watts)	N	Power
A	1309.6667	3	PBM
B	1280.0000	3	PFM

NB: Means with the same letter in the same column are not significantly different

Table E-5 (i): t-Test (LSD) for L2

Alpha	0.05
Error Degrees of Freedom	2
Error Mean Square	41.166667
Critical Value of t	4.30265
Least Significant Difference	22.54

t-Grouping	Mean (Watts)	N	Power
A	994.333	3	PBM
B	1002.000	3	PFM

NB: Means with the same letter in the same column are not significantly different

Table E-5 (j): t-Test (LSD) for L3

Alpha	0.05
Error Degrees of Freedom	2
Error Mean Square	0.666667
Critical Value of t	4.30265
Least Significant Difference	2.8684

t-Grouping	Mean (Watts)	N	Power
A	1612.0000	3	PBM
B	1606.6667	3	PFM

NB: Means with the same letter in the same column are not significantly different

Table E-5 (k): t-Test (LSD) for L4

Alpha	0.05
Error Degrees of Freedom	2
Error Mean Square	3.5
Critical Value of t	4.30265
Least Significant Difference	6.5724

t-Grouping	Mean (Watts)	N	Power
A	792.667	3	PBM
B	778.667	3	PFM

NB: Means with the same letter in the same column are not significantly different

Table E-5 (l): t-Test (LSD) for L5

Alpha	0.05
Error Degrees of Freedom	2
Error Mean Square	1.166667
Critical Value of t	4.30265
Least Significant Difference	3.7946

t-Grouping	Mean (Watts)	N	Power
A	1436.6667	3	PBM
B	1410.0000	3	PFM

NB: Means with the same letter in the same column are not significantly different

Table E-6 (a) (ii): ANOVA Summary for Electrical Energy

Load	R-Square	Coeff Var	Root MSE	Mean Energy	F Value	LSD
L1	0.772256	3.038671	0.003361	0.110618	4.85	<.0481
L2	0.860865	3.984406	0.003581	0.089883	9.16	<.0117
L3	0.748140	4.837422	0.006946	0.143583	5.59	<.0358
L4	0.538341	7.145024	0.004872	0.068183	0.56	<.6585
L5	0.722079	7.126549	0.008902	0.124917	1.30	<.356

Table E-6 (b): Dependent Variable - L1

Source	DF	Sum of Squares	Mean Square	F Value	Pr > F
Model	5	0.00022987	0.00004597	4.07	<.0586
Error	6	0.00006779	0.00001130		
Corrected Total	11	0.00029766			

R-Square	Coeff Var	Root MSE	L1 Mean
0.772256	3.038671	0.003361	0.11061

Source	DF	Anova SS	Mean Square	F Value	Pr > F
Rep	2	0.00006557	0.00003279	2.90	0.1313
Electrical Energy	3	0.00016430	0.00005477	4.85	0.0481

Table E-6 (c): Dependent Variable – L2

Source	DF	Sum of Squares	Mean Square	F Value	Pr > F
Model	5	0.00047614	0.00009523	7.42	<.0150
Error	6	0.00007696	0.00001283		
Corrected Total	11	0.00055310			

R-Square	Coeff Var	Root MSE	L2 Mean
0.860865	3.984406	0.003581	0.089883

Source	DF	Anova SS	Mean Square	F Value	Pr > F
Rep	2	0.00012365	0.00006183	4.82	<.0565
Variety	3	0.00035249	0.00011750	9.16	<.0117

Table E-6 (d): Dependent Variable – L3

Source	DF	Sum of Squares	Mean Square	F Value	Pr > F

Model	5	0.00085983	0.00017197	3.56	0.0767
Error	6	0.00028946	0.00004824		
Corrected Total	11	0.00114928			

R-Square	Coeff Var	Root MSE	L3 Mean
0.748140	4.837422	0.006946	0.143583

Source	DF	Anova SS	Mean Square	F Value	Pr > F
Rep	2	0.00005091	0.00002545	0.53	0.6151
Variety	3	0.00080892	0.00026964	5.59	0.0358

Table E-6 (e): Dependent Variable – L4

Source	DF	Sum of Squares	Mean Square	F Value	Pr > F
Model	5	0.00123542	0.00024708	3.12	0.0994
Error	6	0.00047550	0.00007925		
Corrected Total	11	0.00171092			

R-Square	Coeff Var	Root MSE	L4 Mean
0.722079	7.126549	0.008902	0.

Source	DF	Anova SS	Mean Square	F Value	Pr > F
Rep	2	0.00092517	0.00046258	5.84	0.0391
Electrical Energy	3	0.00031025	0.00010342	1.30	0.3563

Table E-6 (f): Dependent Variable – L5

Source	DF	Sum of Squares	Mean Square	F Value	Pr > F
Model	6	0.00152126	0.00025354	2.89	0.0744
Error	9	0.00079004	0.00008778		
Corrected Total	15	0.00231130			

R-Square	Coeff Var	Root MSE	L5 Mean
0.658184	7.093528	0.009369	0.132081

Source	DF	Anova SS	Mean Square	F Value	Pr > F
Rep	3	0.00079585	0.00026528	3.02	0.0864
Variety	3	0.00072542	0.00024181	2.75	0.1042

Table E-6 (g): t-Test (LSD) for L1

Alpha	0.05

Error Degrees of Freedom	6
Error Mean Square	0.000011
Critical Value of t	2.44691
Least Significant Difference	0.0067

t-Grouping	Mean (kWh)	N	Electrical Energy
A	0.116667	3	EM3
A			
B A	0.110000	3	EFM
B			
B	0.109140	3	EBM
B			
B	0.106667	3	EM1

NB: Means with the same letter in the same column are not significantly different

Table E-6 (h): t-Test (LSD) for L2

Alpha	0.05
Error Degrees of Freedom	6
Error Mean Square	0.000013
Critical Value of t	2.44691
Least Significant Difference	0.0072

t-Grouping	Mean (kWh)	N	Electrical Energy
A	0.096667	3	EM3
A			
B A	0.093333	3	EFM
B			
B C	0.086667	3	EM1
C			
C	0.082867	3	EBM

NB: Means with the same letter in the same column are not significantly different

Table E-6 (i): t-Test (LSD) for L3

Alpha	0.05

Error Degrees of Freedom	6
Error Mean Square	0.000048
Critical Value of t	2.44691
Least Significant Difference	0.0139

t-Grouping	Mean (kWh)	N	Electrical Energy
A	0.156667	3	EM3
A			
B A	0.143333	3	EFM
B			
B	0.140000	3	EM1
B			
B	0.134333	3	EBM

NB: Means with the same letter in the same column are not significantly different

Table E-6 (j): t-Test (LSD) for L4

Alpha	0.05
Error Degrees of Freedom	6
Error Mean Square	0.000024
Critical Value of t	2.44691
Least Significant Difference	0.0097

t-Grouping	Mean (kWh)	N	Electrical Energy
A	0.066667	3	EM1
A	0.070000	3	EFM
A	0.066067	3	EBM
A	0.070000	3	EM3

NB: Means with the same letter in the same column are not significantly different

Table E-6 (k): t-Test (LSD) for L**5**

Alpha	0.05

Error Degrees of Freedom	6
Error Mean Square	0.000079
Critical Value of t	2.44691
Least Significant Difference	0.0178

t-Grouping	Mean (kWh)	N	Electrical Energy
A	0.123333	3	EM1
A	0.123333	3	EFM
A	0.119667	3	EBM
A	0.133333	3	EM3

NB: Means with the same letter in the same column are not significantly different

Appendix F: Measurements of current, voltage, pf, power and electrical energy for selected electrical loads over 20 minutes

Table F: Electrical loads

Electrical loads	Description
L1	5 36W 4ft Fluorescent fittings
L2	5 36W 4ft Fluorescent lights plus 6 100 Watt bulbs
L3	5 36W 4ft Fluorescent lights plus 14 100 Watt bulbs

Table F-1 (a): Measurement of current, voltage, pf, power and electrical energy using load L1 (fluorescent fittings)

Time	**Current**				**Voltage**			**Power**		**Power**		**Electrical Energy**					**Blinks**
(mins)	**(A)**				**(V)**			factor		(W)		(kWh)					
	I1	IBM	IFM	I4	V1	VBM	VFM	pfBM	pfFM	PBM	PFM	EBM	EFM	EM1	EM2	EM3	
0	1.77	1.83	1.8	1.72	230	232	231	0.50	0.57	210	234	0	0	0	0	0	0
5	1.76	1.8	1.77	1.71	230	231	230	0.51	0.58	211	234	0.0176	0.02	0.02	0	0.01	2
5	1.75	1.79	1.76	1.72	230	231	230	0.51	0.58	210	232	0.0175	0.02	0.02	0	0.02	2
5	1.71	1.74	1.73	1.65	228	230	228	0.52	0.58	212	233	0.0177	0.02	0.02	0	0.02	2
5	1.72	1.76	1.74	1.66	229	230	229	0.52	0.59	212	233	0.0177	0.02	0.02	0.1	0.02	2

Table FE-1 (a): Cumulative electrical energy extract

	Current		**Voltage**		**Power**		**Power**		**Electrical Energy**				
	(A)		**(V)**		factor		(W)		(kWh)				
	IBM	IFM	VBM	VFM	pfBM	pfFM	PBM	PFM	EBM	EFM	EM1	EM2	EM3
Average	1.78	1.76	230.8	230	0.512	0.58	211	233.2					
	a	*b*	*c*	*d*	*e*	*f*	*ace*	*bdf*					
Power calculated as V×I× pf from recorded values									210.3	234.8			
Electrical energy (V×I×pf ×time) kWh = (*ace*×20/60), (*bdf*×20/60))									0.07	0.078			
Total energy (kWh) "recorded" in 20 minutes									**0.07**	**0.08**	**0.08**	**0.1**	

0.07

Table F-1 (b): Measurement of current, voltage, pf, power and electrical energy using Load L2 (5×36W fluorescent fittings plus 6×100W incandescent bulbs)

Time	**Current**				**Voltage**			**Power**		**Power**			**Electrical Energy**				**Blinks**
mins)	**(A)**				**(V)**			factor		(W)			(kWh)				
	I1	IBM	IFM	I4	V1	VBM	VFM	pfBM	pfFM	PBM	PFM	EBM	EFM	EM1	EM2	EM3	
			0	3.6	3.59	3.54	3.64	223	226	224	0.92	0.94	751	750	0	0	0
0	0	0															
5	3.65	3.62	3.56	3.62	224	228	227	0.92	0.94	750	757	0.0625	0.07	0.06	0.1	0.07	7
5	3.64	3.61	3.56	3.65	226	225	226	0.92	0.94	755	760	0.0629	0.07	0.06	0	0.07	7
5	3.64	3.61	3.56	3.64	226	226	227	0.95	0.94	755	769	0.0629	0.07	0.06	0.1	0.07	7
			5	3.71	3.59	3.66	3.62	230	231	230	0.91	0.94	777	787	0.0648	0.07	0.07
0.1	0.08	7															

Table FE-1 (b): Cumulative electrical energy extract

	Current		**Voltage**		**Power**		**Power**		**Electrical Energy**				
	(A)		**(V)**		factor		(W)		(kWh)				
	IBM	IFM	VBM	VFM	pfBM	pfFM	PBM	PFM	EBM	EFM	EM1	EM2	EM3
Average	3.63	3.58	227.5	227.5	0.92	0.94	757.6	764.6					
	a	*b*	*c*	*d*	*e*	*f*	*ace*	*bdf*					
Power calculated as V×I× pf from recorded values							760	766					
Electrical energy (V×I×pf ×time) kWh = (*ace*×20/60), (*bdf*×20/60))									0253	0.255			
Total energy (kWh) "recorded" in 20 minutes									**0.253**	**0.28**	**0.25**	**0.3**	**0.29**

Table F-1 (c): Measurement of current, voltage, pf, power and electrical energy using load L3: (5×36W fluorescent fittings plus 14×100W incandescent bulbs)

Time	**Current**				**Voltage**			**Power**		**Power**			**Electrical Energy**				**Blinks**
(mins)	**(A)**				**(V)**			factor		(W)			(kWh)				
	I1	IBM	IFM	I4	V1	VBM	VFM	pfBM	pfFM	PBM	PFM	EBM	EFM	EM1	EM2	EM3	
	0	6.71	6.72	6.66	6.71	222	223	225	0.98	0.99	1478	1480	0	0	0	0	0
0																	

5	6.75	6.75	6.64	6.74	227	229	229	0.98	0.99	1522	1510	0.13	0.15	0.14	0.1	0.15	14
5	6.77	6.75	6.65	6.8	228	229	220	0.98	0.99	1529	1520	0.13	0.14	0.10	0.1	0.12	14
5	6.8	6.77	6.66	6.78	227	226	229	0.98	0.99	1512	1510	0.13	0.13	0.13	0.2	0.14	14
5	6.7	6.71	6.59	6.72	224	226	225	0.98	0.99	1477	1460	0.12	0.14	0.14	0.1	0.14	14

Table FE-1 (c): Cumulative electrical energy extract

	Current		**Voltage**		**Power**		**Power**		**Electrical Energy**				
	(A)		**(V)**		factor		(W)		(kWh)				
	IBM	IFM	VBM	VFM	pfBM	pfFM	PBM	PFM	EBM	EFM	EM1	EM2	E M3
Average			6.75	6.74	226.5	227.6	0.98	0.99	1504	1496.2			
Power calculated as V×I× pf from recorded values							1499	1518.7					
Electrical energy (V×I×pf ×time) kWh = (*ace*×20/60), (*bdf*×20/60))									0.5	0.51			
Total energy (kWh) "recorded" in 20 minutes										**0.51**	**0.56**	**0.51**	**0.51**

0.55

Appendix F-2: Analysis of Current

Table F-2 (a): ANOVA summary for current

Load	R-Square	Coeff Var	Root MSE	Mean Current	F Value	LSD
L1	0.973952	0.491991	0.008539	1.735625	75.51	<.0001
L2	0.971382	0.271723	0.009860	3.628750	62.66	<.0001
L3	0.970393	0.202897	0.013642	6.723750	76.07	<.0001

Table F-2 (b): ANOVA Outputs of Current

Class	Levels					
Rep	4	5	10	15	20	
Error	4	I1	IBM	IFM		I4
Number of observations: 16						

Table F-2 (c): Dependent Variable – L1

Source	DF	Sum of Squares	Mean Square	F Value	Pr > F
Model	6	0.02453750	0.00408958	56.09	<.0001
Error	9	0.00065625	0.00007292		
Corrected Total	15	0.02519375			

R-Square	Coeff Var	Root MSE	L1 Mean
0.973952	0.491991	0.008539	1.735625

Source	DF	Anova SS	Mean Square	F Value	Pr > F
Rep	3	0.00801875	0.00267292	36.66	<.0001
Current	3	0.01651875	0.00550625	75.51	<.0001

Table F-2 (d): Dependent Variable - L2

Source	DF	Sum of Squares	Mean Square	F Value	Pr > F
Model	6	0.02970000	0.00495000	50.91	<.0001
Error	9	0.00087500	0.00009722		
Corrected Total	15	0.03057500			

R-Square	Coeff Var	Root MSE	L2 Mean
0.971382	0.271723	0.009860	3.628750

Source	DF	Anova SS	Mean Square	F Value	Pr > F
Rep	3	0.01142500	0.00380833	39.17	<.0001
Current	3	0.01827500	0.00609167	62.66	<.0001

Table F-2 (e): Dependent Variable - L3

Source	DF	Sum of Squares	Mean Square	F Value	Pr > F
Model	6	0.05490000	0.00915000	49.16	<.0001
Error	9	0.00167500	0.00018611		
Corrected Total	15	0.05657500			

R-Square	Coeff Var	Root MSE	L3 Mean
0.970393	0.202897	0.013642	6.723750

Source	DF	Anova SS	Mean Square	F Value	Pr > F
Rep	3	0.01242500	0.00414167	22.25	<.0002
Current	3	0.04247500	0.01415833	76.07	<.0001

Table F-2 (f): t-Test (LSD) for L1

Alpha	0.05
Error Degrees of Freedom	9
Error Mean Square	0.000073
Critical Value of t	2.26216
Least Significant Difference	0.0137

t-Grouping	Mean (Amps)	N	Current
A	1.772500	4	IBM
B	1.750000	4	IF
C	1.735000	4	I1
D	1.685000	4	I4

NB: Means with the same letter in the same column are not significantly different

Table F-2 (g): t-Test (LSD) for L2

Alpha	0.05
Error Degrees of Freedom	9
Error Mean Square	0.000097
Critical Value of t	2.26216
Least Significant Difference	0.0158

t-Grouping	Mean (Amps)	N	Current
B	3.625000	4	IBM
C	3.575000	4	IFM
A	3.660000	4	I1
A	3.655000	4	I4

NB: Means with the same letter in the same column are not significantly different

Table F-2 (h): t-Test (LSD) for L3

Alpha	0.05
Error Degrees of Freedom	9
Error Mean Square	0.000186
Critical Value of t	2.26216
Least Significant Difference	0.0218

t-Grouping	**Mean (Amps)**	**N**	**Current**
A	6.745000	4	IBM
B	6.635000	4	IFM
A	6.755000	4	I1
A	6.760000	4	I4

NB: Means with the same letter in the same column are not significantly different

Appendix F-3: Analysis of voltage

Table F-3 (a): ANOVA for voltage on different loads

Load	**R-Square**	**Coeff Var**	**Root MSE**	**Mean Voltage**	**F Value**	**LSD**
L1	0.953125	0.125693	0.288675	229.6667	25.00	0.0012
L2	0.845161	0.508305	1.154701	227.1667	1.00	0.42
L3	0.867238	0.408044	0.927961	227.4167	3.58	0.095

Table F-3 (b): ANOVA outputs of voltages

Class	Levels		Values		
Rep	4	5	10	15	20
Error	3	V1	VBM		VFM
Number of observations: 12					

Table F-3 (c): Dependent Variable - L1

Source	**DF**	**Sum of Squares**	**Mean Square**	**F Value**	**Pr > F**
Model	5	10.16666667	2.03333333	24.40	<.0006
Error	6	0.50000000	0.08333333		
Corrected Total	11	10.66666667			

R-Square	Coeff Var	Root MSE	L1 Mean
0.953125	0.125693	0.288675	229.6667

Source	**DF**	**Anova SS**	**Mean Square**	**F Value**	**Pr > F**
Rep	3	6.00000000	2.00000000	24.00	<.0010
Voltage	2	4.16666667	2.08333333	25.00	<.0012

Table F-3 (d): Dependent Variable – L2

Source	**DF**	**Sum of Squares**	**Mean Square**	**F Value**	**Pr > F**
Model	5	43.66666667	8.73333333	6.55	<.0203
Error	6	8.00000000	1.33333333		
Corrected Total	11	51.66666667			

R-Square	Coeff Var	Root MSE	L2 Mean
0.845161	0.508305	1.154701	227.1667

Source	**DF**	**Anova SS**	**Mean Square**	**F Value**	**Pr > F**
Rep	3	41.00000000	13.66666667	10.25	<.0089
Voltage	2	2.66666667	1.33333333	1.00	<.421

Table F-3 (e): Dependent Variable – L3

Source	DF	Sum of Squares	Mean Square	F Value	Pr > F
Model	**5**	33.75000000	6.75000000	7.84	<.0131
Error	6	5.16666667	0.8611111		
Corrected Total	11	38.91666667			

R-Square	Coeff Var	Root MSE	L3 Mean
0.867238	0.408044	0.927961	227.4167

Source	DF	Anova SS	Mean Square	F Value	Pr > F
Rep	3	27.58333333	9.19444444	10.68	<.0081
Voltage	2	6.16666667	3.08333333	3.58	<.0947

Table F-3 (f): t-Test (LSD) for L1

Alpha	0.05
Error Degrees of Freedom	6
Error Mean Square	0.083333
Critical Value of t	2.44691
Least Significant Difference	0.4995

t-Grouping	Mean (Volts)	N	Voltage
A	230.5000	4	VBM
B	229.2500	4	V
B	229.2500	4	VFM

NB: Means with the same letter in the same column are not significantly different

Table F-3 (g): t-Test (LSD) for L2

Alpha	0.05
Error Degrees of Freedom	6
Error Mean Square	1.333333
Critical Value of t	2.44691
Least Significant Difference	1.9979

t-Grouping	Mean (Volts)	N	Voltage
A	227.5000	4	VB
A	227.5000	4	V
A	226.5000	4	VFM

NB: Means with the same letter in the same column are not significantly different

Table F-3 (h): t-Test (LSD) for L3

Alpha	0.05
Error Degrees of Freedom	6
Error Mean Square	0.861111
Critical Value of t	2.44691
Least Significant Difference	1.6056

t-Grouping	Mean (Volts)	N	Voltage
BA	227.5000	4	VBM
B	226.5000		V
A	228.2500	4	VFM

NB: Means with the same letter in the same column are not significantly different

Appendix F-4: Analysis of power factor (pf)

Table F-4 (a): ANOVA for pf

Load	R-Square	Coeff Var	Root MSE	Mean pf	F Value	LSD
L1	0.995962	0.644289	0.003536	0.548750	729.00	0.0001
L2	0.666667	1.313399	0.012247	0.932500	3.00	0.1817
L3	0.666667	0.413416	0.004082	0.987500	3.00	0.1817

Table F-4 (b): ANOVA outputs of pf

Class	Levels	Values			
Rep	4	5	10	15	20
Errr	2	pfBM	pfFM		
Number of observations:	8				

Table F-4 (c): Dependent Variable - L1

Source	DF	Sum of Squares	Mean Square	F Value	Pr > F
Model	4	0.00925000	0.00231250	185.00	<.0006
Error	3	0.00003750	0.00001250		
Corrected Total	7	0.00928750			

R-Square	Coeff Var	Root MSE	L1 Mean
0.995962	0.644289	0.003536	0.548750

Source	DF	Anova SS	Mean Square	F Value	Pr<.F
Rep	3	0.00013750	0.00004583	3.67	<.1571
Variety	1	0.00911250	0.00911250	729.00	<.0001/

Table F-4 (d): Dependent Variable – L2

Source	DF	Sum of Squares	Mean Square	F Value	Pr > F
Model	4	0.00090000	0.00022500	1.50	0.3849
Error	3	0.00045000	0.00015000		
Corrected Total	7	0.00135000			

R-Square	Coeff Var	Root MSE	L2 Mean
0.666667	1.313399	0.012247	0.93250

Source	DF	Anova SS	Mean Square	F Value	Pr > F
Rep	3	0.00045000	0.00015000	1.00	0.5000
Variety	1	0.00045000	0.00045000	3.00	0.1817

Table F-4 (e): Dependent Variable – L3

Source	DF	Sum of Squares	Mean Square	F Value	Pr > F
Model	4	0.00010000	0.00002500	1.50	0.3849
Error	3	0.00005000	0.00001667		
Corrected Total	7	0.00015000			

R-Square	Coeff Var	Root MSE	L3 Mean
0.666667	0.413416	0.004082	0.987500

Source	DF	Anova SS	Mean Square	F Value	Pr > F
Rep	3	0.00005000	0.00001667	1.00	0.5000
Variety	1	0.00005000	0.00005000	3.00	0.1817

Table F-4 (f): t-Test (LSD) for L1

Alpha	0.05
Error Degrees of Freedom	3
Error Mean Square	0.000012
Critical Value of t	3.18245
Least Significant Difference	0.008

t-Grouping	pf Mean	N	Variety
A	0.582500	4	pfFM
B	0.515000	4	pfBM

NB: Means with the same letter in the same column are not significantly different

Table F-4 (g): t-Test (LSD) for L2

Alpha	0.05
Error Degrees of Freedom	3
Error Mean Square	0.00015
Critical Value of t	3.18245
Least Significant Difference	0.0276

t-Grouping	pf Mean	N	Variety
A	0.940000	4	pfFM
A	0.925000	4	pfBM

NB: Means with the same letter in the same column are not significantly

Table F-4 (h): t-Test (LSD) for L3

Alpha	0.05
Error Degrees of Freedom	3
Error Mean Square	0.000017
Critical Value of t	3.18245
Least Significant Difference	0.0092

t-Grouping	pf Mean	N	Variety
A	0.990000	4	
A	0.985000	4	pfBM

NB: Means with the same letter in the same column are not significantly different

Appendix F-5: Analysis of power

Table F-5 (a): ANOVA on power for different loads.

Load	R-Square	Coeff Var	Root MSE	Mean Power	F Value	LSD
L1	0.998554	0.304785	0.677003	222.1250	2064.27	0.0001
L2	0.979921	0.362537	2.768875	763.7500	21.13	0.0193
L3	0.985243	0.294665	4.434712	1505.000	10.17	0.0498

Table F-5 (b): ANOVA outputs of power

Class	Levels	Values
Rep	4	5 10 15 20
Error	2	PBM PFM
Number of observations:	8	

Table F-5 (c): Dependent Variable - L1

Source	DF	Sum of Squares	Mean Square	F Value	Pr > F
Model	4	949.5000000	37.3750000	517.91	<.0001
Error	3	1.3750000	0.4583333		
Corrected Total	7	950.8750000			

R-Square	Coeff Var	Root MSE	L1 Mean
0.998554	0.304785	0.677003	222.1250

Source	DF	Anova SS	Mean Square	F Value	Pr > F
Rep	3	3.3750000	1.1250000	2.45	<.2401
Variety	1	946.1250000	946.1250000	2064.27	<.0001

Table F-5 (d): Dependent Variable – L2

Source	DF	Sum of Squares	Mean Square	F Value	Pr > F
Model	4	1122.500000	280.625000	36.60	<.0070
Error	3	23.000000	7.666667		
Corrected Total	7	1145.500000			

R-Square	Coeff Var	Root MSE	L2 Mean
0.979921	0.362537	2.768875	763.7500

Source	DF	Anova SS	Mean Square	F Value	Pr > F
Rep	3	960.5000000	320.1666667	41.76	<.0060
Variety	1	162.0000000	162.0000000	21.13	<.0193

Table F-5 (e): Dependent Variable – L3

Source	DF	Sum of Squares	Mean Square	F Value	Pr > F
Model	4	3939.000000	984.750000	50.07	<.0044
Error	3	59.000000	19.666667		
Corrected Total	7	3998.000000			

R-Square	Coeff Var	Root MSE	L3 Mean
0.985243	0.294665	4.434712	1505.000

Source	DF	Anova SS	Mean Square	F Value	Pr > F
Rep	3	3739.000000	1246.333333	63.37	<.0033
Variety	1	200.000000	200.000000	10.17	<.0498

Table F-5 (f): t-Test (LSD) for L1

Alpha	0.05
Error Degrees of Freedom	3
Error Mean Square	0.458333
Critical Value of t	3.18245
Least Significant Difference	1.5235

t-Grouping	Mean (Watts)	N	Power
A	233.0000	4	P
B	211.2500	4	

NB: Means with the same letter in the same column are not significantly different

Table F-5 (g): t-Test (LSD) for L2

Alpha	0.05
Error Degrees of Freedom	3
Error Mean Square	7.666667
Critical Value of t	3.18245
Least Significant Difference	6.2309

t-Grouping	Mean (Watts)	N	Power
A	768.250	4	PFM
B	759.250	4	

NB: Means with the same letter in the same coumn are not significantly different

Table F-5 (h): t-Test (LSD) for L3

Alpha	0.05
Error Degrees of Freedom	3
Error Mean Square	19.666667
Critical Value of t	3.18245
Least Significant Difference	9.9796

t-Grouping	Mean (Watts)	N	Power
B	1500.000	4	PFM
A	1510.000	4	PBM

NB: Means with the same letterin the same column are not significantly different

Appendix F-6: Analysis of Electrical Energy

Table F-6 (a): ANOVA summary for electrical energy

Load	R-Square	Coeff Var	Root MSE	Mean	F Value	LSD
L1	0.431865	13.29879	0.002498	0.018781	1.27	<.3416
L2	0.860836	3.91831	0.002628	0.067069	14.16	<.0009
L3	0.658184	7.09352	0.009369	0.132081	2.75	<.1042

Table F-6 (b): ANOVA outputs of electrical energy

Class	Levels	Values			
Rep	4	5	10	15	20
Error	4	EBM	EFM	EM1	EM
Number of observations:	16				

Table F-6 (c): Dependent Variable - L1

Source	DF	Sum of Squares	Mean Square	F Value	Pr > F
Model	6	0.00004268	0.00000711	1.14	0.4124
Error	9	0.00000624			
Corrected Total	15	0.00009882			

R-Square	Coeff Var	Root MSE	L1 Mean
0.431865	13.29879	0.002498	0.018781

Source	DF	Anova SS	Mean Square	F Value	Pr > F
Rep	3	0.00001888	0.00000629	1.01	0.4328
Variety	3	0.00002380	0.00000793	1.27	0.3416

Table F-6 (d): Dependent Variable – L2

Source	DF	Sum of Squares	Mean Square	F Value	Pr > F
Model	6	0.00038448	0.00006408	9.28	0.0020
Error	9	0.00006216	0.00000691		
Corrected Total	15	0.00044663			

R-Square	Coeff Var	Root MSE	L2 Mean
0.860836	3.918310	0.002628	0.067069

Source	DF	Anova SS	Mean Square	F Value	Pr > F
Rep	3	0.00009105	0.00003035	4.39	0.0364
Variety	3	0.00029343	0.00009781	14.16	0.0009

Table F-6 (e): Dependent Variable - L3

Source	DF	Sum of Squares	Mean Square	F Value	Pr > F
Model	6	0.00152126	0.00025354	2.89	0.0744
Error	9	0.00079004	0.00008778		
Corrected Total	15	0.00231130			

R-Square	Coeff Var	Root MSE	L3 Mean
0.658184	7.093528	0.009369	0.132081

Source	DF	Anova SS	Mean Square	F Value	Pr > F
Rep	3	0.00079585	0.00026528	3.02	0.0864
Variety	3	0.00072542	0.00024181	2.75	0.1042

Table F-6 (f): t-Test (LSD) for L1

Alpha	0.05
Error Degrees of Freedom	9
Error Mean Square	6.238E-6
Critical Value of t	2.26216
Least Significant Difference	0.0042

t-Grouping	Mean (kWh)	N	Electrical Energy
A	0.020000	4	EM1
A	0.020000	4	EFM
A	0.017625	4	EBM
A	0.017500	4	EM3

NB: Means with the same letter in the same column are not significantly different

Table F-6 (g): t-Test (LSD) for L1

Alpha	0.05
Error Degrees of Freedom	9
Error Mean Square	6.906E-6
Critical Value of t	2.26216
Least Significant Difference	0.0042

t-Grouping	Mean (kWh)	N	Electrical Energy
B	0.062500	4	EM1
A	0.070000	4	EFM
B	0.063275	4	EBM
A	0.072500	4	EM3

NB: Means with the same letter in the same column are not significantly different

Table F-6 (h): t-Test (LSD) for L3

Alpha	0.05
Error Degrees of Freedom	9
Error Mean Square	0.000088
Critical Value of t	2.26216
Least Significant Difference	0.015

t-Grouping	Mean (kWh)	N	Electrical Energy
B	0.125000	4	EM1
A	0.140000	4	EFM
B A	0.125825	4	EBM
B A	0.137500	4	EM3

NB: Means with the same letter in the same column are not significantly different

Appendix G: Cumulative electrical energy registered for different loads

Table G (a): Cumulative electrical energy registered by 5 meters for 5 loads at 15 minutes each (extracted from Tables FE-1 (a) through (e)).

Energy	**Electrical loads**					**Total Energy**
meters	L1	L2	L3	L4	L5	(kWh)
EBM	0.327	0.249	0.403	0.198	0.359	1.536
EFM	0.33	0.28	0.43	0.21	0.37	1.62
EM1	0.32	0.26	0.43	0.2	0.37	1.58
EM2	0.3	0.3	0.5	0.2	0.4	1.7
EM3	0.35	0.29	0.45	0.21	0.4	1.7

Table G (b): Cumulative electrical energy registered by 5 energy meters for 3 loads at 20 minutes each (extract from Tables FE-1 (a), (b) and (c)).

Energy	**Electrical loads**			**Total Energy**
meters	L1	L2	L3	(kWh)
EBM	0.0705	0.253	0.503	0.827
EM1	0.08	0.25	0.51	0.84
EM2	0.10	0.30	0.51	0.84
EM3	0.07	0.29	0.55	0.91

Appendix H: Output voltages from successive approximation resistor network

Table H (a): Theoretical Design

Design	Resistors	Total sum of resistances up from R23	Jumpers opened successively from J10 to J1										Output (mV)
			R22	R21	R20	R19	R18	R17	R16	R15	R14	R13	
R11	330k	1320030											
R12	330k	990030											
R13	330k	660030										J1	120
R14	160k	330030									J2		160
R15	82k	170030								J3			190.84
R16	47k	88030							J4				211.76
R17	22k	41030						J5					225.95
R18	10k	19030					J6						233.27
R19	4.7k	9030				J7							236.76
R20	2.2k	4330			J8								238.44
R21	1k	2130		J9									239.23
R22	470Ω	1130	J10										239.59
R23	660Ω	660											239.76

Table H (b): Implemented Design

Design	Resistors	Total sum of resistances from R13	Jumpers opened (and left open) successively from J10 to J1										Output Voltage	% Output
			R12	R11	R10	R9	R8	R7	R6	R5	R4	R3		
R1	330k	1286103												
R2	320k	956103												
R3	330k	636103										J1	121.3	50.5
R4	150k	306103									J2		163.2	68
R5	83k	156103								J3			193.5	80.6
R6	39k	73103							J4				215.7	89.9
R7	15k	34103						J5					228	95
R8	10k	19103					J6						233.1	97.1
R9	4.7k	9103				J7							236.7	98.6
R10	2.2k	4403			J8								238.4	99.3
R11	1k	2203		J9									239.2	99.7
R12	553Ω	1203	J10										239.5	99.8
R13	650Ω	650											239.8	99.9

Appendix I: Abstract of Published Journal Paper

Performance of an Anisotropic Magneto-Resistive Electrical Energy Meter

Fredrick M. Kagucia [1], Professor Owino George [2] , Dr. Franklin M. Manene [3]

[1] Post Graduate Student, Dept. of Electrical and Control Eng., Egerton University, Kenya

[2] Department of Mechanical Engineering, Technical University of Kenya

[3] Department of Electrical and Control Engineering, Egerton University, Kenya

Abstract

This paper presents a digital electrical energy meter based on an Anisotropic Magneto-Resistive (AMR) current sensor and an Arduino micro microcontroller. Most energy meters use traditional current sensors with various shortcomings which are overcome by an AMR sensor. The current sensor was tested and found to have a linear output to input characteristic and suitable for metering electrical energy. The meter was designed using Proteus 8 Professional and fabricated on a printed circuit board. A C-language program was developed and stored in the microcontroller to sample voltage and current signals derived from a successive supply voltage divider and the AMR current sensor respectively. The meter computed and displayed on a Liquid Crystal Display (LCD) the electrical energy (kWh), 'real-time' power consumption, power factor, supply voltage and current. The cumulative electrical energy was stored in EEPROM. The meter displays information which is not normally displayed by ordinary domestic electrical energy meters. This information could be used by the consumers and power supply companies to improve the quality of the power supply. By monitoring the power factor and taking appropriate actions, the consumers could pay reduced monthly

bills. The power utility companies could also reduce power distribution costs (due to reduced currents) and improve customer connectivity.

Keywords: *AMR current sensor**,** Arduino micro microcontroller, LCD, Sampling.*

Appendix J: Research Permit

REPUBLIC OF KENYA

NATIONAL COMMISSION FOR SCIENCE, TECHNOLOGY & INNOVATION

Ref No: 868444

Date of Issue: 11/February/2020

RESEARCH LICENSE

This is to Certify that Mr.. FREDRICK MACHARIA KAGUCIA of Egerton University, has been licensed to conduct research in Nakuru on the topic: DESIGN AND PERFORMANCE ANALYSIS OF AN ANISOTROPIC MAGNETO-RESISTIVE ELECTRICAL ENERGY METER for the period ending : 11/February/2021.

License No: NACOSTI/P/20/3704

868444

Applicant Identification Number

Director General
NATIONAL COMMISSION FOR SCIENCE,TECHNOLOGY & INNOVATION

Verification QR Code

NOTE: This is a computer generated License. To verify the authenticity of this document, Scan the QR Code using QR scanner application.